Synthesis and molecular modelling of bio-based polyamides

Thibault Cousin

Thèse

Synthesis and molecular modelling of bio-based amorphous polyamides

Présentée devant
L'institut national des sciences appliquées de Lyon

Pour obtenir
Le grade de docteur

École doctorale
École doctorale Matériaux de Lyon
Spécialité : Matériaux Polymères

Par
Thibault Cousin
(Ingénieur ECPM)

Le 19 mars 2013 devant la Commission d'examen

Jury

M. Alessandro GANDINI — Professeur, Université de Sao Paulo	Rapporteur
M. Jean-Jacques ROBIN — Professeur, Université Montpellier II	Rapporteur
Mme Nadine ESSAYEM — DR, Université Lyon I	Examinateur
M. Jérôme DUPUY — Professeur, INSA de Lyon	Directeur de thèse
Mme. Jocelyne GALY — DR, CNRS	Directeur de thèse
M. Alain ROUSSEAU — IR, INSA Lyon	Membre invité

Ingénierie des Matériaux Polymères, UMR 5223

IMP@INSA

INSA Direction de la Recherche - Ecoles Doctorales – Quinquennal 2011-2015

SIGLE	ECOLE DOCTORALE	NOM ET COORDONNEES DU RESPONSABLE
CHIMIE	**CHIMIE DE LYON** **http://www.edchimie-lyon.fr** Insa : R. GOURDON	M. Jean Marc LANCELIN Université de Lyon – Collège Doctoral Bât ESCPE 43 bd du 11 novembre 1918 69622 VILLEURBANNE Cedex Tél : 04.72.43 13 95 directeur@edchimie-lyon.fr
E.E.A.	**ELECTRONIQUE,** **ELECTROTECHNIQUE, AUTOMATIQUE** **http://edeea.ec-lyon.fr** Secrétariat : M.C. HAVGOUDOUKIAN eea@ec-lyon.fr	M. Gérard SCORLETTI Ecole Centrale de Lyon 36 avenue Guy de Collongue 69134 ECULLY Tél : 04.72.18 60 97 Fax : 04 78 43 37 17 Gerard.scorletti@ec-lyon.fr
E2M2	**EVOLUTION, ECOSYSTEME,** **MICROBIOLOGIE, MODELISATION** **http://e2m2.universite-lyon.fr** Insa : H. CHARLES	Mme Gudrun BORNETTE CNRS UMR 5023 LEHNA Université Claude Bernard Lyon 1 Bât Forel 43 bd du 11 novembre 1918 69622 VILLEURBANNE Cédex Tél : 04.72.43.12.94 e2m2@biomserv.univ-lyon1.fr
EDISS	**INTERDISCIPLINAIRE SCIENCES-** **SANTE** **http://ww2.ibcp.fr/ediss** Sec : Safia AIT CHALAL Insa : M. LAGARDE	M. Didier REVEL Hôpital Louis Pradel Bâtiment Central 28 Avenue Doyen Lépine 69677 BRON Tél : 04.72.68 49 09 Fax :04 72 35 49 16 Didier.revel@creatis.uni-lyon1.fr
INFOMATHS	**INFORMATIQUE ET** **MATHEMATIQUES** http://infomaths.univ-lyon1.fr	M. Johannes KELLENDONK Université Claude Bernard Lyon 1 INFOMATHS Bâtiment Braconnier 43 bd du 11 novembre 1918 69622 VILLEURBANNE Cedex Tél : 04.72. 44.82.94 Fax 04 72 43 16 87 infomaths@univ-lyon1.fr
Matériaux	**MATERIAUX DE LYON** Secrétariat : M. LABOUNE PM : 71.70 –Fax : 87.12 Bat. Saint Exupéry Ed.materiaux@insa-lyon.fr	M. Jean-Yves BUFFIERE INSA de Lyon MATEIS Bâtiment Saint Exupéry 7 avenue Jean Capelle 69621 VILLEURBANNE Cédex Tél : 04.72.43 83 18 Fax 04 72 43 85 28 Jean-yves.buffiere@insa-lyon.fr
MEGA	**MECANIQUE, ENERGETIQUE, GENIE** **CIVIL, ACOUSTIQUE** Secrétariat : M. LABOUNE PM : 71.70 –Fax : 87.12 Bat. Saint Exupéry mega@insa-lyon.fr	M. Philippe BOISSE INSA de Lyon Laboratoire LAMCOS Bâtiment Jacquard 25 bis avenue Jean Capelle 69621 VILLEURBANNE Cedex Tél :04.72.43.71.70 Fax : 04 72 43 72 37 Philippe.boisse@insa-lyon.fr
ScSo	ScSo* M. OBADIA Lionel Sec : Viviane POLSINELLI Insa : J.Y. TOUSSAINT	M. OBADIA Lionel Université Lyon 2 86 rue Pasteur 69365 LYON Cedex 07 Tél : 04.78.69.72.76 Fax : 04.37.28.04.48 Lionel.Obadia@univ-lyon2.fr

*ScSo : Histoire, Geographie, Aménagement, Urbanisme, Archéologie, Science politique, Sociologie, Anthropologie

Abstract

In the current context of oil resources rarefaction, the development of biobased polymers is of major importance. The present work focused on the development of a biobased amorphous polyphthalamide, based on furan-2,5-dicarboxylic acid.

The first part of the study was devoted to the development of a molecular modelling protocol that could calculate the glass transition temperature of polyphthalamides with accuracy. In order to do this, model polyphthalamides based on isophthalic, terephthalic acid and hexamethylene diamine were synthesized and characterized as well as simulated. By comparison between simulated and measured Tg, the protocol was validated.

In a second part of the study, this protocol was applied to FDCA based polyphthalamides. These PPA were also synthesized. It was found that the PA 6-F undertakes a decarboxylation, preventing it from reaching high a molar mass. It was also found that the mechanical and thermal properties decrease as the amount of FDCA in the copolymers increases.

Keywords: Polyamide, polyphthalamide, molecular modelling, molecular dynamics, furan-2,5-dicarboxylic acid, FDCA, biobased polyamides.

Résumé

Dans le contexte actuel de raréfaction des ressources fossiles, le développement des polymères biosourcés est d'une grande importance. Le travail de cette thèse consiste donc en la synthèse et le développement d'un polyphtalamide amorphe à base d'acide furan-2,5-oique.

Dans un premier temps, un protocole de modélisation moléculaire permettant de calculer la Tg de polyphthalamides a été développé. Pour cela, des PPA modèles (basés sur un mélange d'acides isophtaliques et téréphtaliques ainsi que l'hexaméthylène diamine) ont été synthétisés et caractérisés. En comparant les Tg obtenues par modélisation et par mesure en DSC, le protocole de modélisation a été validé.

Dans un deuxième temps, ce protocole a été appliqué à des PPA à base de FDCA. Ces polymères ont également été synthétisés et caractérisés. Il en ressort que le PA 6-F subit une importante décarboxylation durant sa synthèse, l'empêchant d'atteindre une masse molaire importante. Il a aussi été montré que l'ajout de FDCA dans des copolyphthalamides diminuait leurs propriétés thermiques et mécaniques.

Mots-clés: Polyamides biosourcés, polyphtalamides, modélisation moléculaire, dynamique moléculaire, acide furan-2,5-oique, FDCA

Résumé

Dans le contexte actuel de diminution des ressources fossiles et dans une tendance de développement toujours plus important de la chimie verte, de nombreuses recherches portant sur les polymères biosourcés sont aujourd'hui entreprises. Parmi ces polymères biosourcés, des bio-polyamides ont été commercialisés avec succès. Ces polyamides sont principalement à base de PA 11, un polyamide fabriqué par la condensation de l'acide 11-aminoundécanoique, lui-même dérivé de l'huile de ricin. Ce polymère présente des bonnes propriétés d'usage mais a l'inconvénient d'avoir une température de transition vitreuse de l'ordre de 45°C, ce qui l'empêche d'être utilisé pour des applications nécessitant une résistance thermique plus importante. Afin de palier à ce problème, une classe de polyamides semi-aromatiques existe depuis de nombreuses années mais il n'existe aujourd'hui pas d'alternative biosourcée à ces matériaux. Nous nous proposons donc de développer de nouveaux matériaux polyphtalamides (PPA) amorphes biosourcés.

Dans cette thèse, nous nous sommes basés en particulier sur un monomère biosourcé : l'acide furan-2,5-oique, ou FDCA (Figure 1).
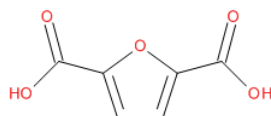
FIGURE 1 – Acide furan-2,5-oique (FDCA)

Ce monomère a été mis sur la liste des composés biosourcés les plus prometteurs pour l'établissement d'une chimie non basée sur des ressources fossiles par le ministère de l'énergie américain. En effet ce monomère pourrait être une alternative intéressante aux acides téréphtaliques et isophtaliques, largement utilisés dans la production de matériaux polymères (notamment le poly(éthylène téréphtalate) PET). De plus, la littérature concernant ce monomère et les polymères qui en découlent n'est pas importante et est contradictoire sur de nombreux points tels que les températures de fusion et de transition vitreuse ainsi que les masses molaires et la réactivité de ceux-ci. Ces différents éléments ont motivé la présente thèse. Cette thèse s'inscrit dans un projet ANR, appelé PolyGlu, et dont le but est la fabrication de polyamides en partant d'une ressource renouvelable, abondante et peu-chère : le glucose. Pour cela, trois partenaires sont impliqués dans ce projet. L'IRCELyon, un laboratoire de catalyse, était en charge de la synthèse d'hydroxymethylfurfural (HMF) à partir de glucose. La société ARKEMA était en charge de la transforma-

7

tion de cet HMF en FDCA et finalement notre laboratoire de l'INSA de Lyon était chargé de la synthèse et la modélisation moléculaire de polyamides à partir de ce FDCA.

Un outil supplémentaire a également été utilisé durant cette thèse : la modélisation moléculaire. En effet, durant les dernières années, la simulation informatique appliquée à la science des matériaux a fait de nombreux progrès et est aujourd'hui plus facilement accessible pour de nombreux laboratoires grâce au développement de la puissance des ordinateurs modernes. Cette simulation permet d'étudier un polymère sans avoir à le synthétiser, ce qui peut être un gain de temps et une économie importante.

Nous nous sommes donc consacrés dans un premier temps au développement d'un protocole robuste de simulation. Pour cela, une série de copolyphtalamides modèles a été synthétisée et caractérisée. Il s'agit de copolymères obtenus par condensation d'un mélange d'acides téréphtalique et isophtalique avec de l'hexaméthylène diamine, avec un taux d'acide téréphtalique inférieur à 50 % afin de synthétiser uniquement des polymères amorphes (Figure 2). En effet, les techniques de modélisation moléculaire utilisés ne prennent pas en compte le phénomène de cristallisation.
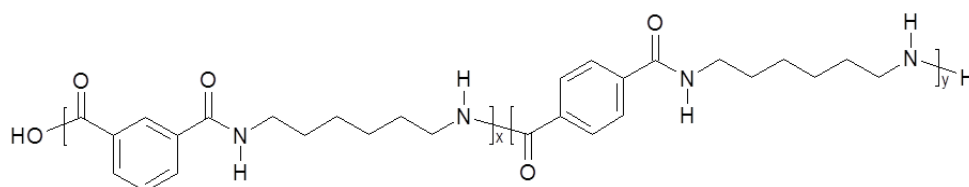

FIGURE 2 – Polyphtalamides modèles synthétisés : PA 6-I/6-T

La synthèse de ces polyphtalamides (PPA) a été faite dans un dispositif fabriqué spécialement à cette intention (à cause des hautes températures nécessaires pour la synthèse des PPA). Ce montage est présenté dans la Figure 2.7 :
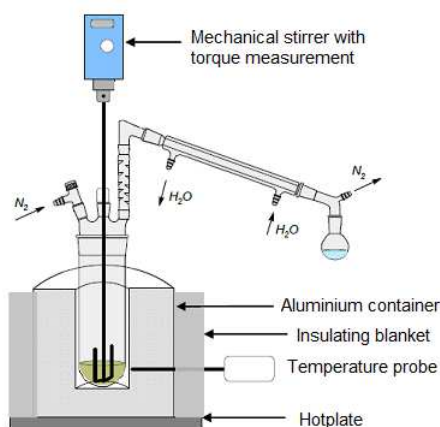

FIGURE 3 – Montage pour la synthèse des polyphtalamides

Ce montage est composé d'un système de chauffe en aluminium, permettant

d'atteindre des températures de l'ordre de 350°C, d'un système de distillation, d'un agitateur mécanique avec mesure du couple d'agitation, le tout sous balayage d'azote. La synthèse se déroule en plusieures étapes : tout d'abord, la diamine en solution (50 wt %) est introduite puis les acides (sous forme de poudre) dans un tube en verre. Les monomères réagissent pour former un sel en solution aqueuse. L'eau est ensuite distillée en augmentant progressivement la température (jusqu'à 260-300°C en fonction de la quantité d'acide téréphtalique). La réaction de polymérisation a lieu dans le fondu, et son avancement est suivi par l'augmentation du couple d'agitation. A la fin de la réaction, le mélange est refroidi à l'air libre et le tube de verre est brisé pour récupérer la cinquantaine de grammes de polymère formée.

La composition chimique des matériaux synthétisés a été vérifiée par RMN du proton, chromatographie d'exclusion stérique (SEC) et viscosimétrie en solution. Les résultats de ces analyses sont présentés dans le Tableau 2.5.

RMN	SEC				Viscosimetrie
Composition (IPA/TPA)	DPn	$\bar{M}_n$	$\bar{M}_w$	$\bar{M}_w$ / $\bar{M}_n$	η_{red} (mL/g)
100 / 0	64	15700	33100	2.1	125
90 / 10	34	8400	20000	2.4	87
80 / 20	66	16200	31000	1.9	130
70 / 30	51	12600	29100	2.3	106
60 / 40	55	13400	38900	2.9	163

TABLE 1 – Composition chimique (RMN), masses molaires (SEC) et viscosité réduite des différents PPA

La répartition des acides dans la chaîne polymère est similaire à celle introduite dans le réacteur, ce qui indique qu'il n'y a pas de pertes d'acide ou de trop grosse différence de réactivité entre les différents monomères. Les masses molaires obtenues sont assez typiques de celles des polyphtalamides, il y a cependant une dispersion de ces masses qui est liée à la faible reproductibilité de la méthode de synthèse.

En parallèle à ces synthèses, deux techniques de modélisation moléculaire ont été utilisées : une méthode basée sur le principe des contributions de groupe et nommée Synthia, et une technique de dynamique moléculaire (MD). La première technique calcule un certain nombre de propriétés des polymères en fonction de leur structure chimique.

Pour ce qui est de la dynamique moléculaire, une approche plus complexe est nécessaire. En effet il faut dans un premier temps "dessiner" le motif répétitif de la chaîne polymère, puis "polymériser" ce motif en créant une chaîne au degré de polymérisation souhaité (ici 20, afin de se rapprocher des masses molaires des PPA synthétisés). La dernière étape de ce processus de construction est de mettre plusieurs chaînes précédemment construites dans une cellule qui se répétera à l'infini dans toutes les directions (frontières périodiques) afin de simuler un matériau en masse et de calculer non seulement les interactions intra mais aussi intermoléculaires (Figure 2.12).

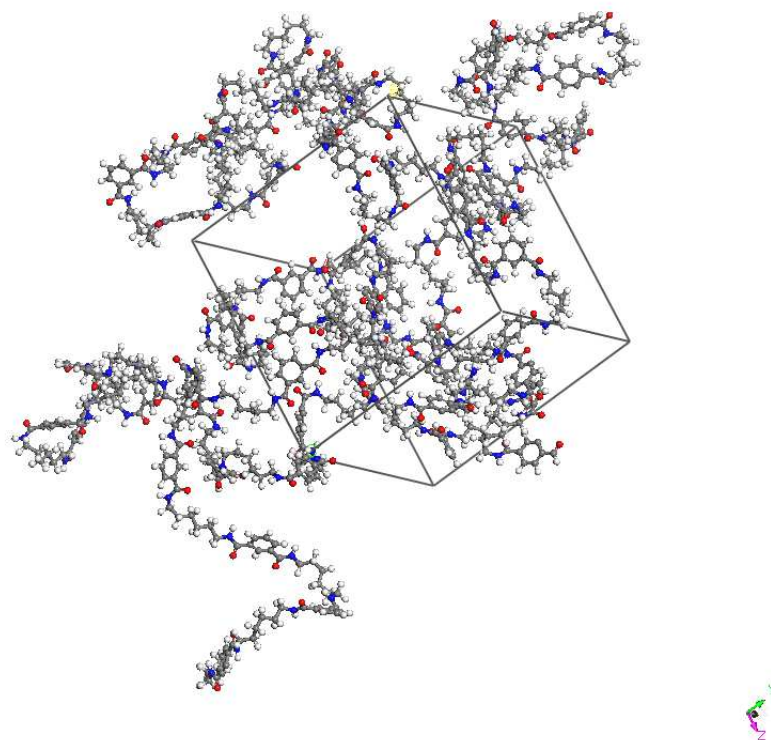La modélisation elle-même consiste à simuler un diagramme densité-température

FIGURE 4 – 3 chaînes de PA 6-I_{80}/6-T_{20} dans une cellule

du polymère afin d'en extraire la température de transition vitreuse. Pour cela, une dynamique moléculaire (résolution des équation de Newton pour chaque atome à chaque instant) de 300 ps a lieu, puis la température du système est diminuée de 10°C et l'étape de dynamique moléculaire recommence. On procède ainsi entre 500 et 300 K afin d'extraire la température de transition vitreuse de cette simulation.

Les résultats de ces deux techniques de modélisation, en comparaison avec les résultats obtenus par DSC pour les matériaux synthétisés sont présentés Figure 5.
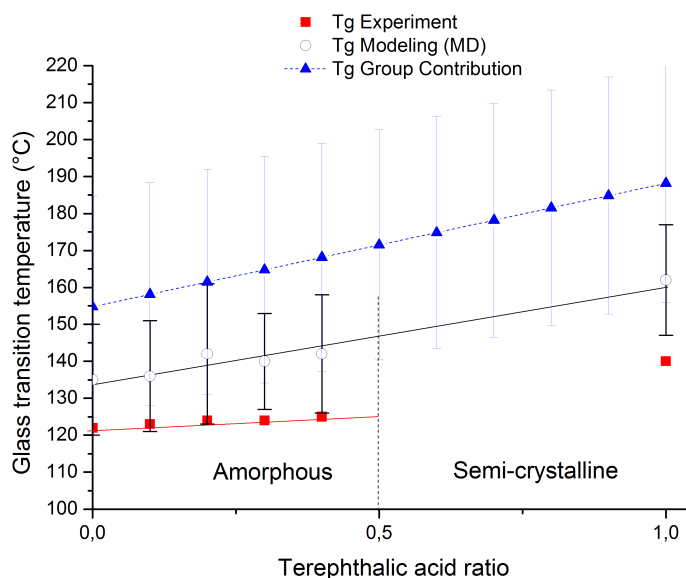
FIGURE 5 – Températures de transition vitreuse en fonction de la quantité d'acide téréphtalique contenu dans les PPA synthétisés

Sur cette figure, on peut voir que les différentes techniques de modélisation montrent la même tendance que les mesures par DSC, à savoir une augmentation de la température de transition vitreuse avec le taux d'acide téréphtalique. La Tg calculée par la méthode des contribution de groupes est clairement plus élevée que la réalité. Les Tg calculées par dynamique moléculaire par contre se rapprochent de celles mesurées par DSC. On peut également observer une différence nette de comportement entre les polyamides amorphes et semi-cristallins. En effet, au dessus de 50 % d'acide téréphtalique, les polymères cristallisent et on peut voir un changement de pente dans l'augmentation de la Tg, ce que les deux techniques de modélisation n'arrivent pas à caractériser. Malgré tout, il semble y avoir une différence fixe d'une vingtaine de degrés entre la dynamique moléculaire et la DSC. Cette différence peut avoir deux origines : la première est la polymolécularité des matériaux synthétisés alors que les matériaux simulés sont isomoléculaires, et la seconde est la différence de vitesse de refroidissement entre une DSC à 10°C/min et une diminution de 10°C sur 50 ps en modélisation qui peut entraîner une mesure de la vitrification précoce du système.

Cependant, comme cette différence de 20°C est fixe, nous pouvons la prendre en compte et utiliser ce protocole pour prédire les températures de transition vitreuse

d'autres polyphtalamides. Le protocole mis en place est donc validé.

Dans une deuxième partie, ce protocole de modélisation a été utilisé pour étudier les propriétés thermiques de polyamides amorphes biosourcés à partir de FDCA. Ces polymères ont également été synthétisés et caractérisés en détails. Pour ces synthèses, un réacteur pilote (1L, 350°C et 50 bars) a été utilisé. Ce réacteur est complètement instrumenté et équipé d'une fenêtre afin de suivre au mieux le déroulement des réactions de polymérisation.

Le protocole de synthèse est en 4 étapes principales, comme présenté sur la Figure 6. La première étape correspond à la formation du sel de polyamide. La deuxième correspond à une augmentation progressive de la température et à une montée en pression (jusque 18-20 bar), ce qui permet d'empêcher la perte de diamine lors de la montée en température. La troisième étape est une lente décompression jusqu'à pression atmosphérique et enfin la dernière étape correspond à la prise en masse, sous vide, du polymère.
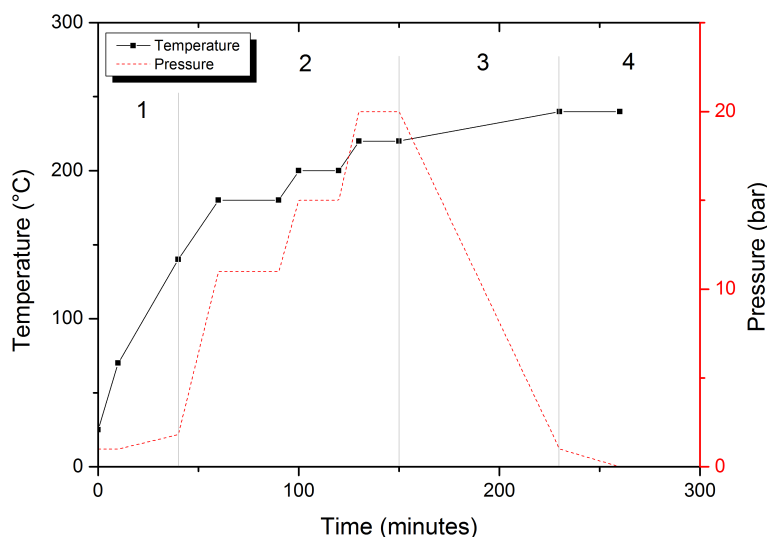
FIGURE 6 – Protocole de synthèse des PPA à partir de FDCA

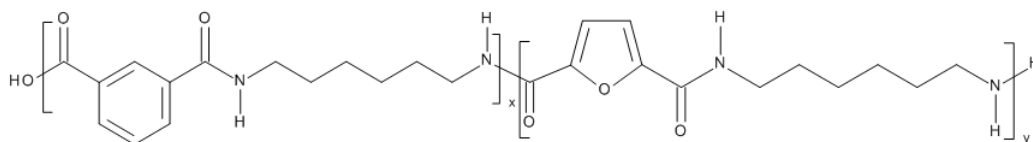Les polyphthalamides ainsi synthétisés devraient être de la forme suivante (Figure 7) :

FIGURE 7 – Formule générale des copolyphtalamides PA 6-I$_{(x)}$/6-F$_{(y)}$

Ces polymères ont été caractérisés comme précédemment par RMN, SEC et viscosimétrie. Les résultats sont présentés dans le Tableau 2.

RMN (IPA/FDCA)	Nomenclature	SEC*			Viscosimetry
		Mn	Mw	PDI	η_{red}
100/0	PA 6-I	15700	33100	2.10	75.0
90/10	PA 6-I$_{90}$/6-F$_{10}$	15300	32700	2.14	67.5
80/20	PA 6-I$_{80}$/6-F$_{20}$	15400	35200	2.29	64.3
70/30	PA 6-I$_{70}$/6-F$_{30}$	14700	32550	2.22	56.4
60/40	PA 6-I$_{60}$/6-F$_{40}$	12150	31400	2.58	46.4
50/50	PA 6-I$_{50}$/6-F$_{50}$	12000	32100	2.68	46.3
0/100	PA 6-F	2400	7300	3.03	15.0

TABLE 2 – Composition, masse molaire et viscosité réduite des PA 6-I$_{(x)}$/6-F$_{(y)}$.
* SEC dans l'HFIP, calibration PMMA

Comme on peut le remarquer dans ce tableau, la répartition des acides dans la chaîne est la même que celle introduite dans le réacteur (RMN du proton). Les masses molaires et viscosités réduites des polyphtalamides sont conformes à ce qui est attendu, sauf dans le cas du PA 6-F, qui présente une masse molaire très faible. De plus, lors de l'analyse par RMN du proton, différents pics inexpliqués sont apparus, et avec d'autant plus d'intensité que le taux de FDCA dans le copolymère est important, comme présenté sur la Figure 8 (pics h, i, j et k).
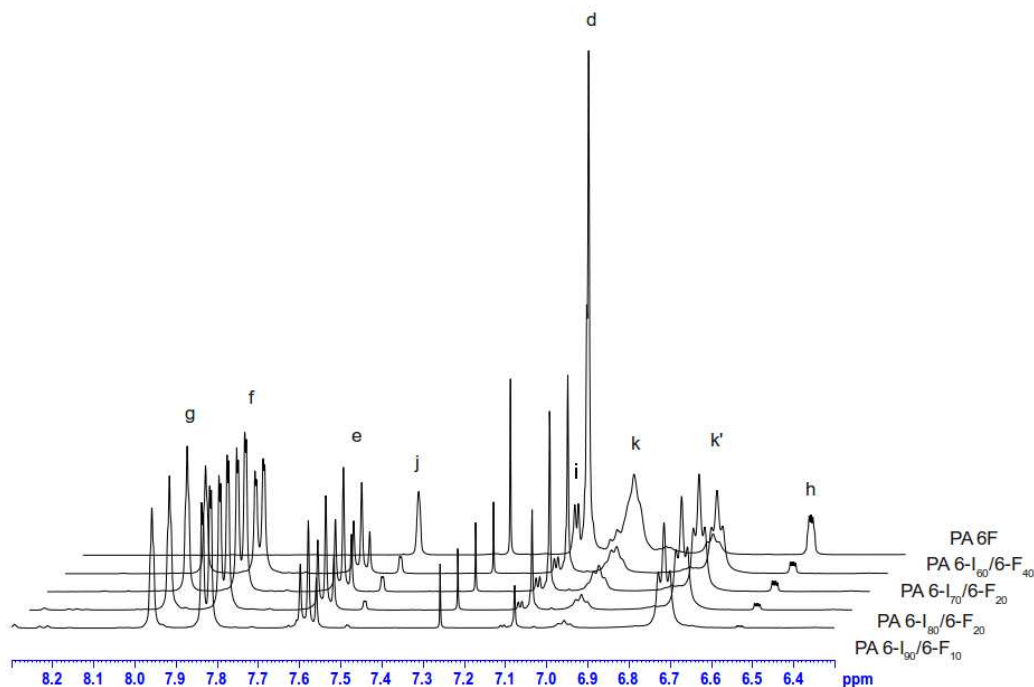

FIGURE 8 – RMN du proton de RMN du proton de PA 6-I$_{(x)}$/6-F$_{(y)}$

14

Afin d'élucider ce phénomène, des analyses complémentaires de RMN du carbone et de RMN 2D (COSY, HSBC, HSQC) ainsi que de la spectroscopie de masse MALDI-TOF ont été effectuées. Ces analyses ont permis de montrer l'existence de la structure présentée sur la Figure 9.
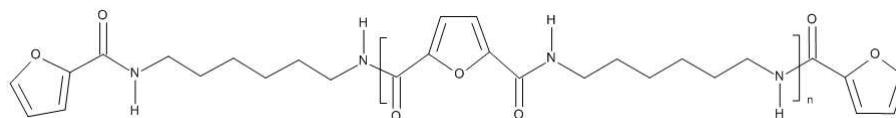

FIGURE 9 – PA 6-F avec des furanes décarboxylés à chaque extrémité

En effet, la présence de furanes décarboxylés à chaque bout de chaîne a été démontrée par MALDI-TOF et RMN. Cette décarboxylation des monomères empêche d'obtenir des hautes masses molaires car ces bouts de chaînes sont non réactifs, ce qui explique la masse molaire faible de l'ordre de 1000-2000 g/mol du PA 6-F.

Les propriétés thermiques de ces copolyamides ont été étudiées par DSC, ATG ainsi que par modélisation moléculaire. Les principaux résultats sont présentés dans la Figure 10.
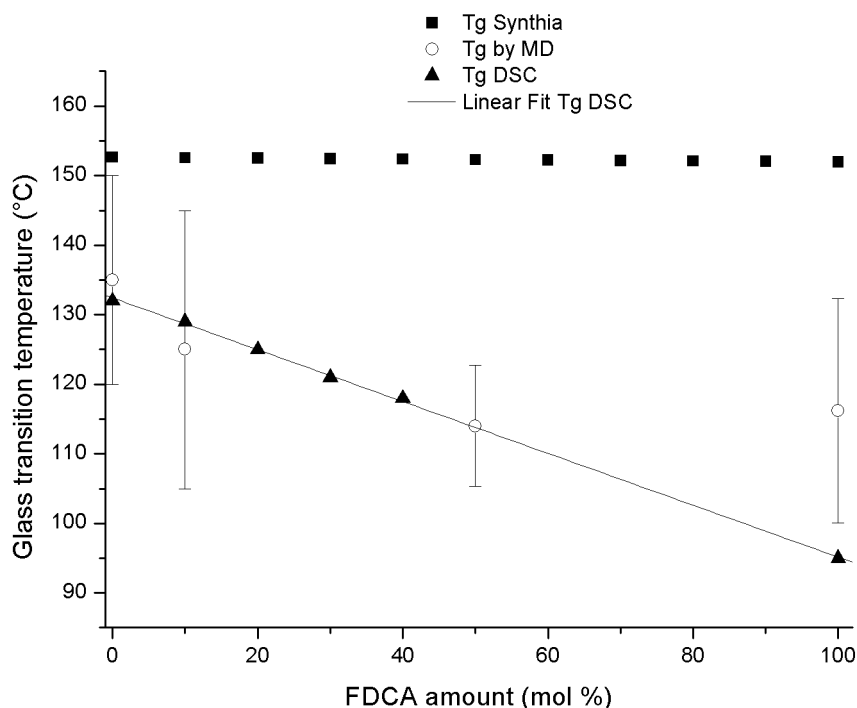
FIGURE 10 – Température de transition vitreuse des différents PA 6-I$_{(x)}$/6-F$_{(y)}$

Dans cette figure, on peut voir que la technique des contributions de groupe (Synthia) n'est pas du tout adaptée à ce système car elle n'observe quasiment aucune diminution de la Tg avec le taux de FDCA, au contraire du protocole de dynamique

moléculaire. La Tg mesurée par DSC et la dynamique moléculaire s'accordent bien jusqu'à 50 % de FDCA dans le copolyamide. Pour ce qui est du PA 6-F, une grande différence est observée (Tg(DSC)=95°C et Tg(MD)=110°C). Cette différence peut provenir de la très faible masse molaire du PA 6-F synthétisé, contrairement au PA 6-F modélisé qui a une masse molaire de 20000 g/mol.

Des tests mécaniques ont également été effectués (traction uni-axiale) après avoir extrudé les PA synthétisés grâce à une micro-extrudeuse (260°C) et injecté dans un moule en forme d'éprouvette de traction (température du moule 80°C). Le module d'Young mesuré pour les différents polymères testés ne semble pas varier en fonction du taux de FDCA. Cependant l'allongement à la rupture et la contrainte à rupture diminuent significativement en ajoutant du FDCA (Figure 11).
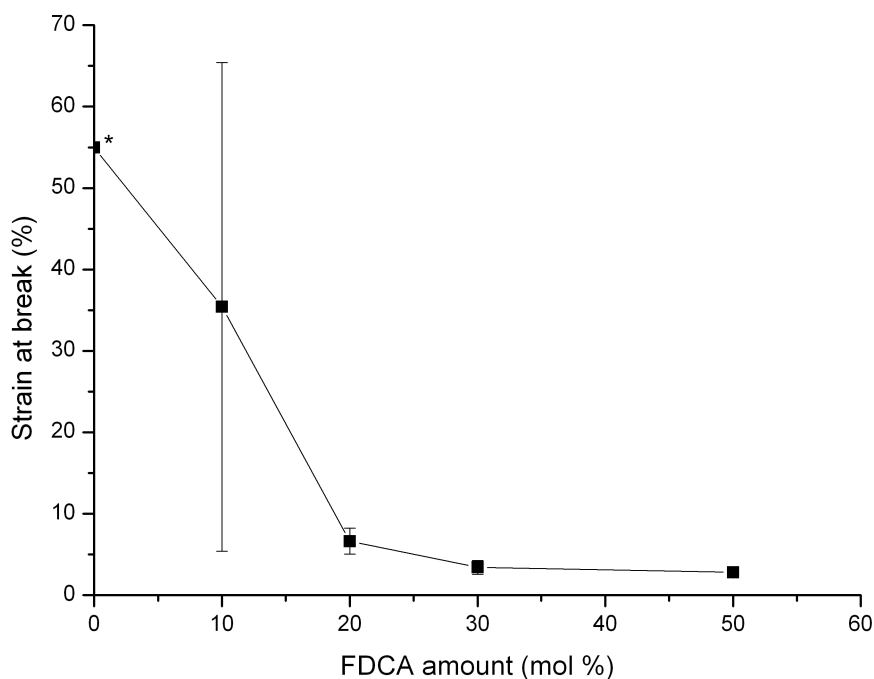
FIGURE 11 – Allongement à la rupture des PA 6-I$_{(x)}$/6-F$_{(y)}$

A la vue de ce graphique, il est clair qu'ajouter du FDCA dans la composition des copolyamides rend le polymère plus fragile. On peut attribuer cela à la différence qu'il y a entre le noyau benzénique de l'acide isophtalique, qui est rigide et plan, ce qui permet aux chaines macromoléculaires de s'organiser par Π-stacking, alors qu'avec l'hétérocycle furanique, moins rigide et non plan, le Π-stacking n'est pas possible. Par ailleurs, il est bien connu que la présence de chaines plus courtes va aussi contribuer à la chute des propriétés mécaniques.

Cette tendance se retrouve également dans les propriétés d'adsorption d'eau des différents PA 6-I$_{(x)}$/6-F$_{(y)}$ (Figure 12). On peut ainsi voir que plus il y a de FDCA dans le polymère, plus la quantité d'eau adsorbée est importante. C'est également

lié à la différence d'hydrophilie entre le benzène et le furane (comportant un atome d'oxygène).
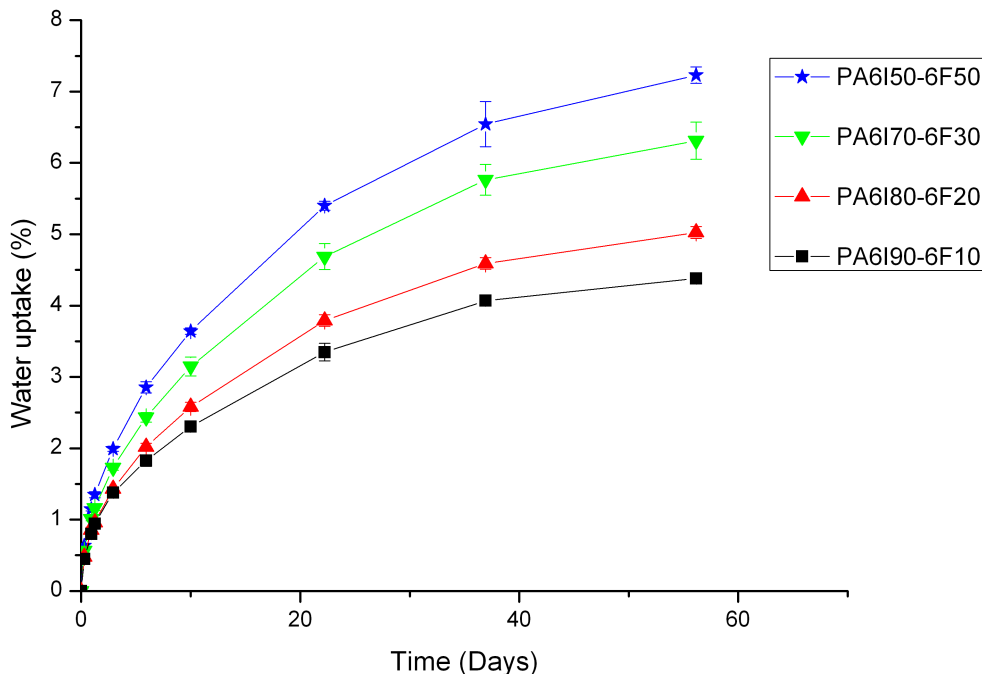

FIGURE 12 – Reprise en eau des différents PA 6-I$_{(x)}$/6-F$_{(y)}$

Pour conclure, le but de cette thèse était la synthèse et la modélisation moléculaire de polyamides semi-aromatiques biosourcés. Pour atteindre ce but, nous avons dans un premier temps développé un protocole de simulation par dynamique moléculaire sur des polyphtalamides modèles (PA 6-I$_{(x)}$/6-F$_{(y)}$). En modélisant et synthétisant en parallèle ces polyamides, nous avons pu établir la validité de ce protocole. Dans un deuxième temps, nous avons appliqué ce protocole sur des polyamides à partir d'acide furan-2,5-oique (FDCA). Des polyamides à base de FDCA ont également été synthétisés. Nous avons mis en évidence la décarboxylation importante du FDCA lors de la synthèse de PA 6-F qui empêche fortement l'augmentation de la masse molaire du polymère lors de sa synthèse, donnant lieu à des propriétés thermiques inférieures à ce que l'on pourrait attendre de ce polymère (grâce à la modélisation).

***

Acknowledgements

Je tiens tout d'abord à remercier les professeurs Jean-François Gérard et Etienne Fleury, directeurs du laboratoire IMP ingénierie des matériaux polymères, pour m'avoir permis d'effectuer ces travaux de thèse au sein de ce laboratoire.

Je souhaite ensuite remercier chaleureusement mes encadrants de thèse Jocelyne Galy, Jérôme Dupuy et Alain Rousseau pour leurs précieux conseils et le soutien qu'ils m'ont apportés. Je tiens tout particulièrement à remercier Alain Rousseau pour son aide indispensable pour l'utilisation du pilote de synthèse. Je souhaite enfin les remercier de la confiance qu'ils m'ont faite lors de ces trois ans.

Je voudrais également remercier les différents partenaires du projet ANR Polyglu pour leurs conseils et suggestions lors de nos réunions. Je tiens à remercier l'équipe de l'IRCELyon et plus particulièrement Nadine Essayem qui était la coordinatrice de l'ANR, mais aussi Franck Rataboul, Rodrigo Lopez de Sousa et Bui Ngoc Quynh. Je voudrais également remercier Jean-Luc Couturier et son équipe chez Arkema pour son expertise.

J'adresse mes remerciements aux rapporteurs de ces travaux de thèse : les professeurs Alessandro Gandini et Jean-Jacques Robin, qui ont accepté de prendre le temps de corriger ce manuscrit et de leurs remarques constructives lors de la soutenance.

Je souhaite remercier les personnes qui ont contribués à cette thèse :
– Je service de RMN de l'IMP : Fernande Boisson, Cécile Chamignon et Annick Waton pour leur aide précieuse dans l'analyse de mes spectres RMN.
– Catherine Ladavière pour le MALDI-TOF.

J'aimerais enfin remercier tous les membres de l'IMP avec lesquels j'ai passé ces trois années pour leur bonne humeur qui a fait passer ces trois ans incroyablement rapidement. Je souhaite plus particulièrement remercier les doctorants et post-doctorants avec lesquels j'ai partagé mon bureau durant toute cette thèse : Florent, Gino, Emilie, Nicolas, Racha, Floriane, Marie, Benjamin, Mohamed pour ces grands fou rires et tous ces bon moments passés avec vous.

Mes derniers remerciements vont à ma famille et mes amis qui ont toujours été là dans les bons moments comme dans les moments de découragement. Merci à eux.

Merci

Thibault Cousin

Contents

Nomenclature

CPU   Central Processing Unit

ΔH_c Heat of polymerization

DFT   Density Functional Theory

DMA   Dynamic Mechanical Analysis

FDCA   Furan-2,5-dicarboxylic acid

FDCE   Furan-2,5-dicarboxylic ester

GPU   Graphics Processing Unit

HMDA   Hexamethyle diamine

HMF   5-hydroxymethyl-2-furancarboxyaldehyde

IPA   Isophthalic acid

MC   Monte Carlo simulation

MD   Molecular Dynamics simualtion

PA6F   Poly(hexamethylene furamide)

PA   Polyamide

PA 6-I   Poly(hexamethylene isophthalamide)

PA 6-T   Poly(hexamethylene terephthalamide)

PA MXD-6   Poly(metaxylylene adipamide)

PPA   Polyphthalamide

PTFE   Poly(tetrafluoroethylene)

QSAR   Quantitative Structure-Activity Relationships

QSPR   Quantitative Structure-Property Relationships

SSP   Solid-State Polymerization

TFAA   Trifluoroacetic anhydride

T_g Glass transition temperature

TGA   Thermogravimetric analysis

T_m Melting temperature

TPA   Terephthalic acid

List of Figures

25

List of Tables

Introduction

The general goal of this study was to synthesize and characterize polyamides materials based on 2,5-furandicarboxylic acid. This monomer has been pointed out as one of the possible biobased alternative to the terephthalic or isophthalic acids. In order to study these new materials a first step will consist in the development of a molecular modelling protocol able to study and predict polyphthalamide properties, then it will be used to study and calculate the expected properties of biobased polytamides and finally the materials will be synthesized and characterized.

Context of the study

With the rarefaction of the oil stocks in the world, a lot of researches are being conducted today on biobased polymer materials. Within these biobased polymers, a class of "bio-polyamides" have been successfully commercialized, mainly PA11 based on 11-aminoundecanoic acid, a biobased monomer derived from castor oil. This polymer is a good engineering polymer but has a glass transition temperature of 45°C which does not allow its use in high temperature applications. Within this context, the search for high performance biobased polyamides is of major importance. High modulus amorphous polyamides based on isophthalic acid (so-called meta-polyphthalamides) have been known for long, but today there is no oil-free alternative to these high-performance polyamides. Achieving the synthesis of such a material is then our goal for this study.

Moreover, the growing interest for the preparation of non-petroleum chemicals has naturally led to the development of the non-food transformation of carbohydrates, which is the most abundant source of renewable materials on earth and among them furanics may be of interest for the preparation of polyesters or polyamides. Indeed there are several monomers derived from furan that could be used to make polyamides in the form of diamines, diesters or diacids. Polyamides made from these monomers have been known for years but a lot of effort is now made on research on the potentially biobased ones.

In this thesis we focused on the biobased monomer 2,5-furandicarboxylic acid (FDCA), which has been assessed to be among the most viable biobased building block for a green polymer industry by the U.S. Department of Energy. Indeed this monomer could be an alternative to the phthalic acids widely used in the polymer industry such as terephthalic and isophthalic acids.

Another interesting point is that the literature on polyamides containing a furan ring is not abundant and mainly of qualitative nature. It was reported that the melting point, glass transition temperature, inherent viscosities or molecular masses vary considerably from one study to the other. Moreover, some previous studies pointed out the low thermal stability of the FDCA, as well as several problems when trying to make polymers with it (reactivity, thermal stability, low molecular weight polymers). All these facts motivated us to study and extensively characterize a series of copolyphthalamides based on FDCA.

Also, usually the process that leads to development of a new material starts with several steps of chemistry optimization, choice of the monomers, etc., followed by an extensive characterization of these polymers. This process is time-consuming and has a substantial cost. In addition, in nowadays situation of quick development of new biobased polymers, a large screening of monomers is required. This is a common new trend of research in polymer and material science, and lot of companies and academic laboratories (including ours) are currently working on this subject.

Simulating polymer properties is considerably less time- consuming than preparing real systems and, therefore, a-priori simulations would allow the development of new materials according to the output of those simulations. In order to speed up this process, recent developments in molecular modelling and computer simulations can be a useful tool. And this tool will be used to predict properties of biobased polyphthalamides prior to their synthesis and characterization.

This study has been carried within a project called "From glucose to polyamide: new processes for hydroxymethylfurfural production and conversion" (acronym "PolyGlu"). The PolyGlu project was financed by the French ANR (Agence Nationale pour la Recherche) and involved three partners:

– IRCELyon (Université Lyon I), a CNRS laboratory, specilized in catalysis, was in charge of the selective conversion of glucose into hydroxymethylfurfural (HMF) through the use of a new generation of solid catalysts.

– Arkema, a french polymer and chemical company, was in charge of the transformation of HMF into FDCA or its derivatives, through clean and industrial catalytic processes.

– IMP@INSA, was our laboratory in charge of the synthesis and modelling of polyamides based on FDCA.

Study approach

The approach of this study will consist of three main parts, corresponding to the three chapters of this thesis:

1. The chapter 1 is a summary of the state of the art concerning the polyamides synthesis and properties and especially polyphthalamides. A focus was also put on the existing studies on the FDCA based polyamides.

2. In the second chapter, a molecular modelling protocol was developed. In order to do this, model polyphthalamides based on terephthalic, isophthalic acids and hexamethylene diamine were synthesized and characterized as well as simulated. The comparison between the simulation and experimental results will prove the accuracy of this modelling protocol.

3. In the chapter 3, the molecular modelling protocol was applied on FDCA based polyamides. A series of copolymers based on FDCA, isophthalic acid and hexamethylene diamine where synthesized and extensively characterized.

Chapter 1

State of the art

Contents

The purpose of this chapter is to introduce the subject of the thesis and to give the reader ideas about the state of the art on the synthesis and characterization of polyamides (PA), polyphthalamides (PPA) and finally on the various techniques of molecular modelling. There will be some historical background described as well as the basic theories needed to understand this thesis.

1 Polyamides

1.1 Historical background

The poly(ϵ–caproamide) was the first polyamide obtained in the history. It was synthesized in 1889 by heating ϵ–aminocaproic acid. In 1927, the two first research groups in fundamental macromolecular chemistry were founded by IG-Farbeindustrie in Germany and DuPont in the United-States. One of the main contributor of this newborn field of science was Wallace Hume Carothers. In 1929, he started the systematic study of the synthesis of a wide variety of polyamides. His work led to the production of several patents on the synthesis of PA starting from amino-acids. He quickly showed the interesting properties of these new materials in the form of textile fibres. He prepared for the first time PA 6-6.

Several patents were published in the following years on the preparation of PA starting from diamine and diacids, with aliphatic, aromatic or alicyclic structures. In 1937 in the USA, the first women stockings were woven from PA 6-6 prepared in

the lab and in the next year, the polycondensation and the spinning of PA 6-6 were developed on a pilot scale.

The industrial development of the PA 6 and PA 6-6 underwent a strong acceleration during the World War II, since these materials were an alternative to silk which became scarce and was used for the manufacturing of parachutes as well as vehicle tires. DuPont started the industrial production of PA 6-6 under the tradename of Nylon®, quickly followed by IG-Farbeindustrie for the PA 6. In 1941, the PA 6 production started in Japan with the german technology of IG-Farbeindustrie. As the war was over, the customers discovered nylon stockings, underwear and shirts. In 1950, 14 industrial plants in 10 countries were producing approximatly 55 kT of PA 6-6 and PA 6. Slowly, other application than textile appeared:

- nylon-bristled toothbrush
- moulded plastic part in replacement of metal or thermoset resins
- extruded films, plates, pipes, etc.
- thermosealable adhesives
- powder for metal coatings, that led to the development of PA 6-10, PA 6-12 or PA 12

In 1940 in France, M. Genas, M. Kastner and J. Zeltner prepared the first grams of amino-11-undecanoic acid, and the corresponding polymer, the PA 11, was commercialized in 1955.

During the first years of their use, PA were mainly a silk substitute and used in textiles. However in the following years of development, the virgin aliphatic polyamide resins became reinforced materials, filled, plasticized, and blended with other plastic materials to extend their properties and possible uses. More than fifty years after their first industrial applications, polyamides still have an extraordinary vitality if we consider the continuous introduction of new types and grades (homopolymers or copolymers, aliphatics or aromatics, random or block, crystallines or amorphous, in blends, as fibers, filled, etc.). All this improvements aim to offer the widest range of properties at the best price.

1.2 Chemistry

1.2.1 General considerations

The amid group (Figure 1.1) is made of 4 main atoms. A carbon atom twice bounded to an oxygen atom and to a secondary nitrogen. A polyamide is then a molecule containing a large number of amide groups.

Four main routes are used for the synthesis of polyamide:
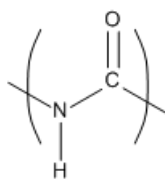
Figure 1.1: Amide group.

  – polycondensation of diamine and diacids (Figure 1.2), or AABB type.
  – interfacial polycondensation of a diamine and an acyl chloride (Figure 1.3), or
    AABB type.
  – polycondensation of amino-acides (Figure 1.4), or AB type.
  – polyaddition of lactams (Figure 1.5), or AB type.
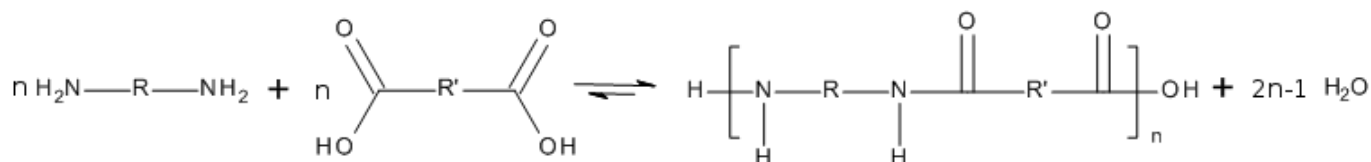
Figure 1.2: Synthesis of a polyamide starting from a diamine and a diacid (AABB).
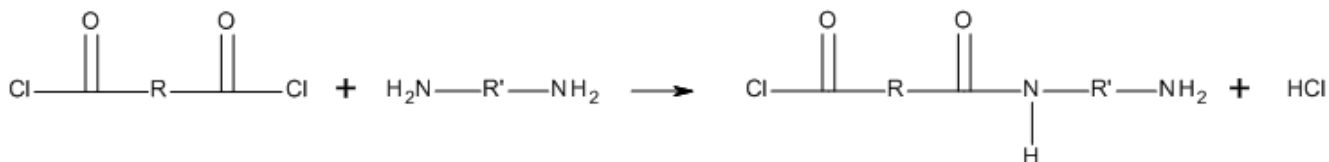
Figure 1.3: Synthesis of a polyamide starting from an acyl chloride and a diamine (AABB).
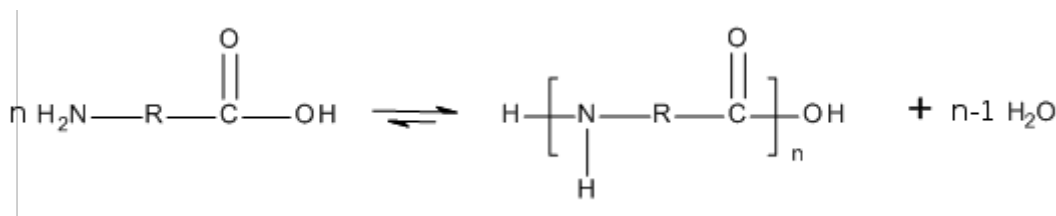
Figure 1.4: Synthesis of a polyamide starting from an α,ω-amino-acid (AB).

    The polyamides synthesized from two different monomers, a diamine and a
diacid, are named PA x-y. In this convention, x is the number of carbon in the
backbone chain of the diamine and y the number of backbone carbons in the diacid
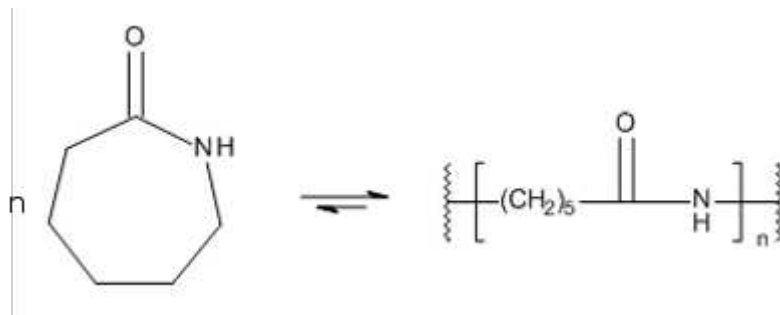
Figure 1.5: Synthesis of a polyamide 6 starting from caprolactam (AB).

molecule. So the polyamide 6-6 is synthesized from the reaction between the 1,6-hexanediamine (or hexamethylene diamine – HMDA) and 1,6-hexanedioc acid (or adipic acid) [1].

When an aromatic monomer is introduced in the polymer, the number of carbon in the nomenclature is replaced by a typical abbreviation for the monomer. As an example, the polymer made by the condensation of terephthalic acid with hexamethylene diamine will be called PA 6-T, where the T stands for terephthalic acid. Another example would be the poly(hexamethylene isophthalamide) PA 6-I, made by the condensation of HMDA with isophthalic acid.

The polyamides synthesized from amino-acids or lactams are named PA X , where X is also the number of carbon atoms in the backbone of the monomer chain.

1.2.2 AABB type polyamide chemistry

Salt formation The usual AABB type polyamide is synthesized through the reaction of a diacid and a diamine, plus several additives. The diacid intermediates are generally crystalline powders, with high melting points, whereas diamines are usually liquids or hard-to-handle solids (melting points in the range 0-60°C). This fundamental difference between the physical state of the two monomers may lead to problems when mixing them directly.

The usual industrial process for the manufacture of this type of PA uses a ionic salt solution of the monomers instead of the monomers by themselves, see figure 1.6. Indeed, an aqueous solution of the monomers could be handled much more easily. As the diacid and diamine chain length increases, the solubility in water of the corresponding salt deacreases. For example, hexamethylenediammonium adipate (the PA 6-6 salt), can easily be handled as a 50 % solution at 50°C, whereas PA 12-12 salt is essentially insoluble.

Moreover, the measurement of the pH is a simple method to monitor the reaction stoichiometry, since amines are weak bases whereas the diacids used are also weak
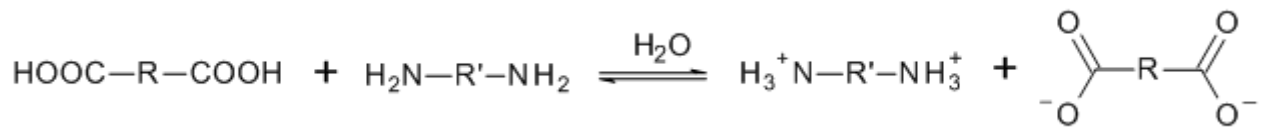
Figure 1.6: Formation of a PA salt.
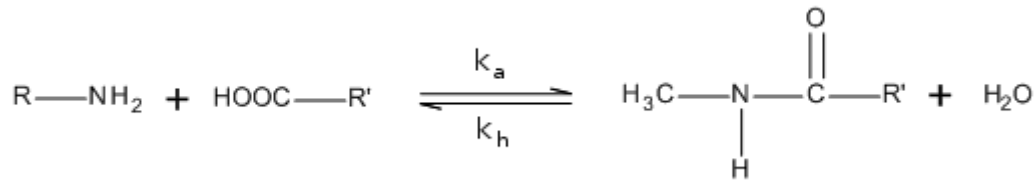
Figure 1.7: Polycondensation equilibrium

acids. When the two components are mixed in water, an acid/base equilibrium takes place. At the equivalence, i.e. a 1:1 stoichiometric ratio between diacid and diamine, the pH is approximately equal to (Eq. (1.1)):

$$pH_{equivalence} = \frac{\log K_B - \log K_W - \log K_A}{2} \tag{1.1}$$

where K_W is the dissociation constant of water and K_A and K_B are the second dissociation constant of the acid and base (diamine). The equivalence pH of dilute 6-6, 6-9, 6-10 and 6-12 salts is about 7.6 [2].

It is also possible to use a diester instead of a diacid for the synthesis of AABB type polyamides. In this case, there is no salt formation step. The reaction occurs directly between the diester and the diamine, and instead of releasing water, the reaction could release methyl or ethyl alcohol.

Polycondensation equilibrium Polycondensation of polyamides is an equilibrated reaction, meaning that the reaction could go towards the formation of the polymer (the polymerization) or backwards to the monomers (depolymerization). The general equation of the polycondensation is showed on figure 1.7, where k_a is the reaction constant of the amidation and k_h the reaction constant of the hydrolysis.

The equilibrium constant K_c of the polycondensation is the following (Eq. (1.2)):

$$K_c = \frac{k_a}{k_h} = \frac{[NHCO]\,[H_2O]}{[NH_2]\,[COOH]} \tag{1.2}$$

Any change in the concentration of the reactants and products will cause the system to change to achieve the ratio equal to K_c, the thermodynamical equilibrium state. For example, if the ratio is smaller than K_c, amidation will take place, and if higher than K_c, hydrolysis will occur. From this equation, it is clear that in order to push the reaction towards polycondensation, i.e. direct reaction, the concentration of water must be kept as low as possible.

Another important point is that polyamidation reaction is an exothermic reaction. Hence, low temperatures favor the polymerization reaction, while high temperatures favor the hydrolysis of the polymer. For aliphatic polyamides, in general the heat of polymerization ΔH_c averages around -27 kJ/mol [2].

Kinetics   The reaction of polyamidation is a second order reaction, when the conversion is lower than 90%. Above 90 % of conversion, the amount of water is low, as well as the concentration of chain-ends. Moreover, the increasing viscosity of the reaction mixture may lead to heterogeneity of the temperature and several physical phenomena could occur. Some studies have pointed out an apparent third-order reaction above 90 % of conversion with a possible acid catalysis [3–6].

The general equation of the kinetics of the AABB type polymerization in stoichiometric conditions ($[COOH] = [NH_2]$) is showed on equation (1.3).

$$\frac{-d\,[COOH]}{dt} = k_a\,[COOH]\,[NH_2] \tag{1.3}$$

After integration and with $[COOH]_0$ the initial acid concentration, the final kinetic equation of the AABB type polymerization is the following (Eq. (1.4)):

$$\frac{1}{[COOH]^2} - \frac{1}{[COOH]_0^2} = 2k_a t \tag{1.4}$$

In the case of non-stoichiometric conditions, if $[COOH] - [NH_2] = D$, the equation (1.3) becomes:

$$\frac{-d\,[COOH]}{dt} = k_a\,[COOH]\,[COOH - D] \tag{1.5}$$

After integration, the final kinetic equation (1.4) becomes:

$$\frac{1}{D^2} \ln \frac{[COOH]}{[NH_2]} + \frac{1}{D} \frac{1}{[COOH]} = k_a t + C \tag{1.6}$$

where C is an integration constant.

In these rate expression, two important simplifying assumptions have been made [7]:

 – The rate of reaction of a functional group is independent of the size of the polymer chain to which it is attached
 – The reverse reaction (hydrolysis) is neglected. It is only valid for low water content

1.2.3   Interfacial polycondensation between diamines and acyl chlorides

Acyl chlorides (also known as acid chlorides) are carboxylic acids with the OH group replaced by a chlorine atom. Acyl chlorides are not found in nature because they are highly reactive. They are normally formed by nucleophilic substitution of carboxylic acids by PCl_3, PCl_5 and $SOCl_2$.

These acyl chlorides being more reactive than diacids, it is possible to make polyamides at room temperature by interfacial polycondensation between a diacyl chloride and a diamine. One of the major drawback of these polymerization is that the small molecule released during the condensation reaction is not water as in the classic diacid/diamine reaction, but is HCl gaz, which is of course very corrosive and dangerous. Another drawback preventing this technique to be used massively in the industry is the need of important amounts of organic solvents for the solubilization of the acyl chlorides. Generally the solvents used are dichloromethane or cyclohexane.

However, the interfacial polycondensation may be of interest for the synthesis of aromatic polyamides, which fusion temperatures are too high to be able to synthesize them through classic polymerization. Other specific applications may need the interfacial technique, such as the fabrication of nano or micrometer sized capsules for drug delivery [8], or in-situ polymerization of carbon fibers polyamide composites [9].

1.2.4   AB type polyamide chemistry

The synthesis of the AB type PA is made by ring-opening of lactams or the condensation of amino acids.

Polymerization of aminoacids   The condensation of amino-acids is similar to the condensation of a diamine with a diacid, except that the two functionnal groups are on the same molecule. This structural feature prevent deviation from the stoichiometry of the reactants. Thus there is no need to make a salt prior to the reaction. The monomer is just heated up to its melting point (around 190°C for the 11-amino-undecanoic acid, the PA 11 monomer), and the polymerization proceeds

in the melt, with removal of the water produced by the condensation reaction (figure 1.4).

Polymerization of lactams   In the case of the polymerization of lactams, the chemical route towards the polymer is a bit more complicated. The ring-opening and the polymerization of lactams is done by three main reactions:

1. Ring-opening by the hydrolysis of the lactam by water into an amino acid (figure 1.8)
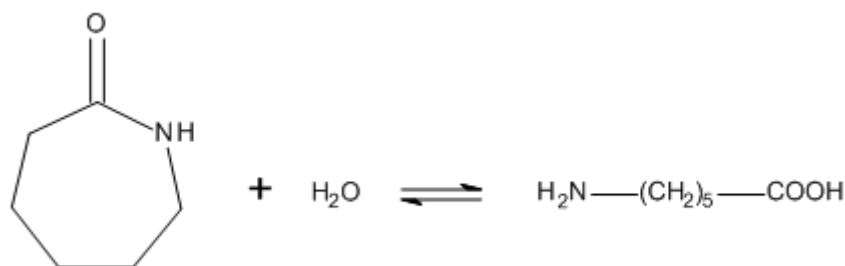
Figure 1.8: Ring-opening of a lactam by water.

2. Condensation of two amino acids, with the elimination of water (figure 1.9)
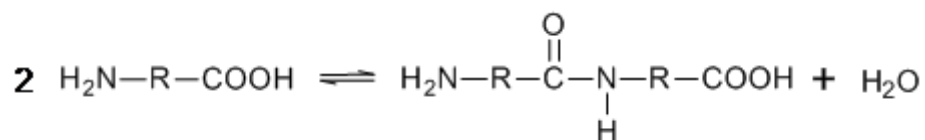
Figure 1.9: Condensation of two amino acids.

3. Addition of a lactam to a polymer chain end (figure 1.10)
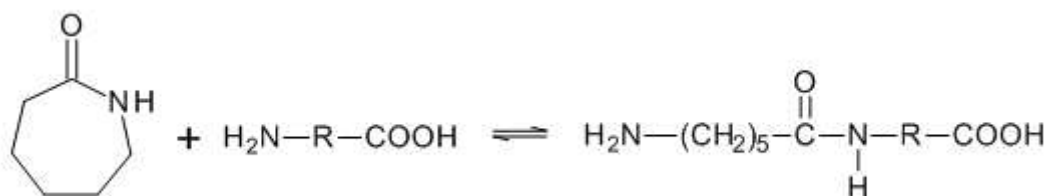
Figure 1.10: Addition of a lactam to a polymer chain end.

At the beginning of the synthesis, when there is a big amount of water in the reaction mixture, it is the second reaction (figure 1.9) that is predominant. However,

when the water is removed from the reactor and the water amount drops to less than 5 %, it is the third reaction (figure 1.10) that dominates.

The reaction between the two aminoacids is the reaction which controls the final molar mass of the polymer. It could be catalysed by acids. Some complications may arise when there is an equilibrium between monomer, cyclic oligomers and the polymer. This is particulary the case for the synthesis of PA 6, where a cyclic oligomer equilibrium is significant. Rings incorporating up to nine caprolactams units have been detected [10]. These cyclic oligomers needs to be removed from the reaction mixture in order to continue the reaction. This supplementary step may lead to problems on an industrial point of view.

Kinetics   The kinetics of the polymerization of AB type PA is close to the AABB type one. Indeed, the only changes that should be done in the equations is that $[COOH] = [NH_2]$ always, because the two functional groups are supported on the same molecule. This cancels all stoichiometry problems. However one should be cautious when dealing with the kinetics of the lactam polymerization. As showed above, three reactions are involved in this polymerization, not only the condensation of amino-acids. This two supplementary reactions have to be taken into account.

1.2.5   Additives and fillers

Besides dyes and pigments, a wide variety of additives could be incorporated into polyamides, either during the polycondensation, during the extrusion process or during the drying [11]. All this additives are added to the polymer material in order to improve several of its properties such as:

– resistance to oxidation in hot conditions or to outdoor weather: antioxidants, UV scavengers
– processing aids: demolding agents, internal or external lubricants
– fire behaviour: flame and fire retardants
– creep and stiffness resistance: fibers and reinforcing fillers, nucleating agents
– flexibility: plasticizers and elastomeric modifiers
– impact resistance: elastomeric modifiers

In order to be efficient, these additives should be finely dispersed in the polymer matrix, and have a good affinity with it.

According to the desired functions for applications, it is possible to incorporate in polyamides fibers and other reinforcing agents, for instance to optimize:

– rigidity, mechanical strength and heat distortion temperature under load: glass fibers, titanate, carbon, ceramics

– dimensional stability under heat and the thermal coefficient of expansion, while limiting the warping of the moulded objects: mineral fillers such as glass beads, silicates (talc, mica), calcium carbonate

– friction coefficient: graphite powders, bronze, molybdenum disulfide, poly (tetrafluoroethylene) (PTFE)

– electrical properties: powders and carbon fibers, metal fibers.

Another method for improving the properties of the polyamides is to blend them with other polymer materials such as polyolefins (to decrease their water absorption), elastomers (to increase their impact properties), etc.

1.3 Properties

1.3.1 Physical properties

Density Polyamides have a density that could go from 1.04 to 1.15 (for the PA 6), depending on the crystallinity ratio. They are generally translucent or opaque depending on the thickness of the material. However they could also be transparent under certain conditions, i.e. amorphous PA are transparent.

Water absorption Polyamides are very moisture sensitive. Because of their chemical structure, the amide group tends to form high hydrogen bonding with water. So the material absorbs a big amount of water which acts as a plasticizer for the PA. In normal conditions and about 50 % of humidity, polyamides absorb around 2.5% of water (in weight), as shown on table 1.1, which changes their mechanical properties [11].

In this table, the water uptake in several hygroscopic conditions are displayed for aliphatic polyamides (4-6, 6-6, 6 and 11) as well as for semi-aromatic polyamides such as PA 6/6-T (copolymer made from the condensation of caprolactam and hexametylene diamine with terephthalic acid), PA 6-I (made from the condensation of hexamethylene diamine with isophthalic acid) or the PA MXD-6 (condensation of metaxylene diamine with adipic acid).

The rate of moisture pickup depends on the polyamide type, temperature, the crystallinity and the thickness of the material. It is roughly proportional to the square of the thickness and decreases with increasing relative humidity.

The amount of water absorbed at the equilibrium depends on the methylene/ amide ratio ($CH_2/CONH$). Indeed, by increasing the number of amide groups in the polymer chain, the number of possible hydrogen bonding between the PA and water increases. This explains why the PA 4-6 is one of the most hygroscopic material whereas PA 11 is one of the less water absorbing material. This water

PA	Percent water absorbed at 23°C	
	50% RH	100% RH
4-6	3.8	15.0
6-6	2.5	8.5
6	2.8	9.5
11	1.0	1.9
6/6-T	1.9	6.0
6-I	2.0	6.0
MXD-6	1.9	5.8

Table 1.1: Water absorbtion of some polyamides [2].

absorption is reversible, so the PA material has to be dried before melt processing, in order to avoid its hydrolysis.

Resistance to chemicals and solvents   Polyamides have a good resistance to aliphatic and aromatic solvents, engine fuels (use of PA 12 as car gas tank), lubricants, oils and aqueous solutions of many inorganic chemicals (such as inorganic salts). Polyamides exhibit a moderate resistance to mild base solution, but only a limited resistance to acids, phenols, oxidizing agents and a few chlorinated hydrocarbons (especially at high temperature) [2]. The best measurement and assurance of chemical resistance of PA comes from their numerous successful commercial applications, as injection moulded parts, films and fibres in exposition to gasoline, grease, oils and salts.

Crystallinity   The presence of the polar amide groups allows hydrogen bonding between the carbonyl and NH groups in adjacent sections of the polyamide chains. For common polyamides such as PA 6-6 and PA 6, the regular spatial alignment of amide groups allows a high degree of hydrogen bonding to be developed when chains are aligned together, giving rise to a crystalline structure in that region with typically a 40-50 % degree of crystallinity. These polyamides are semicrystalline materials that can be thought as a combination of ordered crystalline regions and more random amorphous areas having a much lower concentration of hydrogen bonding. This semicrystalline structure gives rise to the good balance of properties [12]. Polyamides 11 and 12, which have more methylene groups between the amide functions, have a

lower crystallinity degree of about 20 to 30 %

The crystalline regions contribute to the stiffness, strength, chemical resistance, creep resistance, temperature stability, and electrical properties; the amorphous areas contribute to the impact resistance and high elongation at break.

The crystallinity can be disrupted by substituents on the chains that interfere with the alignment process. Amorphous polyamides are produced by deliberately engineering this effect, eg, PA 6/3-T or PA T/MD-T, which uses trimethyl-substituted hexamethylenediamine isomers combined with terephthalic acid. The introduction of isophthalic acid (a meta isomer of the terephthalic acid) also disrupt the alignment of the hydrogen bonds and gives rise to amorphous polyamides.

Electrical properties   Polyamides are reasonably good insulators at low temperature and when the humidity level is low. Injection moulded parts are used in a variety of connectors, terminals, harness and many other devices. These parts are used in low-frequency, moderate voltage applications, that need reasonable dielectric properties but good mechanical, thermal and chemical properties.

The main differences in the PA dielectric properties are related to the amount of water they can absorb. Their volume resistivity is in the scale of 10^{15} ohm.cm when dry, but it can drop by as much as 6 orders of magnitude at 50% relative humidity for the most moisture sensitive polyamides. PA dielectric constant is in the order of 4 (at 100 Hz) when dry, but could increase up to 22 (at 100Hz) for the PA 4-6 at 50% RH [2].

1.3.2   Mechanical properties

Generally, polyamides have a high mechanical resistance (see table 1.2), and in particular a good creep resistance at room temperature. They are rigid materials, especially the aromatic PA, with a good resistance to cyclic stress [13].

The mechanical properties of PA change in function of their water content as said previously. When they are dry, they are more brittle materials but when they have a higher amount of adsorbed water, they have a plasticized polymer material behaviour.

1.3.3   Thermal properties

Polyamides having a stereoregular structure are generally crystalline and have a sharp fusion, with a low viscosity in the molten state. The usual PA have a melting temperature of about 200°C or more and a glass transition temperature around 50-70°C (see table 1.3). These high glass transition and melting temperatures make

PA good materials for high temperature uses [13].

The methylene chain length of the polyamide has an influence on its melting temperature. Indeed, the methylene/amide ratio is an important parameter that has a big influence on the thermal properties of polyamides, as showed on figure 1.11.

Among the PA derived from α, ω-aminoacids or the corresponding lactams, those having an odd number of chain atoms (PA 7) have higher metling points than those having an even number of chain atoms (PA 6). Polyamides derived from the condensation of diacids and diamines generally have high melting points in the case of even-even (PA 6-10). When one of the monomer has an odd number of carbon atoms, the melting point of the corresponding polymer drops significantly (PA 6-9). These differences come from the alignment of the hydrogen bonds in the polyamides, granting them their high cohesive energy and then their high melting points (Figure 1.12). When the AABB type PA has an odd number of carbons, the alignment is disrupted and the melting point drops significantly.

The melting point of PA is reduced by the introduction of methyl branches or N-alkylation. This branches prevent ordering of the polymer chains in the form of crystallites and thus decrease the crystallinity of this polyamides. Introducing aromatic p-phenylene groups increase the melting point of these PA. However, the introduction of m-phenylene linkage decreases the melting point of polyamides. In order to tailor the melting point of the synthesized polyamides, it is possible to copolymerize polyamides from different monomers.

Properties	Units	PA 6	PA 11	PA 12	PA 6-6	PA 4-6	PA6-10
Stress at break	MPa	80	60	55	85	100	70
Strain at break	%	50	300	250	45	30	50
Yield modulus	MPa	3200	–	1450	2800	3300	1500
Flexural modulus	MPa	2200	1000	1400	2840	3300	2500

Table 1.2: Mechanical properties of some usual polyamides [13].

Properties	Units	PA 6	PA 11	PA 12	PA 6-6	PA 4-6	PA6-10
T_m	°C	220	185	175	260	295	215
T_g	°C	50-60	46	37	57	80	50

Table 1.3: Thermal properties of some usual polyamides [13].
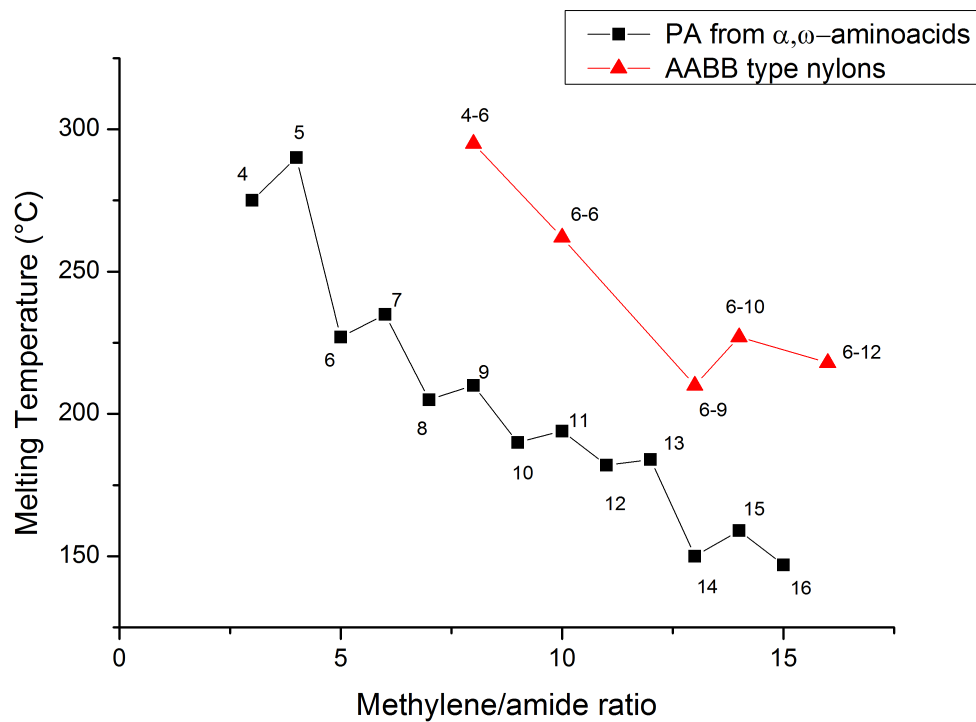
Figure 1.11: Melting temperatures of aliphatic polyamides [13]
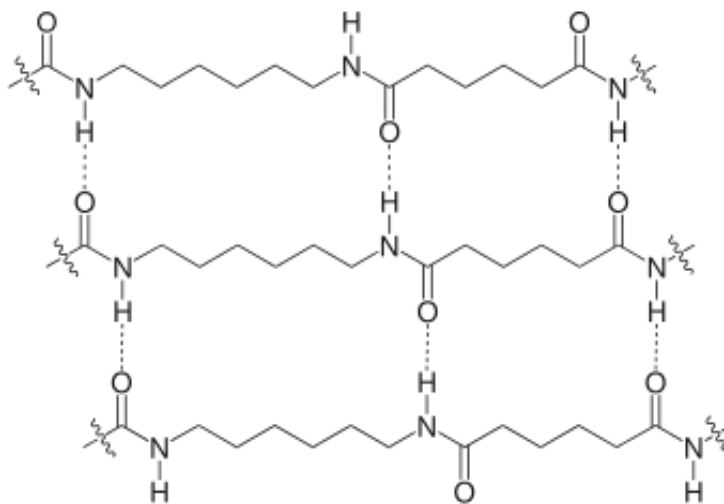
Figure 1.12: Polyamide 6-6 struture

1.4 Processing of polyamides

Polyamides are thermoplastics that could be processed by several methods. The common requirement for all process methods is that the polyamide powder or pellets have to be dried before processing, in order to avoid hydrolysis during all the time where the PA is melted. The main techniques used for polyamides processing are injection molding and extrusion. However other techniques are available such as blow molding, rotomolding or RTM (Resin Transfer Molding) for composites forming.

1.4.1 Injection molding

Injection molding is the main method used for the processing of polyamides materials (nearly 60 % of the polyamide materials objects produced were injected [12]). Polyamides have a sharp melting and a relatively low melt viscosity and this has to be taken into account when making molds. The general temperature range for the processing of several polyamides is shown on table 1.4 [14].

Polyamide	Process temperature (°C)	Mold temperature (°C)
PA 6	250-290	80
PA 6-6	290-300	80-100
PA 4-6	315	120
PA 6-10	270	80
PA 11	210-260	80
PA 12	200-250	70-80
PA MXD6	250-280	130
Polyphthalamides	327-332	135-150

Table 1.4: Injection-molding process temperatures for different polyamides [14]

Significant mold shrinkage occurs with PA, mainly on account of the increase in density with crystallization. This can give rise to voiding and sink marks in moldings. The dimensional stability can be much improved by using reinforcing agents or nucleated materials.

1.4.2 Extrusion

Extrusion accounts for about 30% of polyamide produced and is used in various processes. Most extrusion operations require high viscosity (high molar mass) PA in order to give a high melt strength to maintain the shape of the extrudate. Generally

PA are extruded in the form of pipes, films or profiles. They can also be co-extruded in order to coat another polymer material such as PVC for example.

2   Polyphthalamides

2.1   Introduction

Polyphthalamides (PPA) are situated between usual aliphatic polyamides and fully aromatic polyamides (Aramids, such as Kevlar®). They are made by the reaction between aliphatic diamines and aromatic diacids. Other co-monomers could be used, but usually the term polyphthalamide applies only when at least 55% of the acid part is composed of terephthalic (TPA, Figure 1.13) or isophthalic (IPA, Figure 1.14) acid derivatives [15]. These acids bring an aromatic ring in the polymer chain backbone, which gives the PPA their common name: *semi-aromatic polyamides.*
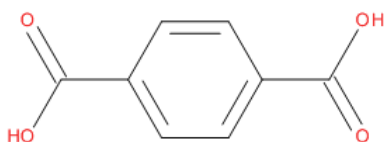
Figure 1.13: Terephthalic acid (benzene-1,4-dicarboxylic acid).
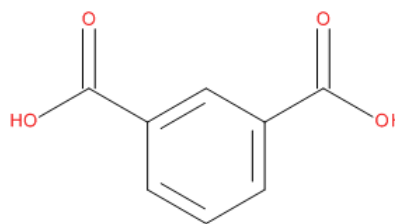
Figure 1.14: Isophthalic acid (benzene-1,3-dicarboxylic acid)

The polyphthalamides could be semi-crystalline or amorphous, depending on the combination of monomers used. Several PPA of each category are commercial products [2]. The semi-crystalline PPA are based on PA 6-T, made from the reaction between hexamethylene diamine and terephthalic acid, with other monomers such as adipic acid. This aromaticity of the TPA gives the polymer chain a rigidity that leads to high glass transition and melting temperatures. The PA 6-T has also higher chemical, mechanical and thermal resistances than aliphatic polyamides such as PA 6-6 [16].

When more than 55% of the acid part of the polymer is made of isophthalic acid, the resulting material is amorphous [17]. Amorphous materials tend to have lower mechanical and thermal properties, but one of their interesting feature could be their transparency. Indeed, transparent amorphous PPA with a good resistance to stress cracking in contact with chemicals is of great industrial interest [13].

2.2 Synthesis

2.2.1 Chemistry

The chemistry involved in the synthesis of polyphthalamides is the same as the one for polyamides synthesis. Stoichiometric amounts of terephthalic and/or isophthalic acids, aliphatic diamines, additional comonomers, encapping agents, etc. are mixed with catalyst (if any) in water in a reactor. The reaction mixture is then heated and the water is gradually removed, up to the desired viscosity. The major and first PPA that has been synthesized is the PA 6-T. The two monomers are mixed in an autoclave, the temperature is increased and the water which is produced by the reaction is removed (Figure 1.15).
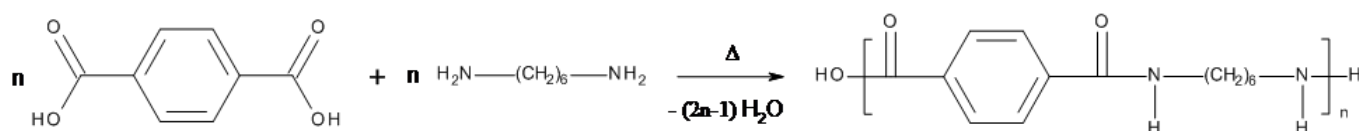
Figure 1.15: Synthesis of PA 6-T

The major problem with this polymer is its very high-melting temperature (370°C), granting good thermal properties but making its processing very difficult (degradation before reaching melting point). Moreover, at 370°C several secondary reactions could happen, leading to branching and decomposition (see 2.2.2 and 2.2.3). Interfacial polymerization is possible and can be carried out at low temperature but is not economic.

A two-step process is more often used in the industry when making polyphthalamides with high melting points (PPA composed of a majority of PA 6-T). The first step consist of the synthesis in autoclave of a low molar mass polymer, which should have the same composition as the final PPA. Then, in a second step, this prepolymer is further polymerized using SSP (Solid-State Polymerization). This SSP is carried out at low temperature (above the polymer glass transition and below its melting-point, usually between 200 to 300°C), under inert atmosphere or vacuum [18].

Other PPA that are processable have been known for long [19–27]. They are based on PA 6-T with co-monomers that lowers its melting point to about 300°C (see Figure 1.16), making the material suitable for injection molding or extrusion processes. An eutectic behaviour is observed for several co-PPA based on PA 6-T [17].
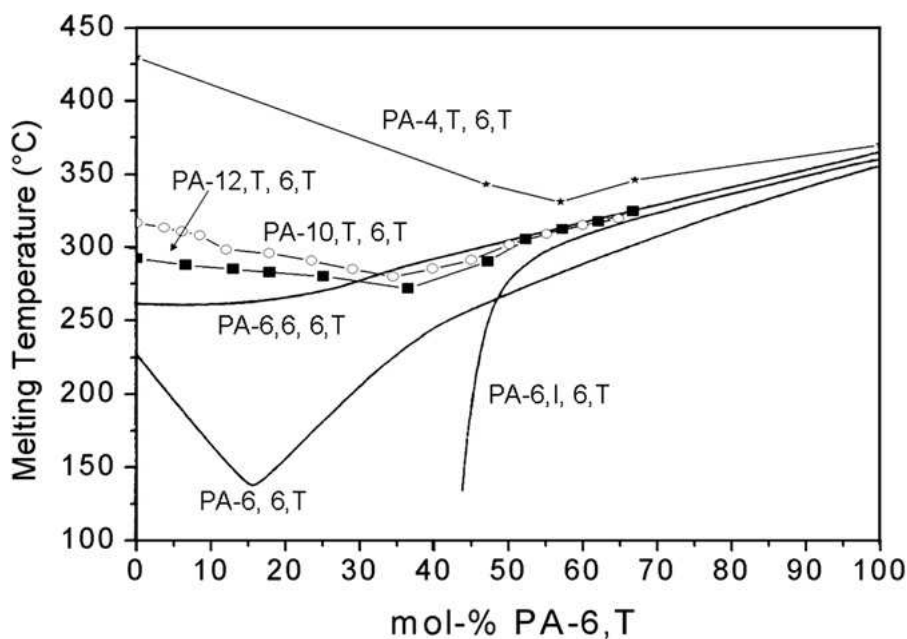
Figure 1.16: Melting point of several copolyphthalamides [17].

These high melting point but still processable polymer materials are of great
industrial interest. Indeed for several applications in the automotive or electronic
industry, a combination of high thermal, mechanical, chemical and electrical resis-
tance is required. These needs could be fulfilled by the use of PPA.

2.2.2   Thermal degradation

The thermal degradation is the degradation that occurs at high temperature and
under the absence of oxygen. This degradation may happen during the synthesis of
polyamides, at temperatures above 250°C, and lead to the thermal decomposition
of the polymer and/or the monomers. Indeed the diacids could suffer a decarboxy-
lation, while diamines could suffer from a deamination. The main products formed
by these decompositions are water, carbon dioxide and ammonia [28].

The reaction that leads to the formation of CO_2 and water takes place between
two carboxylic chain ends (from the polymer or the monomer), and is presented in
figure 1.17.

The stability of polyamides is the reflection of the inherent stability of their
corresponding monomers. Except for the odd-even alternation, the thermal stability
of aliphatic dicarboxylic acids increases with the chain length of the monomer, as
shown on table 1.5.

However, other compounds in the polyamide structure may have much lower
thermal stability and thus decrease the overall stability of the polymer. This is

R—CONH—(CH$_2$)$_5$-COOH **+** HOOC—(CH$_2$)$_5$—NHCO—R'

$\longrightarrow$ R—CONH—(CH$_2$)$_5$-CO(CH$_2$)$_5$-NHCO—R' **+** CO$_2$ **+** H$_2$O
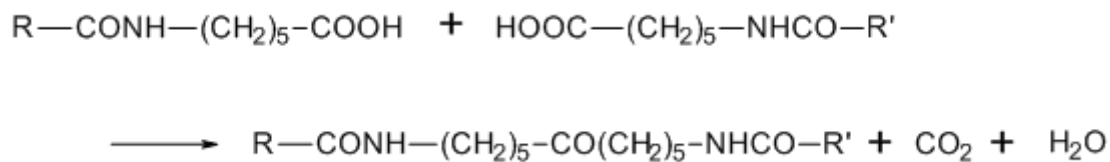
Figure 1.17: Decarboxylation during polyamide synthesis

Name	Number of methylene units	Decarboxylation temperature (°C)
Oxalic	0	166-180
Malonic	1	140-160
Succinic	2	290-310
Glutaric	3	280-290
Adipic	4	300-320
Pimelic	5	290-310
Suberic	6	340-360
Azelaic	7	320-340
Sebacic	8	350-370

Table 1.5: Thermal stability of dicarboxylic acids [28].

especially the case when monomers can cyclize to 5 to 7-membered rings. Succinic acid, glutaric acid, tetramethylenediamine and 5-aminohexanoic acid have a high tendency to form cycles, even when the monomers are part of the polymer chain. Adipic acid and 6-aminohexanoic acid have only a moderate tendency to cyclize, so PA 6 and PA 6-6 are more stable and could be obtained with higher molecular weights than PA 4-4, PA 4-5 and PA 5.

The formation of ammonia during the synthesis of some polyamides could be explained by the following reaction (figure 1.18)

Figure 1.18: Reaction between two terminal amines

2.2.3   Degradation due to the diamines

The diamines, which are volatile compounds, are a major source of degradations, side-reactions, and loss of stoichiometry. Indeed, linear aliphatic diamines have low melting and boiling temperatures compared to the equivalent diacids (see figure 1.19 and table 1.6).

Number of methylene unit	Melting Temperature (°C)	Boiling Temperature (°C)
2	9	116
3	-12	140
4	27	158
5	9	180
6	42	205
7	29	224
8	50	225
9	35	258
10	59	-
12	68	-

Table 1.6: Melting and boiling temperatures of linear aliphatic diamines

This relatively low boiling point of the diamines compared to the temperatures at which the polyamide syntheses are carried out, may lead to a loose of the stoichiometry of the reactants by water steam extraction of diamine during the water removal phase of the PA synthesis [29]. This deviation from the 1:1 stoichiometry
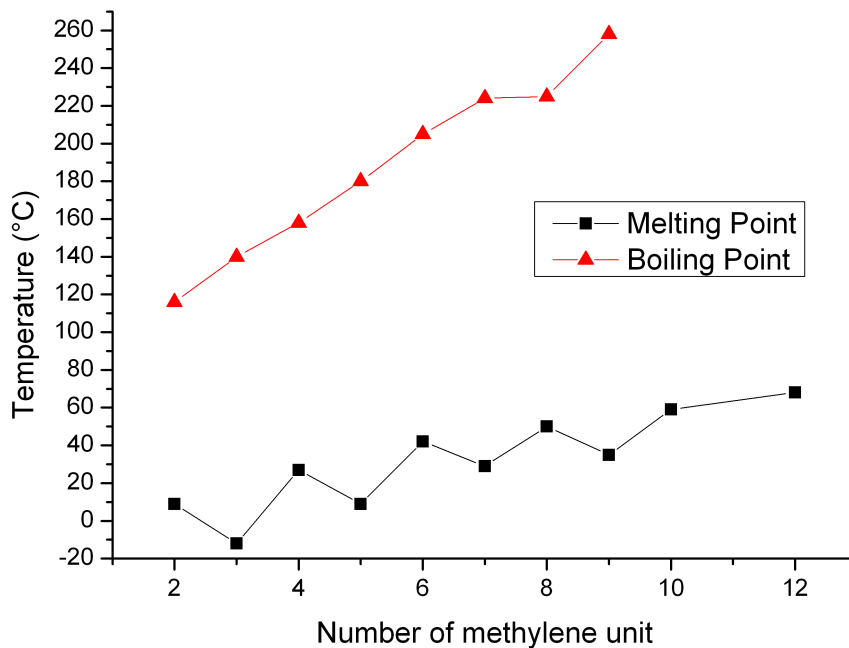
Figure 1.19: Melting and boiling temperatures of linear aliphatic diamines

between diacids and diamines decreases the average degree of polymerization of the final polymer.

2.3 Properties

The copolyphthalamides are being used in several industries such as electronic devices, automotive, packaging or sports articles. Indeed PPA have remarkably high mechanical and thermal strength, which could find uses for example as metal replacement in vehicles in order to reduce car's weight.

A table summarizing the main thermal and mechanical properties of PPA, compared to classical aliphatic polyamides is presented in table 1.7.

Properties	Units	Aliphatic PA			Semi-crystalline PPA			Amorphous PPA
		PA 6	PA 6-6	PA 11	PA 6/6-T	PA 6-T/6-I	PA MXD6	PA 6-I
Density	g/cm^3	1.13	1.14	1.04	1.18	1.18	1.22	1.18
Water absorption (50%RH)	%	2.8	2.5	1.0	1.9	1.7	1.9	2
T_m	°C	215	265	187	295	320	243	–
T_g	°C	50	57	46	110	125	90	125
Stress at break	MPa	80	85	60	100	105	101	110
Strain at break	%	50	45	300	10	10	2	50

Table 1.7: Properties of usual PPA in comparison with classical aliphatic PA. [2, 13]

In this table we can see that polyphthalamides have a higher density (1.18 to 1.22) than aliphatic polyamides. This is due to the stacking of the benzene rings, which leads to dense materials. However, PPA are still light materials compared to ceramics (3-5) or metals (5-10). Polyphthalamides have consequently higher glass transition and melting temperatures compared to aliphatic PA. This feature make them suitable for high temperature applications (around 100°C), where rigid materials are needed (high heat deflection temperatures).

3   Polyamides from furan monomers

3.1   Introduction

The growing interest for the preparation of non-petroleum chemicals has naturally led to the development of the non-food transformation of carbohydrates, which is the most abundant source of renewable materials on earth [30]. Indeed, through photosynthesis (Equation (1.7)), vast amounts of biomass are produced.

$$nCO_2 + nH_2O \rightarrow (CH_2O)_n + nO_2 \tag{1.7}$$
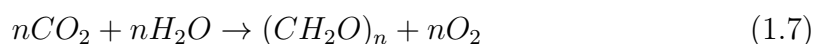
Out of the approximately 170 billion tons of biomass produced every year, 75% are in the form of carbohydrates. Among these carbohydrates, furanics compounds may be of interest in the preparation of non-petroleum based polymer materials such as polyesters or polyamides [31].

Furan derivatives are present in nature in a wide variety of forms and structures. They could be found in living organisms (animals and plants) in small amounts. Their main uses until nowadays, were in the pharmaceutical and fine chemistry industries. But recently, new ways to obtain furan based chemicals from bio-resources (agriculture wastes, etc.) open new possibilities of large scale use for this family of chemicals. These new uses could be as bio-fuel or as reactant for the production of plastic materials.
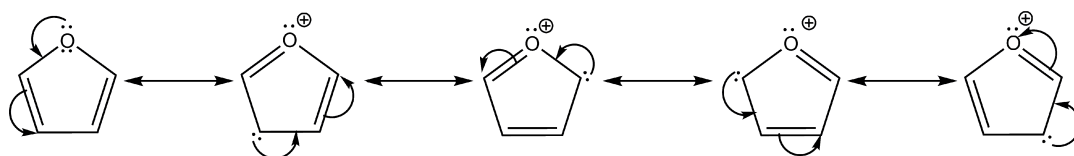
Figure 1.20: Resonance forms of the furan molecule.

The furan molecule is a 5-member heterocycle, which grant this molecule very peculiar chemical properties. Indeed, because of its contributing structures (see figure 1.20), furan is sensitive to nucleophilic substitution reactions — such as alkylations, halogenations, sulphonations, nitrations etc.— regioselectively in C2 and/or C5 positions [32].

In comparison with its heterocyclic equivalents (pyrole and thiophene), the furan present less aromaticity and a much higher dienic behaviour. As a consequence of this dienic nature, furan can undergo quite easily Diels-Alder reactions as shown on figure 1.21 [33–36]. Several applications using the reversible nature of the Diels-Alder

reaction employ furan derivative to make thermo-reversible cross-linked polymer networks.
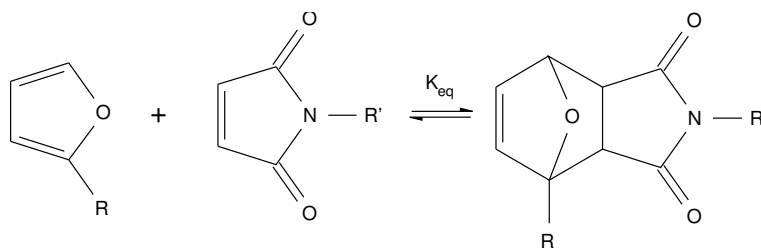
Figure 1.21: Diels-Alder reaction of a furan derivative.

However, when substituting the furan ring with acid in positions 2 and 5, such as the FDCA, the Diels-Adler reaction could not occur anymore.

3.2 Furanics monomers

Because there will be in the next years a rarefaction of the oil resources, a lot of effort is put today on the exchange of the classical monomers (for PPA) to furan-based equivalent monomers, since these monomers could be bio-based [37]. There are several monomers derived from furan and that could be used to make polyamides. They could be diamines, diesters or diacids. Indeed PA made of aromatic diacids, diamines, etc. have been known for years [38].

Two basic furanics monomers are readily accessible from renewable resources: furfural (*2-furancarboxaldehyde*, Figure 1.22) and *5-hydroxymethylfurfural* (also called HMF, Figure 1.23). This two chemicals have been identified as "platform chemicals" for the future transition from oil-based chemistry and material science to a greener chemistry [39].
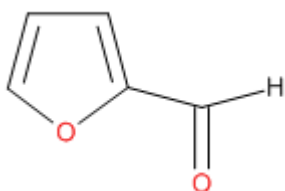
Figure 1.22: Furfural
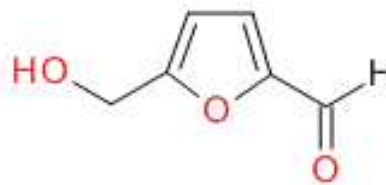
Figure 1.23: 5-Hydroxymethylfurfural (HMF)

From furfural and HMF, a variety of high potential organic chemical interme-diates could be obtained. Among the intermediates derived from furfural, the fur-

furyl alcohol, *2,5-bis(hydroxymethyl)-furan* (figure 1.24) and *2,5-bis(hydroxymethyl)-tetrahydrofuran* (figure 1.25) may be the most interesting chemicals.
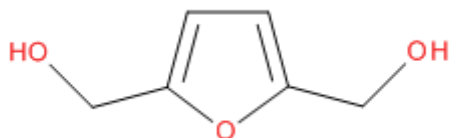
Figure 1.24: 2,5-Bis(hydroxymethyl)-furan
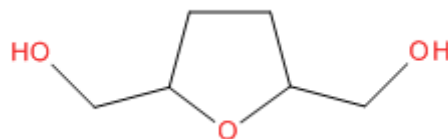
Figure 1.25: 2,5-Bis(hydroxy-methyl)tetrahydrofuran)

In the case of the second platform furanic chemical, HMF has been used for the manufacture of phenolic resins, but the most promising ensuing chemicals are the 2,5-disubstituted furan derivatives. Indeed they could replace their aromatic counterparts, such as terephthalic acid and/or isophthalic acid. In the particular case of the manufacturing of polyamides, two intermediates appear to be of particular interest: the *furan-2,5-dicarboxylic acid* (FDCA, figure 1.26) and its diester counterpart (FDCE, figure 1.27). The diester can be a methyl, ethyl, ester.

These structure seemed to be close to the isophthalic acid structure (Figure 1.14).
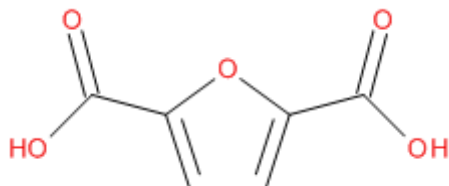
Figure 1.26: Furan-2,5-dicarboxylic acid (FDCA)
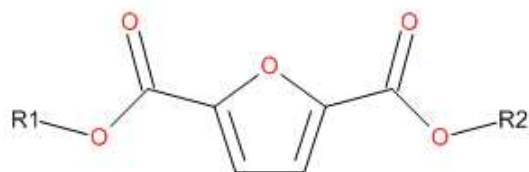
Figure 1.27: Furan-2,5-dicarboxylic ester (FDCE)

Others structures, such as 2,2'-bis(5-chloroformyl-2-furyl)propane (1.28), could also be used to synthesize polymers. Indeed this furanic monomer is readily prepared from commercial furoates and could be used in the synthesis of furanics polyamides [40].

3.2.1 Production of HMF from glucose

HMF is a rather unstable molecule, which can be found in natural products such as honey and a variety of heat processed food, as a product of the degradation of carbohydrates. Several reviews have been recently published on the transformation of biomass to HMF and other chemicals such as furfural [37, 41, 42].
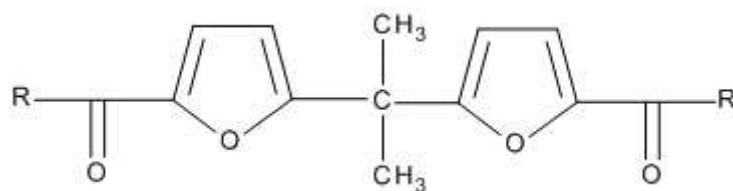
Figure 1.28: 2,2'-bis(5-chloroformyl-2-furyl)propane if R=Cl.

The synthesis of HMF is based on the triple dehydration of hexoses (sugars). The main problem with this synthesis is that it produces a lot of side products alongside HMF (Figure 1.29), and HMF is obtained with a low selectivity and low yield. Indeed if the dehydration is pushed further than a triple one, levulinic acid and formic acid are obtained or by reaction of the HMF with himself, water soluble polymers are obtained. All these side-products are really difficult to separate from HMF since they all are (partially) water soluble polar organic acids or hydroxydes. In order to
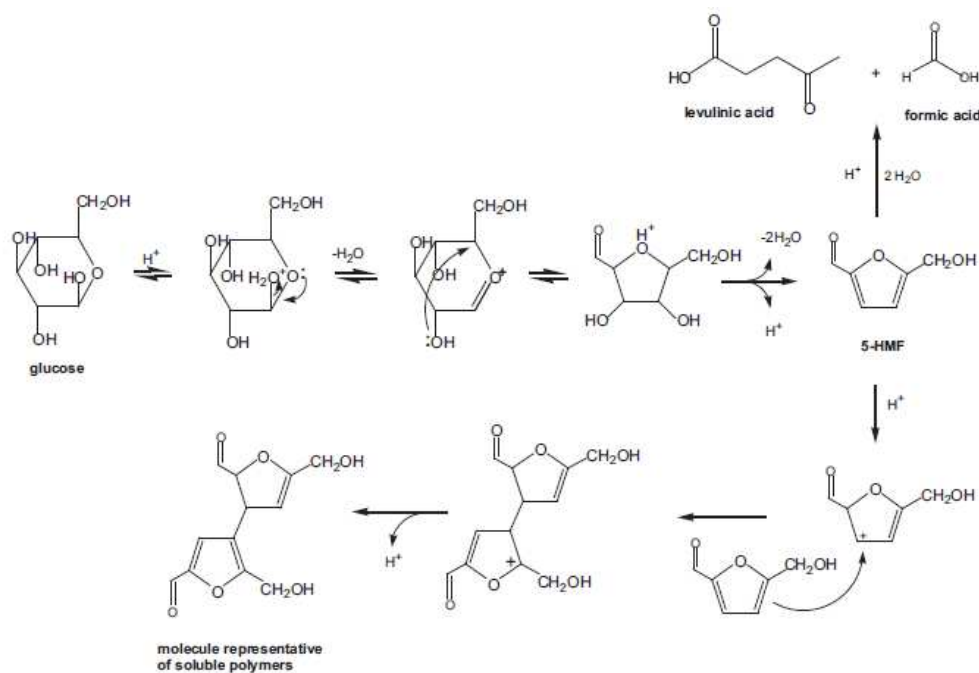
Figure 1.29: Production scheme of 5-hydroxymethylfurfural (HMF) [43]

prevent these side reactions and increase the yield and selectivity of the synthesis of HMF, which could put a curb on the developement of several biobased polymers and chemicals, a lot of research is being carried on that subject. Scientists have thought about changing the reaction conditions or the catalytic system used [37, 44, 45], the process either by using extraction solvents [46] or continuous process [47] or even

micro-wave assisted reactions [48].

3.2.2   Oxidation of HMF into FDCA and FDCE

As we know, one of the goals of HMF is to be converted into FDCA to make polymers. This reaction could be done through the use of noble metal catalysts (carbon or aluminia supported platinium) [49, 50]. In these reaction systems, the oxidation of 5-HMF favorably proceeds to the deep oxidation to diacid when the reaction was performed under oxygen pressure at controlled pH value. The oxidation of 5-HMF in aqueous phase to FDCA was demonstrated with a near-quantitative yield on a Pt/Al_2O_3 catalyst in basic reaction conditions at 60°C [51].

More recently, other teams found that the oxidation of HMF to FDCA could be done with good results with the use of TiO_2 supported gold nanoparticles [52–55]. The partial oxidation of 5-hydroxymethyl-2-furfural (HMF) over the Au nanoparticles supported on TiO_2 resulted in the formation of 5-hydroxymethyl-2-furancarboxylic acid (HMFCA) and furandicarboxylic acid (FDCA) (Figure 1.30). In some reactions, byproducts derived from HMF degradation were observed, this being an indication of the low activity of catalysts for HMF oxidation. In addition, the repeated absence of the 5-formyl-2-furancarboxylic acid intermediate (FFCA) in these experiments confirmed that the oxidation of the hydroxyl group in 5-hydroxymethyl-2-furfural is the rate limiting step of the reaction while FFCA, if formed, is quickly transformed to FDCA .
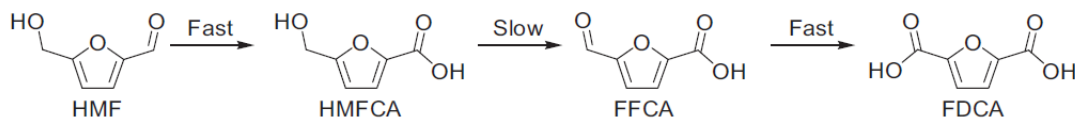
Figure 1.30: Production scheme FDCA [52]

The transformation of raw materials such as glucose or cellulose to HMF and to FDCA has been observed, but the separation of byproducts and the production of good yields in a viable way from an economical point of view still needs a lot of research. Very recently, a dutch company, Avantium, claimed that they found a method for the production of FDCA from raw renewable resources which could compete with terephthalic acid in terms of price. They claimed that their process is a two steps process [56]:

 – The catalytic dehydration of the carbohydrate feedstock in an alcohol, such as methanol, to make Alkoxymethyl-Furfural (RMF), such as methoxymethyl furfural (MMF).

– The catalytic oxidation of RMF in acetic acid to make FDCA.

3.3   Polymerisation

3.3.1   Aliphatic polymers

The synthesis of polyamides using furan derivatives has been known since the 60's. It was studied qualitatively by different groups in Germany [57] and in Japan [58–60]. Recently other studies have been carried out much more extensively on this subject.

Many of these studies showed contradictory results. Some studies claim that polyamides made from FDCA and various aliphatic diamines were amorphous while other studies showed melting points for the same polymers. However all studies agreed on the poor thermal stability of the FDCA.

A study by Hopff and Krieger [61] in 1961 showed the decarboxylation temperatures of several heteroatomic dicarboxylic acids as well as the decarboxylation and melting temperature of the hexamethylene diammonium salts of these diacids. The main results are presented in the table 1.8.

	Acid form		Hexamethylene diamonium salt	
Acid	Tm (°C)	Td (°C)	Tm (°C)	Td (°C)
Adipic	153	286	202	186
FDCA	151	271	261	228

Table 1.8: Melting (Tm) and decarboxylation temperatures (Td) of several acids and corresponding hexamethylene diammonium salts [61]

In this table it is clear that the melting temperature of the diammonium salts are higher than their decarboxylation temperatures. In the case of the FDCA based salt, the melting temperature is 33°C higher than its thermal decomposition. This may lead to several problems during melt polycondensation such as the loss of some monomers and then a loss of stoichiometry. Also partially decarboxylated diacids become monoacids and then prevent the chain growth and so the production of high molar mass polyamides.

According to the paper by Brown [62], two mechanisms are involved in this decarboxylation. It is either a unimolecular (equation (1.8)) or a bimolecular (equation (1.9)) electrophilic substitution of the CO_2 by a H^+ proton in solution.

$$RCOOH \rightarrow RCOO^- + H^+ \rightarrow RH + CO_2 \qquad (1.8)$$

$$RCOOH + H^+ \rightarrow RH + H^+ + CO_2 \qquad (1.9)$$
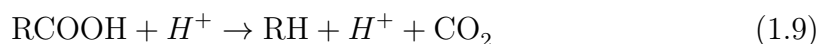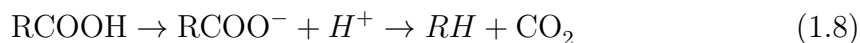
Both mechanisms lead to a RH product which is a nonreactive monomer, preventing the growth of the polymer chain. This decarboxylation has to be avoided at maximum in order to synthesize a material with good properties.

Despite this problem, some research teams managed to synthesize various polyamides with FDCA. They used several strategies to avoid this decarboxylation. One of that comes in mind easily is to choose another chemical path than melt polycondensation. So several teams did interfacial polymerization with 2,5-furandicarboxylic chlorides and various chain length diamines [63, 64]. With this method, high molar mass PPA could be synthesized, such as a 51 000 g/mol (HFIP SEC, PMMA calibration) PA 2-F or a 31 000 g/mol PA 3-F, synthesized by Yutaka and al. at Canon (Japan). However, only glass transition temperatures were measured and not melting temperatures.

Other teams used melt polycondensation or solution polycondensation but starting from the dimethyl (or ethyl) esters of the FDCA. In particular a paper by Grosshardt and al. [65] showed that the reaction between FDCE and aliphatic diamines was possible and they characterized the products. They also compared different polymerisation techniques such as bulk, solution and interfacial polymerisations. In the bulk polymerisation, the reactions where performed using a catalyst: the *(4-chlorobutyl)dihydroxyzinc*. The reactants (FDCE + diamines) where introduced in stoichiometric quantities in order to obtain molar mass as high as possible. The polymerisation was then carried out at 140°C during 2 hours under a 3 bar pressure of nitrogen. This pressure role is to prevent the volatilization of the volatile diamines.

In a second step, the reaction mixture was heated at 180°C during 2 hours, then at 200°C during also 2 hours and finally at 220°C during an hour. These different increases in the temperature came also with a decrease of the pressure to less than 100 Pa for the elimination of the by-products and remaining monomers. The reaction scheme is presented in figure 1.31
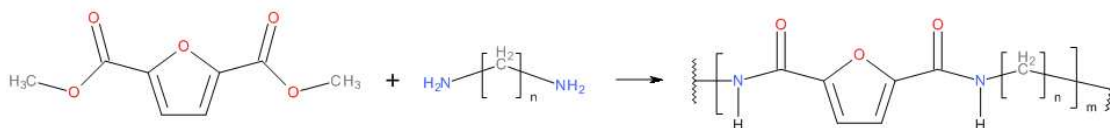
Figure 1.31: Synthesis of aliphatic polyamide from FDCE and various diamines.

The results of this protocol are presented in table 1.9, where PA x-F means the polyamide obtained through the polycondensation of the diamine of chain length x with the FDCE. The noticeable results are that the molar mass of all the polymers synthesized are not very high for PPA (Mn between 5160-7000 g/mol and Mw between 11000-20000 g/mol).

	Diamine	$\bar{M}_n{}^*$(g/mol)	$\bar{M}_w{}^*$(g/mol)	T_g °C	
				DSC	DMA
PA 6-F	1,6-hexanediamine	5160	13845	110	109
PA 8-F	1,8-octanediamine	4299	11130	82	84
PA 10-F	1,10-decanediamine	5266	12748	70	70
PA 12-F	1,12-dodecanediamine	6970	18837	68	71

Table 1.9: Influence of the chain length of the diamine on the molar mass and glass transition temperature [65]. * SEC in HFIP, PMMA standards.
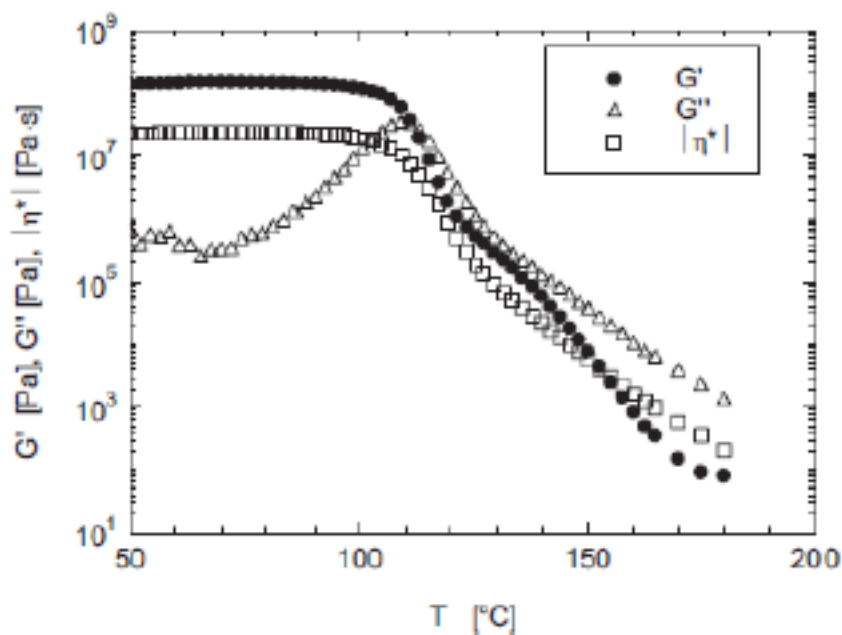
Figure 1.32: DMA analysis of PA 6F.

An example of the analysis of the synthesized polymer is presented in figure 1.32, showing the result of the dynamic mechanical analysis (DMA) of the PA 6-F, where the glass transition temperature of the polymer is observed at 109°C (maximum of G").

Another effect is the decrease of the glass transition temperature as the chain length of the diamine increases, which is normal because it increases the flexibility of the chain and increases the distance between amide groups. All the polymers synthesized in this studies where amorphous polyamides.

So finally despite the unstability of FDCA, making furan based polyamides was achieved. A summary of the melting (for the paper that mention a semi-crystalline polymer) and glass transition temperatures, obtained through these different studies, is shown on the table 1.10.

PA x-F	Synthesis method	Tg (°C)	Tm (°C)	Mn (g/mol)	Mw (g/mol)	Ref
PA 2-F	Solution	206			51000	[63]
	Melt	159			3700	
PA 3-F	Solution	179			31000	[63]
	Melt	150			3200	
PA 4-F			250			[66]
PA 6-F	Melt		175			[57]
			175			[64]
			155-175			[66]
	Melt ester	110		5160	13845	[65]
			175			[64]
	Solution		155			[57]
PA 8-F	Melt ester	84		4299	11130	[65]
	Solution		125			[57]
PA 10-F	Melt ester	70		5266	12748	[65]
	Solution		130			[57]
PA 12-F	Melt ester	68		6970	18837	[65]

Table 1.10: Glass and melting temperatures and molar mass for different FDCA based polyamides

In this table, the "Melt" synthesis method means a classical melt polycondensation between a diacid and a diamine, whereas the "Melt ester" stands for a melt polycondensation between a diester and a diamine. The "Solution" method stands for the polycondensation of a diacyl chlorine and a diamine in solution or interfacial polycondensation.

This table clearly points out the contradictions of the various studies that exist on the synthesis of FDCA based polyamides. Indeed, several studies showed semi-crystalline polymers by measuring melting temperatures whereas other studies where only able to measure glass transitions and not melting temperatures.

An other way of showing these results is displayed on figure 1.33. On this figure, the characteristic temperature of the analogous PA x-T, polymers made of terephthalic acid and various aliphatic diamines, are shown for comparison.

It clearly appears that the melting temperature of a furan-based PA is considerably lower than the terephthalic based PA. This may be caused by the non-planar structure of the FDCA, compared to the benzene ring. This feature disrupt the crystallization of the polymer. The difference in the Tg value is smaller but with the same trend.
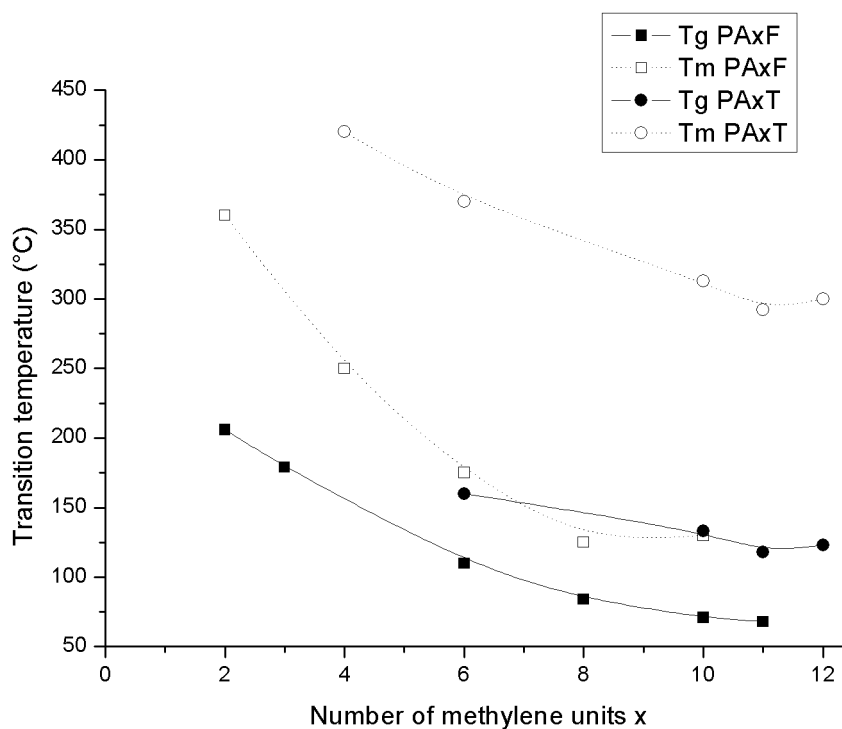
Figure 1.33: Glass transition and melting temperatures of a series of PAx-T and PAx-F depending on the number of methylene units in the repeating unit. [57, 61, 63, 64, 66].

3.3.2 Aromatic polyamides

In parallel to the studies on aliphatic PA, other studies have been carried out on the synthesis of aromatic polyamides from FDCA and aromatic diamines such

as the 1,4-phenylenediamine [67]. These synthesis were performed in solution in a mixture of N-methylpyrolidone/pyridin, which gave the best yields. The reactants where introduced in stoichiometric quantities in presence of LiCl, $CaCO_3$ and triphenylphosphite at 90°C for 20 hours. The reaction scheme is presented in figure 1.34
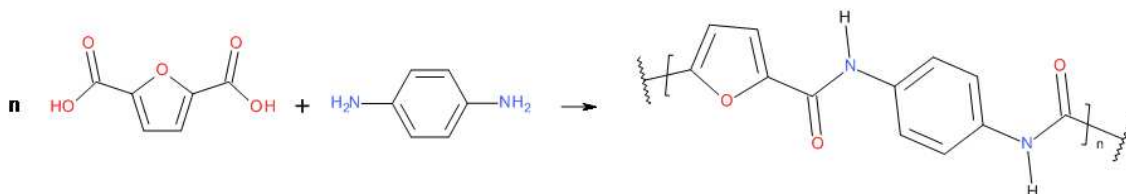
Figure 1.34: Synthesis of an aromatic polyamide from FDCA and 1,4-phenylenediamine.

The resulting polymer is only soluble in N-methylpyrolidone with 4% of LiCl. Solutions of this polymer have proven to have a lyotropic liquid crystal behaviour. This PA has quite high molar mass ($\bar{M}_n = 20000$ g/mol and $\bar{M}_w = 10^5$ g/mol) and kevlar-like properties, its terephthalic equivalent. This material has a glass transition temperature of about 325°C and a degradation temperature around 400°C.

4   Computer simulation of polymers

By definition, a computer simulation, a computer model, or a computational model is a computer program, or network of computers, that attempts to simulate an abstract model of a particular system. Computer simulations have become a useful part of mathematical modelling of many natural systems in physics (computational physics), astrophysics, chemistry and biology, human systems in economics, psychology, social science, and engineering.

It can be used to explore and gain new insights into new technology, and to estimate the performance of systems too complex for analytical solutions. For example, the study of the motion of more than two interacting bodies, even by the simple laws of Newtonian mechanics become essentially unsolvable analytically. However by using a computer, it is possible to get the answer at any desired accuracy. Most of the materials science deals with the properties of systems of many atoms or molecules, and with many usually meaning much more than two. So if we wish to compute the properties of a liquid (a particularly complicated example), there is no hope of finding the answer only with paper and pencil.

4.1   History of computer simulation

The first uses that were made of computers was in the early 1940's, to solve problems on the "Manhattan Project", the making of the nuclear bomb during the World War II. During this war, computers were also used in cryptography. The first uses in the "civilian" research were carried out in the field of statistical physics in the 1950's.

The early history of computer simulation illustrates the role of computers as ways to "measure" properties that could not be measured by other techniques. Some areas of physics appeared to have little need for simulations because very good analytical theories were available (e.g., to predict the properties of dilute gases or harmonic crystalline solids). However in other areas, few if any exact theoretical results were known, and progress was much limited by the lack of unambiguous tests to assess the quality of approximate theories.

The first computer simulation of a liquid was carried almost 60 years ago, in 1953, by Metropolis [68]. This simulation laid the foundations of modern Monte Carlo simulations (MC). In this method, atoms or particles are randomly chosen and randomly displaced to a nearby position. Energy considerations dictate whether the trial move is "accepted" or not. MC proved to be a very powerful tool for the equilibration of complex systems because of their ability to overcome free energy barriers that limit the motion of these systems in configuration space. However, this MC technique is not designed to study the dynamic properties of many body systems. That is why an alternative technique was developed: Molecular Dynamics (MD). MD simulation is based on the solution of the classical equations of motion (Newton's equation) for each particle in the system.

In 1955, the first simulation of a non-linear crystal (1D) using molecular dynamics was carried out by Fermi, Pasta and Ulam [69]. The following year, in 1956, Alder and Wainwright simulated hard sphere with MD techniques [70], the first step towards the simulation of atoms dynamics.

During the following decade, several tools were developed in order to increase the potential of the computer simulation in the field of statistical and molecular physics. Thus, several integrators such as the Verlet integrator, computing tool such as neighbour lists were developed. Crystal systems, polymer, biological systems, interfaces, copolymers, have all been subjects of study with MD simulations.

With the exponential increase of the computer power, the 1980's saw the development of quantum simulation techniques such as *ab-initio* calculations, Car-Parrinello method in quantum chemistry [71], Gaussian simulations, etc.

In the 1990's, the effort of development of the computer simulations was more

on the coding itself, in order to take the maximum advantage of the massive parallel
computers that were made at this time. Simulations were also developed in new
thermodynamical ensembles such as the grand-canonical ensemble. In the last years,
new hardware material has become popular: GPU's (Graphics Processing Unit).
Indeed, calculation on massively parallel GPU's could be much more efficient than
more traditional CPU's (Central Processing Unit), but this change in the hardware
has to be sided by a change in the algorithms and coding language [72].

4.2   General considerations

4.2.1   Different scales
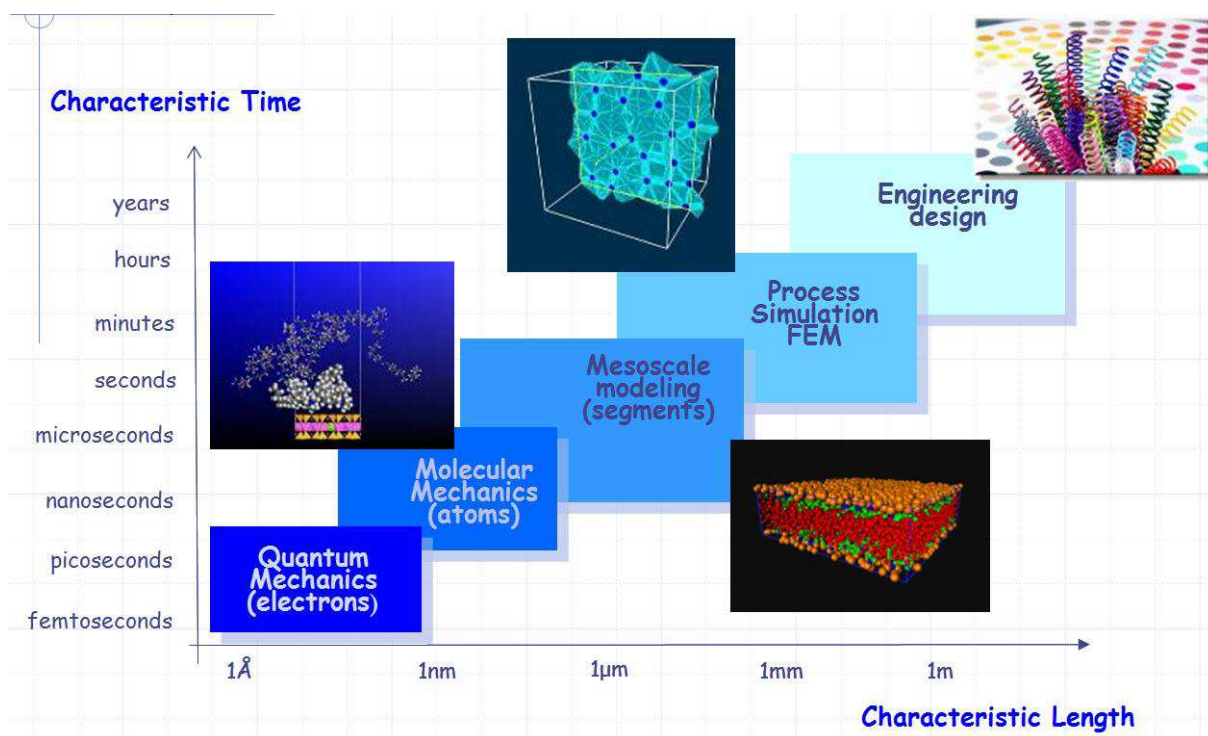
Figure 1.35: Multiscale molecular modelling.

The words *molecular modelling* regroup a wide set of very different techniques
(quantum, atomistic, mesoscale methods, etc.). These techniques are different in
terms of time and space scales on which they apply and so on their use (see figure
1.35) [73]).
At the smallest scale, it is quantum methods that are used. The quantum methods
regroup *ab-initio* techniques such as Hartree-Fock or the density functional theory
(DFT). These theories do not use system dependent parameters of semi-empirical
databases. They are only based upon the quantum mechanics equations, the equa-

tions that governs the electrons and nucleus behaviour. One of the main issue with this method is the huge number of elements that need to be calculated on systems that have more than hundred atoms. So this method is not very efficient for the molecular modelling of macroscopic material properties.

The scale that stands just above this one is the molecular dynamics (MD). This method could be applied to systems 10000 times bigger than quantum mechanics and on time-scales up to dozens of nanoseconds. This method is based upon statistical mechanics calculations. So it is here the classical mechanics (Newtonian equations of movement) that is applied on a big number of elements, where the "statistics" word comes from.

To each particle of the system (atom), several parameters are associated, for example the charge of the atom, its valence, the nature of its chemical bonds or its Van der Waals radius. These parameters are determined by *ab-initio* calculations or are experimental values. When all particles in the system have associated parameters, the principles of the classical mechanics applies: calculation of the forces that apply on the system and calculation of the equations of motion.

However this scale might not be sufficient for some problems in the field of material science. Indeed in the polymer science, polymer chains usually have relaxation times on the order of 1 second, while the crystallisation phenomena could take up to several tenths of seconds. So to treat these sort of problems, a superior scale to the MD one exists: the mesoscale. In this mesoscale method, atoms are grouped in "blobs" that could contain from few atoms to several tenths of atoms. Then MD calculations are done not on the atoms but on the groups of atoms, which are considered as one big particle with average parameters of the containing atoms. This method decreases a lot the calculation time compared to MD and allows the study of longer time and space-scales such as copolymers self-assembly, diffusion and transport properties, etc.

Even higher scale methods exist but will not be treated here since they deal more about object conception and process engineering, not on material science. Most of the calculations that were done for this study where performed on the atomistic scale with molecular dynamics techniques.

4.2.2   Is a computer simulation an experiment?

Computer simulations can play a significant role by providing essentially exact results for problems in statistical mechanics that otherwise would be soluble only by approximate theories or totally insoluble. From this sense computer simulations is a direct test of theories. Indeed the equations solved in the simulation are exact

(Newton's equations of motion, that have been verified since several centuries). So if the output of the simulation is in contradiction with the result expected by a proposed theory, the theory has to be false because the simulation could not be false (if the input parameters are correct).

From another point of view, the results of computer simulations may also be compared to those of real experiments. This is the duality of the computer simulation. On the one hand, it is a test of the model used in the computer simulations. On the other hand, if the model is proven to be a good one, the simulations can offer insights to the experimentalists and assist in the interpretation of new results.

Due to their connecting role, these techniques are often called "computer experiments" [74].

4.3   Atomistic simulation – Molecular dynamics

During the computer simulation on the atomistic scale, the intra- and inter-chains interactions are calculated with a great accuracy. Indeed each atom has some special characteristics (charge, Van der Waals radius, etc.) depending on its electronical surroundings. Each atom is given a "type" or a "class" in function of its surroundings and this will lead the atom's behavior during the simulation. All atoms of the same kind (sp^2 carbon, carbon in a carboxylic acid group, secondary amine, etc.) will be of the same type.

These types are defined at the beginning of the simulation and will not change during the calculation. Types are known before the simulation, either calculated by *ab-inito* methods or determined empirically.

The fundamental principles of the molecular dynamics is the use of the classical (Newtonian) equations of motions to describe the movements of the system. This equation is written for the i atom:

$$\frac{-\partial V}{\partial R_i} = m_i \frac{\partial^2 R_i}{\partial t^2} \tag{1.10}$$

where R_i are the coordinates of the atom, m_i its mass and V a potential. This potential V is an empirical potential, also called by the simulation software *forcefield*. It describes the surface of potential energy of n atoms. The accuracy of a simulation depends on the ability of the forcefield to describe the interactions taking place in the system.

The simulations goes through several steps:

1. all coordinates of the atoms of the system in the initial configuration are known

2. Newton's equation is resolved for each atom of the system

3. the resulting movement for the time-step of the simulation is applied

4. all new coordinates of the atoms are calculated. The system is in a new state.

5. a new iteration is applied on the new state of the system, ...

The time average of the particles speed, quantity of movement, etc. could be related to macroscopic physical properties at the end of the simulation. A more detailed bibliography and theoretical description of the different molecular modelling techniques used are presented in chapter 2 and Appendix A.

4.4 Applications

Beginning in theoretical physics, the method of MD gained popularity in material science and since the 1970s also in biochemistry and biophysics. The first macromolecular molecular dynamics simulation was published in 1977 [75]. In chemistry, MD serves as an important tool in protein structure determination and refinement using experimental tools such as X-ray crystallography and NMR.

It has also been applied with limited success as a method of refining protein structure predictions. In physics, MD is used to examine the dynamics of atomic-level phenomena that cannot be directly observed, such as thin film growth and ion-subplantation. It is also used to examine the physical properties of nanotechnological devices that have not or cannot yet be created.

In applied mathematics and theoretical physics, molecular dynamics is a part of the research realm of dynamical systems, ergodic theory, atomic, molecular, and optical physics and statistical mechanics in general. The concepts of energy conservation and molecular entropy come from thermodynamics. Some techniques to calculate conformational entropy such as principal components analysis come from information theory. Mathematical techniques such as the transfer operator become applicable when MD is seen as a Markov chain. Also, there is a large community of mathematicians working on volume preserving, symplectic integrators for more computationally efficient MD simulations.

MD can also be seen as a special case of the discrete element method (DEM) in which the particles have spherical shape (e.g. with the size of their van der Waals radii).

References

[1] E. Maréchal, "Polycondensation et polyaddition," *Les Techniques de l'Ingénieur*, 1998.

[2] M. Kohan, *Nylons Plastics Handbook*.   New York: Carl Hanser Verlag, 1995.

[3] K. Tai, H. Teranishi, Y. Arai, and T. Tagawa, "The kinetics of hydrolytic polymerization of ϵ-caprolactam," *Journal of Applied Polymer Science*, vol. 24, no. 1, pp. 211–224, 1979. [Online]. Available: http://dx.doi.org/10.1002/app.1979.070240119

[4] ——, "The kinetics of hydrolytic polymerization of ϵ-caprolactam. II. Determination of the kinetic and thermodynamic constants by least-squares curve fitting," *Journal of Applied Polymer Science*, vol. 25, no. 1, pp. 77–87, 1980. [Online]. Available: http://dx.doi.org/10.1002/app.1980.070250108

[5] R. G. Griskey and B. I. Lee, "Thermally induced solid-state polymerization in nylon 66," *Journal of Applied Polymer Science*, vol. 10, no. 1, pp. 105–111, 1966. [Online]. Available: http://dx.doi.org/10.1002/app.1966.070100108

[6] I. K. Miller and Z. J., *Condensation Polymerization and Polymerization Mechanisms*.   American Chemical Society, 1985, ch. 8, pp. 159–173. [Online]. Available: http://pubs.acs.org/doi/abs/10.1021/bk-1985-0285.ch008

[7] P. Rempp and E. W. Merrill, *Polymer Synthesis*.   John Wiley & Sons, Dec. 1998.

[8] C. Scott, D. Wu, C.-C. Ho, and C. C. Co, "Liquid-Core Capsules via Interfacial Polymerization: A Free-Radical Analogy of the Nylon Rope Trick," *Journal of the American Chemical Society*, vol. 127, no. 12, pp. 4160–4161, 2005. [Online]. Available: http://pubs.acs.org/doi/abs/10.1021/ja044532h

[9] E. C. Botelho, N. Scherbakoff, M. C. Rezende, A. M. Kawamoto, and J. Sciamareli, "Synthesis of Polyamide 6/6 by Interfacial Polycondensation with the Simultaneous Impregnation of Carbon Fibers," *Macromolecules*, vol. 34, no. 10, pp. 3367–3375, 2001. [Online]. Available: http://pubs.acs.org/doi/abs/10.1021/ma000902k

[10] H. K. Reimschuessel, "Nylon 6. Chemistry and mechanisms," *Journal of Polymer Science: Macromolecular Reviews*, vol. 12, no. 1, pp. 65–139, 1977. [Online]. Available: http://dx.doi.org/10.1002/pol.1977.230120102

[11] J. Trotignon, J. Verdu, A. Dobraczynski, and M. Piperaud, *Matières Plastiques*. Nathan - AFNOR, 2006.

[12] H. Mark, "Polyamides, Plastics."

[13] B. Guerin, "Polyamides," *Les Techniques de l'Ingénieur*, 1994.

[14] *ISO 1874-2 Plastics – Polyamide (PA) moulding and extrusion materials*, ISO International Organization for Standardization, Geneva (CH) Std. ISO 1874-2:2006(E), 2006. [Online]. Available: http://www.iso.org

[15] *ASTM D5336 - 09 Standard Specification for Polyphthalamide (PPA) Injection Molding Materials*, ASTM International, West Conshohocken, PA Std. ASTM D5336 - 09, 2009. [Online]. Available: http://www.astm.org

[16] C. Leboeuf and D. A. Harbourne, "Synthesis of semi-crystalline polyphthalamides through reactive extrusion of hexamethylene terephthalamide oligomer with lower melting, semi-crystalline or amorphous polyamides," Patent WO 1999/061 509, 1999. [Online]. Available: http://www.patentlens.net/patentlens/patent/WO_1999_061509_A1/en

[17] T. F. Novitsky, C. A. Lange, L. J. Mathias, S. Osborn, R. Ayotte, and S. Manning, "Eutectic melting behavior of polyamide 10,T-co-6,T and 12,T-co-6,T copolyterephthalamides," *Polymer*, vol. 51, no. 11, pp. 2417–2425, 2010. [Online]. Available: http://www.sciencedirect.com/science/article/B6TXW-4YRHCW1-6/2/89b03fca78d6d1748494f32d151627ed

[18] S. N. Vouyiouka and C. D. Papaspyrides, *Solid-State Polymerization*. John Wiley & Sons, Inc., 2002.

[19] R. B. Rashbrook, C. W. Alexander, and E. C. Bland, "Dryer screen made from poly(2-methyl-1,5-pentylene) terephthalamide," Patent US 5 112 685, 1992, Hoechst Celanese Corp. [Online]. Available: http://www.patentlens.net/patentlens/patent/US_5112685/en

[20] W. Poppe, Y.-T. Chen, L. Autry, and J. Richardson, "Crystalline polyamide composition from dicarboxylic acid mixture and diamine," Patent US 4 603 166, 1986, Amoco Corporation. [Online]. Available: http://www.patentlens.net/patentlens/patent/US_4603166/en

[21] J. Richardson, W. Poppe, B. Bolton, and E. E. Paschke, "Polycondensation process with mean dispersion residence time," Patent US4 831 108, 1989, Amoco Corporation.

[22] H. Reimann, G. Pipper, H.-P. Weiss, C. Plachetta, E. M. Koch, G. Blinne, W. Goetz, and P. Steiert, "Partially aromatic polyamides with a reduced triamine content," Patent EP0 299 444, 1989, BASF Aktiengesellschaft.

[23] P.-Y. Lahary and J. Coquard, "Semi-crystalline, semi-aromatic copolyamides," Patent WO9 115 537, 1991, Rhône-Poulenc Chimie.

[24] S. L.-K. Mok and R. Pagilagan, "Terephthalic acid copolyamides," Patent WO9 210 525, 1992, Du Pont Canada INC.

[25] R. Gabler, "Amorphous polyamides from a mixture of an alkyl substituted aliphatic diamine and unsubstituted aliphatic diamine," Patent US3 294 758, 1966, Grace W R & CO.

[26] G. Schade, N. Vollkommer, and H. Wemheuer, "Method of preparing modified or unmodified poly-(alkylpentamethyleneterephthalamide)," Patent US 4 163 101, 1979, Dynamit Nobel Aktiengesellschaft.

[27] G. Bier, F. Blaschke, H. aus der Funten, and G. Schade, "Transparent Polyamides," Patent US 4 111 921, 1978, Dynamit Nobel Aktiengesellschaft.

[28] H. K. Reimschuessel and G. J. Dege, "Polyamides: Decarboxylation and desamination in nylon 6 equilibrium polymer," *Journal of Polymer Science Part A-1: Polymer Chemistry*, vol. 8, no. 11, pp. 3265–3283, 1970. [Online]. Available: http://dx.doi.org/10.1002/pol.1970.150081120

[29] P.-Y. Lahary and J. Coquard, "Semi-crystalline, semi-aromatic copolyamides," Patent EP 0 522 027 B1, 1995, Nyltech France.

[30] H. Röper, "Renewable Raw Materials in Europe - Industrial Utilisation of Starch and Sugar," *Starch*, vol. 54, no. 3-4, pp. 89–99, 2002. [Online]. Available: http://dx.doi.org/10.1002/1521-379X(200204)54:3/4<89::AID-STAR89>3.0.CO

[31] B. Sillion, "Aromatic and Heterocyclic Polymers - What Future?" *High Performance Polymers*, vol. 11, no. 4, pp. 417–436, 1999. [Online]. Available: http://hip.sagepub.com/content/11/4/417.abstract

[32] A. Gandini and M. Belgacem, "Furans in Polymer Chemistry," *Progress in Polymer Science*, vol. 22, pp. 1203–1379, 1997.

[33] H. Laita, S. Boufi, and A. Gandini, "The application of the Diels-Alder reaction to polymers bearing furan moieties. 1. Reactions with maleimides," *European Polymer Journal*, vol. 33, no. 8, pp. 1203–1211, 1997. [Online]. Available: http://www.sciencedirect.com/science/article/B6TWW-3SP3089-3/2/c63673961683956a7b8cb10f86cce4d4

[34] Y. Liu, C. Hsieh, and Y. Chen, "Thermally reversible cross-linked polyamides and thermo-responsive gels by means of Diels-Alder reaction," *Polymer*, vol. 47, no. 8, pp. 2581–2586, 2006. [Online]. Available: http://www.sciencedirect.com/science/article/B6TXW-4JF97NN-3/2/7cb73af6d457ca060afa44171816ec9b

[35] N. Teramoto, Y. Arai, and M. Shibata, "Thermo-reversible Diels-Alder polymerization of difurfurylidene trehalose and bismaleimides," *Carbohydrate Polymers*, vol. 64, no. 1, pp. 78–84, 2006. [Online]. Available: http://www.sciencedirect.com/science/article/B6TFD-4HR72GX-6/2/e4f8d6faa067a917693baae65c161f8b

[36] B. J. Adzima, H. A. Aguirre, C. J. Kloxin, T. F. Scott, and C. N. Bowman, "Rheological and Chemical Analysis of Reverse Gelation in a Covalently Cross-

Linked Diels-Alder Polymer Network," *Macromolecules*, vol. 41, no. 23, pp. 9112–9117, 2008. [Online]. Available: http://dx.doi.org/10.1021/ma801863d

[37] C. Moreau, M. N. Belgacem, and A. Gandini, "Recent Catalytic Advances in the Chemistry of Substituted Furans from Carbohydrates and in the Ensuing Polymers," *Topics in Catalysis*, vol. 27, no. 1, pp. 11–30, 2004. [Online]. Available: http://dx.doi.org/10.1023/B:TOCA.0000013537.13540.0e

[38] J. M. Garcia, F. C. Garcia, F. Serna, and J. L. de la Peña, "High-performance aromatic polyamides," *Progress in Polymer Science*, vol. 35, no. 5, pp. 623–686, 2010. [Online]. Available: http://www.sciencedirect.com/science/article/B6TX2-4X9NV3D-1/2/fb9b2d372e9dd04b13d662d516140f50

[39] T. Werpy and G. Petersen, "Top Value Added Chemicals From Biomass," US Department of Energy, Tech. Rep., 2004.

[40] S. Gharbi and A. Gandini, "Polyamides incorporating furan moieties. 1. Interfacial polycondensation of 2,2â€šÂ¬Â²-bis(5-chloroformyl-2-furyl)propane with 1,6-diaminohexane," *Acta Polymerica*, vol. 50, no. 8, pp. 293–297, 1999. [Online]. Available: http://dx.doi.org/10.1002/(SICI)1521-4044(19990801)50:8<293::AID-APOL293>3.0.CO

[41] A. Corma, S. Iborra, and A. Velty, "Chemical Routes for the Transformation of Biomass into Chemicals," *Chemical Reviews*, vol. 107, no. 6, pp. 2411–2502, 2007. [Online]. Available: http://dx.doi.org/10.1021/cr050989d

[42] J. Lewkowski, "Synthesis, Chemistry and Applications of 5-Hydroxymethylfurfural and Its Derivatives," *ChemInform*, vol. 34, 2003. [Online]. Available: http://dx.doi.org/10.1002/chin.200302269

[43] F. Chambon, F. Rataboul, C. Pinel, A. Cabiac, E. Guillon, and N. Essayem, "Cellulose hydrothermal conversion promoted by heterogeneous Bronsted and Lewis acids: Remarkable efficiency of solid Lewis acids to produce lactic acid," *Applied Catalysis B: Environmental*, vol. 105, pp. 171 – 181, 2011. [Online]. Available: http://www.sciencedirect.com/science/article/pii/S092633731100172X

[44] X. Tong, Y. Ma, and Y. Li, "Biomass into chemicals: Conversion of sugars to furan derivatives by catalytic processes," *Applied Catalysis A: General*, vol. 385, no. 1-2, pp. 1–13, 2010. [Online]. Available: http://www.sciencedirect.com/science/article/B6TF5-50G065V-1/2/e097b20439a02e1b24941c7cfe9dca65

[45] N. Essayem, R. Lopes De Souza, and F. Rataboul, "Method for Producing 5-Hydroxymethylfurfural," Patent WO 2012/156 479, 2012, CNRS.

[46] M. Kröger, U. Prüβe, and K. Vorlop, "A new approach for the production of 2,5-furandicarboxylic acid by in situ oxidation of 5-hydroxymethylfurfural starting from fructose," *Topics in Catalysis*, vol. 13, no. 3, pp. 237–242, 2000. [Online]. Available: http://dx.doi.org/10.1023/A:1009017929727

[47] C. V. McNeff, D. T. Nowlan, L. C. McNeff, B. Yan, and R. L. Fedie, "Continuous production of 5-hydroxymethylfurfural from simple and complex carbohydrates," *Applied Catalysis A: General*, vol. 384, no. 1-2, pp. 65–69, 2010. [Online]. Available: http://www.sciencedirect.com/science/article/B6TF5-508X3CD-7/2/7d039c58b8792abc902c0055ee7b0eff

[48] M. Möller, F. Harnisch, and U. Schröder, "Microwave-assisted hydrothermal degradation of fructose and glucose in subcritical water," *Biomass and Bioenergy*, vol. 39, pp. 389 – 398, 2012. [Online]. Available: http://www.sciencedirect.com/science/article/pii/S0961953412000463

[49] P. Vinke, W. van der Poel, and H. van Bekkum, "Platinum Catalyzed Oxidation of 5-Hydroxymethylfurfural," in *New Developments in Selective Oxidation*, ser. Studies in Surface Science and Catalysis, G. Centi and F. Trifiro, Eds.   Elsevier, 1990, vol. 55, pp. 147–158. [Online]. Available: http://www.sciencedirect.com/science/article/pii/S0167299108601445

[50] ——, "On the oxygen tolerance of noble metal catalysts in liquid phase alcohol oxidations the influence of the support on catalyst deactivation," in *Heterogeneous Catalysis and Fine Chemicals II Proceedings of the 2nd International Symposium*, ser. Studies in Surface Science and Catalysis, M. Guisnet, J. Barrault, C. Bouchoule, D. Duprez, G. Pärot, R. Maurel, and C. Montassier, Eds.   Elsevier, 1991, vol. 59, pp. 385–394. [Online]. Available: http://www.sciencedirect.com/science/article/pii/S0167299108611453

[51] P. Mäki-Arvela, B. Holmbom, T. Salmi, and D. Y. Murzin, "Recent Progress in Synthesis of Fine and Specialty Chemicals from Wood and Other Biomass by Heterogeneous Catalytic Processes," *Catalysis Reviews*, vol. 49, no. 3, pp. 197–340, 2007. [Online]. Available: http://www.tandfonline.com/doi/abs/10.1080/01614940701313127

[52] S. Albonetti, T. Pasini, A. Lolli, M. Blosi, M. Piccinini, N. Dimitratos, J. A. Lopez-Sanchez, D. J. Morgan, A. F. Carley, G. J. Hutchings, and F. Cavani, "Selective oxidation of 5-hydroxymethyl-2-furfural over TiO2-supported gold-copper catalysts prepared from preformed nanoparticles: Effect of Au/Cu ratio," *Catalysis Today*, 2012. [Online]. Available: http://www.sciencedirect.com/science/article/pii/S0920586112004051

[53] A. Boisen, T. Christensen, W. Fu, Y. Gorbanev, T. Hansen, J. Jensen, S. Klitgaard, S. Pedersen, A. Riisager, T. Ståhlberg, and J. Woodley, "Process integration for the conversion of glucose to 2,5-furandicarboxylic acid," *Chemical Engineering Research and Design*, vol. 87, no. 9, pp. 1318–1327, 2009. [Online]. Available: http://www.sciencedirect.com/science/article/pii/S0263876209001464

[54] Y. Gorbanev, S. Klitgaard, J. Woodley, C. H. Christensen, and A. Riisager, "Gold-Catalyzed Aerobic Oxidation of 5-Hydroxymethylfurfural in Water at Ambient Temperature," *ChemSusChem*, vol. 2, no. 7, pp. 672–675, 2009. [Online]. Available: http://dx.doi.org/10.1002/cssc.200900059

[55] O. Casanova, S. Iborra, and A. Corma, "Biomass into Chemicals: Aerobic Oxidation of 5-Hydroxymethyl-2-furfural into 2,5-Furandicarboxylic Acid with Gold Nanoparticle Catalysts," *ChemSusChem*, vol. 2, no. 12, pp. 1138–1144, 2009. [Online]. Available: http://dx.doi.org/10.1002/cssc.200900137

[56] Avantium. "http://avantium.com/yxy/YXY-technology/YXY-process-technology.html". [Online]. Available: http://avantium.com/yxy/YXY-technology/YXY-process-technology.html

[57] H. Hopff and A. Kreiger, *Makromolecular Chemie*, vol. 47, p. 93, 1961.

[58] N. Ogata, Y. Hosoda, and G. Suzuki, "Active polycondensation of monomers having hetero atoms," *Polymer Journal*, vol. 6, no. 5, pp. 412–418, 1974.

[59] N. Ogata, K. Sanui, and K. Okouchi, "Active polycondensation of dicarboxylic acid derivatives having b-hetero atoms," *Polymer Journal*, vol. 5, no. 2, pp. 186–194, 1973.

[60] N. Ogata and K. Shimamura, "Active Polycondensation of diesters having heterocyclic nuclei," *Polymer Journal*, vol. 7, no. 1, pp. 72–78, 1975.

[61] H. Hopff and A. Krieger, "Über Decarboxylierung und Dissoziation heterocyclischer Dicarbonsäuren," *Helvetica Chimica Acta*, vol. 44, no. 4, pp. 1058–1063, 1961. [Online]. Available: http://onlinelibrary.wiley.com/doi/10.1002/hlca.19610440425/abstract

[62] B. R. Brown, "The mechanism of thermal decarboxylation," *Quarterly Reviews, Chemical Society*, vol. 5, no. 2, pp. 131–146, Jan. 1951. [Online]. Available: http://pubs.rsc.org/en/content/articlelanding/1951/qr/qr9510500131

[63] K. Yutaka, T. Miura, K. Matsuda, and T. Komuro, "Polyamide compound and molded article thereof," Patent Application WO 2012/132 792 A1, 2012. [Online]. Available: http://www.patentlens.net/patentlens/patent/WO_2012_132792_A1/en

[64] P. M. Heertjes and G. J. Kok, "Polycondensation products of 2,5-furandicarboxylic acid," *Delft Progress Report Series A*, vol. 1, pp. 59–63, 1974.

[65] O. Grosshardt, U. Fehrencacher, K. Kowollik, B. Tübke, N. Dingenouts, and M. Wilhem, "Synthese und Characterisierung von Polyestern und Polyamiden auf der Basis von Furan-2,5-dicarbonsäure," *Chemie Ingenieur Technik*, vol. 11, p. 81, 2009.

[66] J. A. Moore and W. W. Bunting, "Polyesters and polyamides containing isomeric furan dicarboxylic acids," *Polymer science and technology*, vol. 31, pp. 51–91. [Online]. Available: http://cat.inist.fr/?aModele=afficheN&cpsidt= 8738230

[67] A. Mitiakoudis and A. Gandini, "Synthesis and characterization of furanic polyamides," *Macromolecules*, vol. 24, no. 4, pp. 830–835, 1991. [Online]. Available: http://dx.doi.org/10.1021/ma00004a003

[68] N. Metropolis, A. W. Rosenbluth, M. N. Rosenbluth, A. H. Teller, and E. Teller, "Equation of State Calculations by Fast Computing Machines," *The Journal of Chemical Physics*, vol. 21, no. 6, pp. 1087–1092, 1953. [Online]. Available: http://link.aip.org/link/?JCP/21/1087/1

[69] A. P. Mason, J. Z. Norman, H. Bambi, and K. C. David, "Fermi, Pasta, Ulam and the Birth of Experimental Mathematics," *American Scientist*, vol. 92, no. 3, p. 214, May 2009.

[70] B. J. Alder and T. E. Wainwright, "Phase Transition for a Hard Sphere System," *The Journal of Chemical Physics*, vol. 27, no. 5, pp. 1208–1209, 1957. [Online]. Available: http://link.aip.org/link/?JCP/27/1208/1

[71] R. Car and M. Parrinello, "Unified Approach for Molecular Dynamics and Density-Functional Theory," *Physical Review Letters*, vol. 55, pp. 2471–2474, Nov 1985. [Online]. Available: http://link.aps.org/doi/10.1103/PhysRevLett. 55.2471

[72] J. E. Stone, D. J. Hardy, I. S. Ufimtsev, and K. Schulten, "GPU-accelerated molecular modeling coming of age," *Journal of Molecular Graphics and Modelling*, vol. 29, no. 2, pp. 116–125, 2010. [Online]. Available: http://www.sciencedirect.com/science/article/pii/S1093326310000914

[73] "The Mose Laboratory - University of Trieste," http://www.mose.units.it/Lists-/Multiscale%20Molecular%20Modeling/AllItems.aspx. [Online]. Available: http://www.mose.units.it/Lists/Multiscale;http://allitems.aspx

[74] A. H. Vagelis, "Atomistic Molecular Dynamics Simulations of Polymer Melt Viscoelasticity," Ph.D. dissertation, University of Patras, 2001.

[75] J. A. McCammon, B. R. Gelin, and M. Karplus, "Dynamics of folded proteins," *Nature*, vol. 267, pp. 585–590, Jun. 1977.

Chapter 2

Synthesis and simulation of model polyphthalamides

Contents

This chapter is dedicated to the synthesis and the simulation of model polyphthalamides (PPA). These model PPA will be used for the development of a simulation protocol able to predict the glass transition temperature of several other polyphthalamide analogue materials.

1 Introduction

Generally the process that leads to the development of a new material involves several steps of chemistry optimization of its synthesis, including choice of the monomers, the catalysis, etc. followed by a rigorous characterization of the produced materials. This process is time-consuming and may be very expensive.

Simulating polymer properties is considerably less time consuming than preparing real systems and, therefore, *a-priori* simulations would allow the development of new materials according to the output of those simulations. In order to speed up this process, recent developments in molecular modelling and computer simulations has made possible the study and simulation of polymer materials in details [1]. Moreover, in nowadays situation of quick development of new biobased polymers, large screening of monomers is required. This is a common new trend of research in polymer and material science, and lot of companies and academic laboratories are currently working on this subject.

The aim of this chapter is to investigate PPA properties with the use of molecular modelling and computer simulation methods in comparison with experimental data. On this base, only amorphous PPA were synthesized and studied. These amorphous PPA are not really interesting for their thermal and mechanical properties, but they are important for the molecular modelling. Indeed the atomistic simulation cannot take into account the crystallization process, which occurs on a much larger space and time-scale.

In this chapter, we will focus on the one hand on the synthesis and characterization of amorphous PPA and on the other hand on their molecular modelling mainly by molecular dynamics (MD) in the aim of establishing a robust protocol that will allow the study of other PPA.

The first pages of this chapter will be consecrated to a general presentation of the monomers used in our syntheses and the presentation of the synthesis protocol and characterization techniques. Then a section will be dedicated to the simulation techniques used for the study of the PPA glass transitions. Finally, in the last part we will compare the simulation results with the experimental data and conclude on the validity and accuracy of the simulation protocol we developed.

2 Experimental methods

2.1 Synthesis

2.1.1 Materials

Diacids   Polyphthalamides are composed of a majority of aromatic acids — mainly terephthalic acid (TPA) and/or isophthalic acid (IPA) — condensed with an aliphatic diamine. The diacids used are presented in figure 2.1 and 2.2.
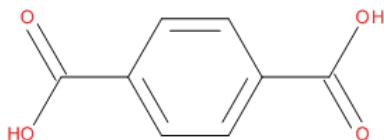
Figure 2.1: Terephthalic acid (benzene-1,4-dicarboxylic acid)
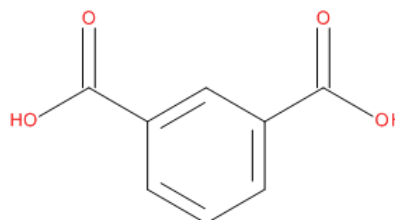
Figure 2.2: Isophthalic acid (benzene-1,3-dicarboxylic acid)

Terephthalic acid is an aromatic diacid produced by the oxidation, in the presence of O_2 of the air, of *p-xylene*, as shown on figure 2.3. The commercial process used acetic acid as solvent and a catalyst composed of cobalt and manganese salts, with a bromide promoter [2]. Its main use is the production of polyethylene terephthate (PET) for the production of plastic bottles (more than 30 million tonnes of TPA produced in 2006).

Several companies are working on the improvement of this process with the use for example of super-critical CO_2 as a solvent [3, 4]. Another research path for the production of terephthalic acid was its production from biobased resources such as
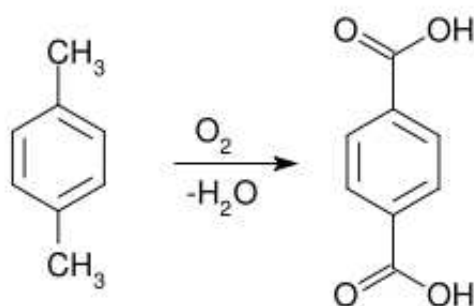
Figure 2.3: Oxidation of p-xylene by O_2 in the air

limonene [5, 6], which was recently put on the first steps of industrialisation process. Terephthalic acid comes as a white powder. Its main properties are listed in table 2.1.

Isophthalic acid is an isomer of terephthalic acid (meta-phthalic acid instead of para-phthalic acid for the TPA). It is synthesized with the same process as TPA but starting from *m-xylene*. Its properties are listed in table 2.1. Isophthalic acid is mainly used (in the form of acyl chloride) in the production of the fire-resistant Nomex® meta-aramid fiber (figure 2.4) from DuPont.
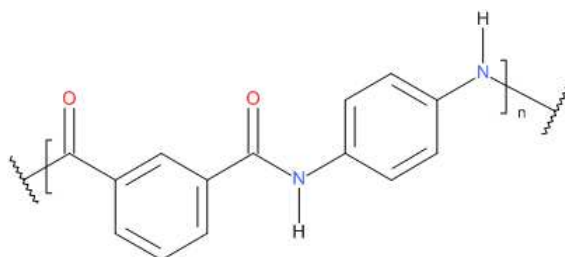
Figure 2.4: Poly(phenylene isophthalamide), also named Nomex®

Diamine   Hexamethylene diamine (HMDA), 1,6-hexane diamine, is a classical monomer used for the synthesis of polyamides. It is a linear aliphatic diamine with a chain length of 6 carbons between the two amine functions. The chemical structure of HMDA is presented in figure 2.5.
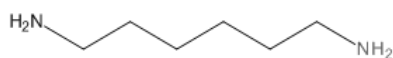
Figure 2.5: 1,6-hexane diamine

IUPAC Name	Molecular formula	Molar mass (g/mol)	Density	Melting point	Boiling Point	Water Solubility	Supplier
Benzene-1,4-dicarboxylic acid	$C_8H_6O_4$	166.13	1.522	sub. 402°C	-	0.02g/L	BP Chemicals
Benzene-1,3-dicarboxylic acid	$C_8H_6O_4$	166.13	1.526	345°C	-	insoluble	BP Chemicals
Hexane-1,6-diamine	$C_6H_{16}N_2$	116.21	0.84	42°C	205°C	490 g/L	Sigma-Aldrich

Table 2.1: Properties of the monomers used

HMDA is a white solid at room temperature, and is highly soluble in water and alcohols (methyl and ethyl). Its main properties are listed in the table 2.1.

2.1.2   Synthesis of polyphthalamides

Introduction   As said in the introduction and bibliography chapter, synthesis of polyphthalamides were carried out. These synthesis of model PPA were done in traditional laboratory glassware by mixing aromatic diacids, TPA and IPA, with an aliphatic diamine, HMDA. The reaction that occurred was a polycondensation reaction.

The polycondensation reaction is a step-by-step reaction between acid and amine chain ends between monomers and/or chains of various lengths. At each step, a small molecule is eliminated. Here with TPA, IPA and HMDA, molecules of water were eliminated. The acids and diamine do not react directly with each other. The chemical species go to a salty state where the acid is in the carboxylate form and the amine in the ammonium form, as shown on figure 2.6.

Another important fact about polycondensation reaction is that it is an equilibrated reaction, so the stoichiometry of the reactants is a very important parameter. It has a direct influence on the molar mass of the synthesized polymers.

Synthesis set-up   The different syntheses were carried out in the following set-up (Figure 2.7).

It is composed of a glass tube of approximately 200 mL that fits in an aluminium container. This container is surrounded by an insulating blanket and stands on an electrical heating device. This set-up was constructed especially for this purpose
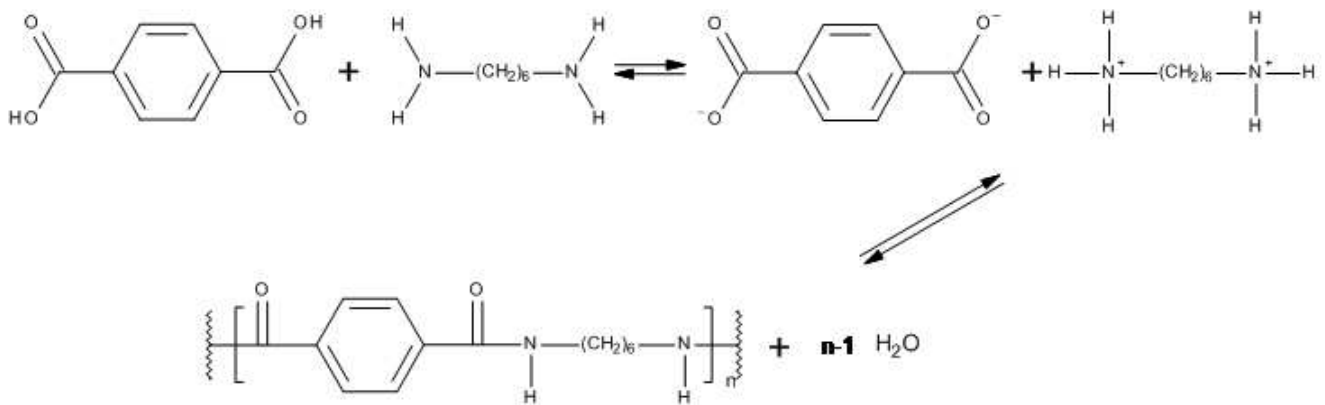
Figure 2.6: Polycondensation reaction scheme PA 6-T
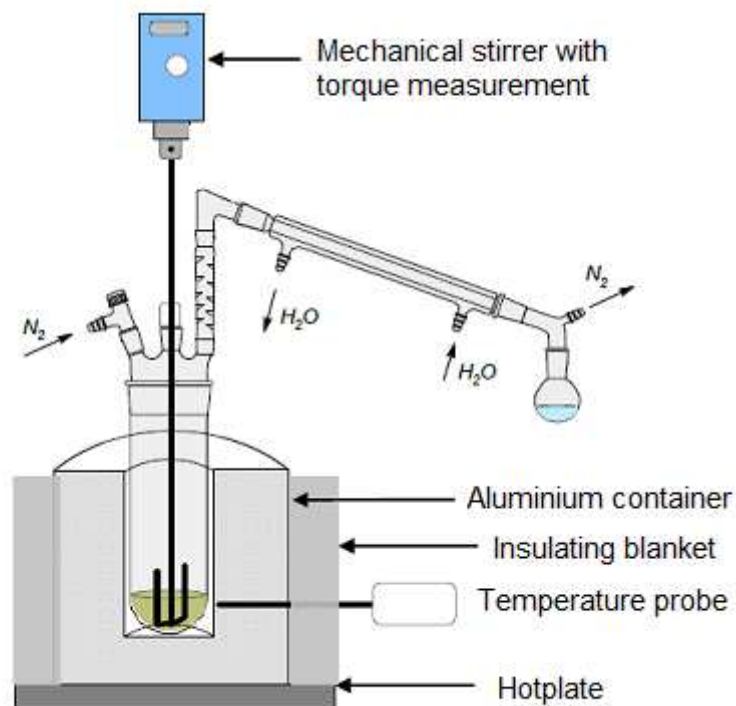
Figure 2.7: Synthesis set-up

because the temperatures needed for polyamide synthesis are much higher than the ones achievable by a traditional oil bath. On the top of the glass tube, a three-ways reactor head is adjusted. Through one of the ways goes the stirrer, the second one is dedicated to the nitrogen flow and on top of the last one is standing a fractionating column, with a condenser and a receiving flask. This distillation device was needed for the separation of the water and the diamine vapour that may form during the reaction. Indeed it was suitable that all the diamine stayed in the reaction mixture to keep the right stoichiometry between reactants, while the water — product of the reaction — was removed.

During the different PPA syntheses, three parameters were followed:
 – the temperature
 – the torque
 – the amount of distilled water

These three parameters allow the control of the advancement of the reaction and its kinetics. The temperature measured is the temperature of the aluminium container, not the temperature inside the reactor. The torque is measured with the stirrer system, which has got a torque measurement system built-in. Finally the amount of distilled water is measured with the graduated receiving flask of the distillation set-up.

At the end of the reaction, around 40 grams of PPA are obtained.

Protocol   The syntheses of the PPA were carried out by following this protocol:
 – First the diamine is weighted and introduced in the glass tube with a certain amount a water (from 10 to 20 grams) to help the homogenisation of the reaction mixture. The diamine should completely be dissolved in the water at room temperature. As an example, for the synthesis of a PA 6-I, 21.4g of HMDA is poured in the reactor with 20 grams of water.
 – Then the mixture of acid is added in the glass tube (29.4g of isophthalic acid). The acids are in the form of an insoluble powder,that should progressively disappear as the PA salt is formed. This reaction is exothermic and the solution temperature increases up to 50°C.
 – The glass tube is adjusted to the reactor's head and 2 to 3 nitrogen flushes are performed to remove all the oxygen in the experimental set-up.
 – Temperature is slowly increased to around 160°C. At this temperature, the salt should be entirely formed (no insoluble powder present [1]) and the water

---

1. Visual inspection of the reaction mixture by lowering the heating device from time to time should be performed to check the homogeneity of the reaction.

that was added at the beginning is slowly distilled.

– Then the temperature is further increased to the reaction temperature (from 260 to 300°C, depending on the amount of TPA in the mixture). In the example (PA 6-I), the temperature is increased to 260°C.

– Reaction advancement is followed by the increase of the stirring torque and the amount of water distilled. For this example, the torque increases from 0 to 5.6 N.cm when the reaction was stopped.

– When the reaction is said to be complete enough, the heating device is lowered and the glass tube is slowly cooled down to room temperature.

– Finally, when the system is at room temperature, the glass tube is recovered and broken to collect the polymer material formed.

The amount of HMDA in the distillates was controlled during the first syntheses that were performed. This was done using a refractometry technique. Indeed the refractive index of the diamine is at 20°C: $n_{20} = 1.439$, which is different from the one of water: $n_{20} = 1.333$. This allows the construction of a master curve (Figure 2.8) of the refractive index of a hexamethylene diamine water solution as a function of the concentration.

Equation	y = a + b*x		
		Value	Standard Error
Refractive index at 20°C	Intercept	1,3324	0,00102
	Slope	0,00163	3,36043E-5
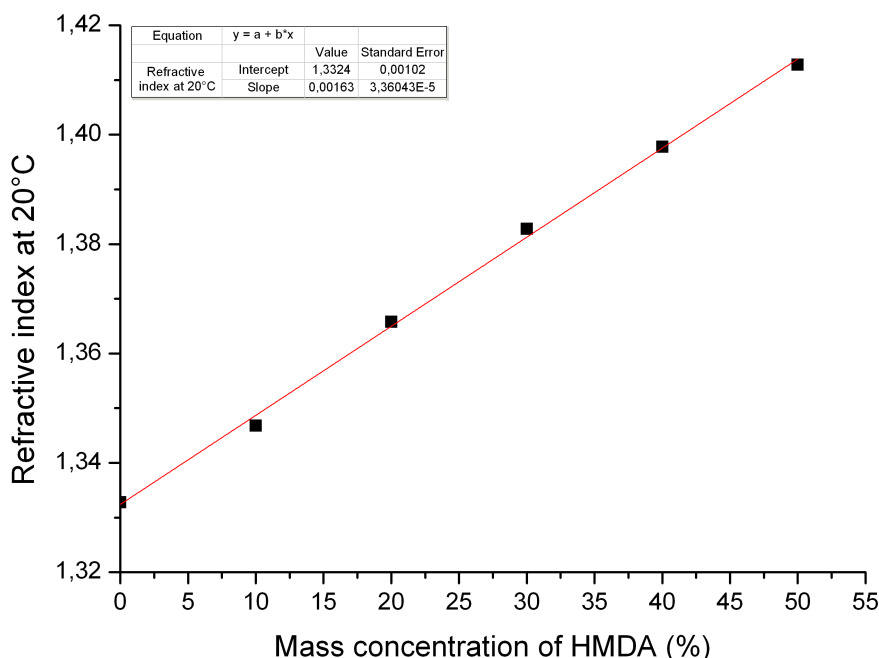
Figure 2.8: Refractive index of HMDA solutions

With this technique it was shown that approximately 2 to 3 mol % of the diamine were lost during the synthesis. So in order to compensate this loss, the HMDA was put in a light excess of about 2 mol % at the beginning of the reaction.

2.2   Polyphthalamides characterizations

2.2.1   Structure and composition characterization

After the synthesis of the polyphthalamides, the first important parameters to be characterized were the composition and chemical structure. Indeed the molar mass of the polymer, its polydispersity, the repartition of the different co monomers have a big influence on all the other macroscopic properties of the material. The characterisation techniques that have been used are the following:

1. solution viscosimetry

2. [1]H nuclear magnetic resonance

3. size-exclusion chromatography

Solution viscosimetry   The solution viscosimetry is a technique that allows the measurement of reduced and intrinsic viscosities of polymer solutions. The intrinsic viscosity can be linked to the molar mass of the polymer through the well-known Mark-Houwink relation. So this technique allows a quick estimation of the molar mass of the synthesized polymer, since it is a quick and cheap analysis. The main problem of these relationships is that they are only valid for linear, unmodified polymers. So even if the absolute determination of the molar mass by viscosimetry is not possible since our PPA are copolymers, this technique could still give an order of magnitude of $\bar{M}_n$.

Polymer solution at a concentration of 5 g/L in a 1/1 (by weight) mixture of phenol and 1,2-dichlorobenzene were analysed in a Ubbeholde viscosimetric device. In order to solubilize the materials, the mixtures containing the polymer and the solvent were heated with stirring at 135°C during 2h. The solution was then cooled and poured into an Ubbeholde viscosimeter tube, lying in a thermostated water bath at 25°C. The reduced viscosity (η_{red}) of the polymer was calculated using the solvent flow time and the polymer solution flow time in the viscosimeter (equation (2.1)):

$$\eta_{red} = \frac{t - t_0}{t_0 C}(mL/g) \tag{2.1}$$

In this equation, t is the polymer solution flow time, t_0 the solvent flow time and C the concentration of the solution in $g\,mL^{-1}$.

It is also possible to extract the intrinsic viscosity from this experiment by following the method provided in a paper by Solomon and Ciuta [7]. In this paper they propose an empirical relationship between the intrinsic viscosity of a polymer

diluted solution and its specific and relative viscosities, as shown on equation (2.2).

$$[\eta] = \frac{1}{c}\sqrt{2(\eta_{sp} - \ln\eta_{rel})} \tag{2.2}$$

In this equation, $[\eta]$ is the intrinsic viscosity, c the mass concentration of the solution and η_{sp} and η_{rel} the specific and relative viscosities.

It is also known that for solution time flows longer than 100 seconds, the specific viscosity is (equation 2.3):

$$\eta_{sp} = \frac{\eta - \eta_0}{\eta_0} \simeq \frac{t - t_0}{t_0} \tag{2.3}$$

and the relative viscosity (equation (2.4)):

$$\eta_{rel} = \frac{\eta}{\eta_0} \simeq \frac{t}{t_0} \tag{2.4}$$

where t and t_0 represent the solution and solvent flow times.

So by adding these two equations in the equation (2.2), the equation (2.5) is obtained:

$$[\eta] = \frac{1}{c}\sqrt{2(\frac{t - t_0}{t_0} - \ln(\frac{t}{t_0}))} \tag{2.5}$$

NMR analysis   NMR is a powerful technique that could provide a lot of informations. On the one hand, with ^{1}H nuclear magnetic resonance it is possible to obtain informations such as the average number molar mass, the composition of the copolyamide, the nature of the chain ends, etc.

^{1}H NMR   ^{1}H NMR analysis were performed on the various polymers modified by *N-Trifluoroacetylation* [8]. It was necessary to derivatize the polymers because polyamides are insoluble in most common solvents, due to very high hydrogen bonding and non-bonded interactions. In order to bypass this problem, reactions between the different polyamides and trifluoroacetic anhydride (TFAA) were performed in $CHCl_3$ as shown in figure 2.9.

Solutions were prepared using $CDCl_3$ with excess TFAA to achieve the solubilization of the polymers by using the following procedure. The different PA were weighted (20 mg for ^{1}H) and introduced into the NMR tube, then 0.5 mL of TFAA was added into the tube, followed by 0.5 mL of $CDCl_3$. The NMR tube was then manually stirred every 30 min until complete dissolution (approximately 2 to 3 hours). The different spectrums were collected at 300 K on an Avance III Bruker 400 MHz spectrometer.
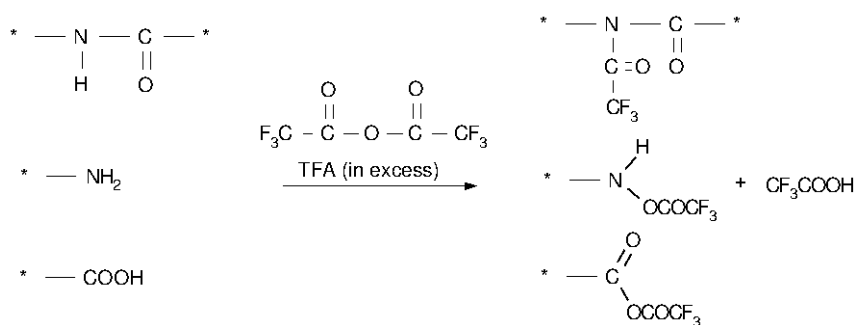
Figure 2.9: Trifluoroacetylation of the polyamide chemical units

SEC analysis   The last technique that was used to characterized the molar mass distribution of the several copolyamides synthesized was size-exclusion chromatography. This technique is based on the difference in hydrodynamic volume between polymer chains of various chain lengths. Indeed a long chain polymer material occupies a much higher volume in solution than a shorter chain polymer.

This is explained by the dependence of the radius of gyration of a polymer chain to its chain length. Indeed, the radius of gyration of a polymer chain is defined as the root mean square distance of the object's parts from its center of gravity and corresponds to the radius of the statistical volume occupied by a polymer chain. Several models of polymer chains exist and are split into two types: "ideal" and "real" models. However all models agree on a dependence of the type showed on the following equation [9]:

$$R_g \sim N^\nu \tag{2.6}$$

where R_g is the radius of gyration and N the number of monomer or repeating units in the chain. This equation is the Flory's mean field approach, where ν depends on how "good" the solvent is for the polymer. For good solvent, $\nu = 3/5$; for bad solvent, $\nu = 1/3$. Therefore polymer in good solvent has larger size and behaves like a fractal object. In bad solvent it behaves like a solid sphere. In the so called θ solvent, $\nu = 1/2$, which is the result of simple random walk. The chain behaves as if it were an ideal chain.

In all cases, the radius of gyration increases as the chain length increases and so does the hydrodynamic volume.

Size Exclusion Chromatography experiments were performed on derivatized [10] polymers in THF because PPA are not soluble in THF. The reaction process was close to the NMR one. A reaction between the PA and TFAA was performed in CHCl$_3$. This reaction was carried out at room temperature for 10 hours. After 10

hours, the solvent was evaporated and the modified polymer solubilized in THF at 1g/L.

After this step of chemical modification, the materials were tested on a Shimadzu SEC equipped with 3 Waters HR5E columns. Three detectors were used: Refractive Index (RI Shimadzu RID-10A), viscosimeter and light scattering (Viscotek TDA). With the combination of these 3 detectors, no column calibration was needed and absolute molar mass could be measured if dn/dc is known. The dn/dc values were calculated using a fixed concentration of the polymer solution at 1g/L.

This modification changes the molar mass of the PPA, because every free hydrogen in amide ($CO-NH$), carboxylic acid (COOH), and the first one for amine (NH_2) were replaced by a $COCF_3$ group. If we consider that the chemical modification is total, the molar mass were subjected to a big change. Indeed the molar mass of a hydrogen atom is close to 1 g/mol, whereas the $COCF_3$ group weight is 97 g/mol. So in order to present molar mass of unmodified PA, the molar mass of the modified repeating unit was calculated, and the degree of polymerization of the modified PA was calculated using the SEC results. Then by multiplying this $\bar{DP}_n$ with the unmodified repeating unit weight, the "real" molar mass of the polymers could be found.

2.3 Thermal properties

2.3.1 Differential Scanning Calorimetry

Differential Scanning Calorimetry tests were performed using a Thermal Analysis (TA) Q20 instrument, at a heating/cooling rate of 10°C/min, under nitrogen gas flow (50 mL/min). Samples were heated at 330°C, cooled to 25°C and then a second cycle (from 25°C to 330°C and back to 25°C) was applied. The glass transition temperature was measured at the onset during the second cooling cycle, the first one annealing the thermal history of the material. The glass transition was measured during the cooling because during the simulation procedure, the T_g was also estimated during a cooling process.

2.3.2 Thermogravimetric analysis (TGA)

Thermogravimetric analysis were performed on the various model PPA synthesized. This analysis characterized the thermal degradation of a material by measuring its weight loss vs. temperature or vs. time during an isothermal test.

The analyses were carried on a Thermal Analysis TA ATG Q500 apparatus. In this analysis, the weight of a sample (a few milligrams of polymer) was mea-

sured continuously while the temperature was increased at a 10°C/min rate up to 600 °C. The sample was under nitrogen flow (90 mL/min) during all analysis, to prevent thermo-oxidative degradation. The weight loss was then plotted versus the temperature of the apparatus.

3 Simulation techniques

The molecular modelling approach is separated into two axes: the first one through the use of Quantitative Structure-Property Relationships method, and the second one using molecular dynamics simulations

3.1 Quantitative Structure-Property Relationships method

3.1.1 Introduction and historical point of view

The first molecular simulation technique that was used during this study was the so-called Quantitative Structure-Property Relationships (QSPR) method. This method allows a quick screen of chemicals (organics, drugs, polymers, etc.) for a wide range of properties. This method is also more often called QSAR for Quantitative Structure–Activity relationships when applied to biological systems, especially in the pharmaceutical industry.

QSPR are based on the assumption that the structure of a molecule (i.e. its geometric, steric and electronic properties) must contain the features responsible for its physical, chemical, and biological properties, and on the ability to represent the chemical by one, or more, numerical descriptor(s). This assumption was made at the end of the 19th century, but since this method needs extensive databases to complete quantitative and accurate calculation, its practical use is more recent.

It has been nearly 40 years since the QSAR modeling was firstly used into the practice of agrochemistry, drug design, toxicology, industrial and environmental chemistry. Its growing power in the following years may also be attributed to the rapid and extensive development in methodologies and computational techniques that have allowed to refine the many variables and approaches used in this modelling approach [11, 12]. This technique is nowadays widely used in the drug discovery process in the pharmaceutical industry.

The application of the QSAR methodology to material science is much more recent. Previous QSPR approaches have relied on statistical interpolation from observed structure-property relationships using functional group contribution methods [13, 14]. These approaches restricted property predictions to those polymers

comprised of a specific set of known chemical groups. But for the application of this method in a accurate way to polymer materials, topological information have to be taken into account.

3.1.2 Synthia

The QSPR software that was used for the present study is the Synthia [15] software from Accelrys company.

Synthia uses topological informations and more specifically connectivity indices derived from graph theory [16]. In mathematics and computer science, graph theory is the study of graphs, which are mathematical structures used to model pairwise relations between objects from a certain collection. So Synthia is essentially based upon individual atoms and bonds. With no database of functional group contributions required, properties can be predicted for polymers comprised of the nine elements: carbon, hydrogen, nitrogen, oxygen, silicon, sulfur, fluorine, chlorine, and bromine. Synthia is based on works conducted by Dr. Jozef Bicerano of The Dow Chemical Company, where the methodology has been extensively tested in practical work [17].

3.2 Molecular dynamics simulation

A theoretical background of molecular dynamics (MD) is provided in appendix A.

In our project, the aim of these simulations was to produce a density vs. temperature chart, from which the glass transition temperature of the modelled polymer could be extracted. All simulations were performed with the Material Studio software [18], also from the Accelrys company, using the COMPASS forcefield [19, 20]. The simulations were carried out in 3 steps:
  – polymer chain construction and preparation of the simulation
  – running the simulation itself
  – extraction of the results from the simulation data
These 3 steps are explained in details below.

3.2.1 Preparation of the simulation

The first step of every simulation is the definition of the system, such as defining the number of atoms in the system, several parameters (temperature, pressure), the boundaries... In our case, for MD simulations, this definition consists on the construction of the polymer chains in a state as close as possible to the reality. In order to achieve this goal, the first phase was the building of the polymer repeating

unit, as showed on figure 2.10, and to define the head (h) and tail (t) atoms of the
repetitive unit.
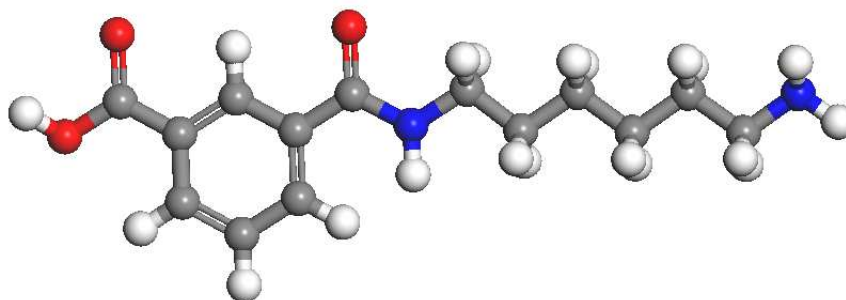
Figure 2.10: Repeating unit of a PA 6I.

Then, the polymer chain itself is constructed at the desired chain length by
repeating the units. It is possible to chose the repeating pattern, such as head-to-
tail, hh, or tt. A random torsion angle is applied between the consecutive repeating
units during the construction, and the chain ends are tailored in order to respect
the reality (figure 2.11), i.e. on one chain end a carboxylic acid group and on the
other end an amine chain end.

After this construction step, the chain undertook a geometry optimization step
by using the Forcite Plus module of the Materials Studio software, with Smart
Algorithm method. This algorithm is a cascade of the steepest-descend, ABNR
(Adjusted Basis set Newton-Raphson), and quasi-Newton methods as the system
approaches its equilibrium.

Copolymers could also be constructed by using the same process. Two repeating
units are defined, then a copolymer chain is constructed, either random or any other
copolymer structure with the use of reaction probabilities.

The last step of the preparation is the construction of the "bulk" system. Indeed,
the construction of the polymer chain was representative of an isolated molecule in
the vacuum. However in reality a chain is never isolated, but surrounded by many
other chains. In order to calculate these interactions between different chain, a bulk
system has to be created. This construction was performed by the Amorphous Cell
of the module of the Materials Studio. Periodic "cells" were defined, in which a
certain number of chains was packed. The simulation of a cell with only one chain
but a very long one would be as accurate than the simulation of a cell filled with
several shorter chains. However the simulation with shorter chains would runs much
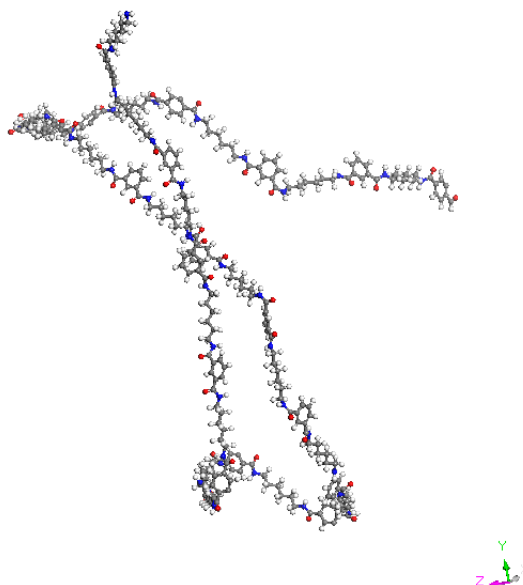
Figure 2.11: Chain of PA 6-I_{80}/6-T_{20} with 20 repeating units.

faster because the system would have more degrees of freedom and would go to an equilibrium state much faster. This is true up to a certain point, indeed if the chains are too short, the intra-molecular interactions would be underestimated compared to inter-molecular interactions. So we choose in this thesis to put in every cell constructed 3 chains made by 20 repetitive units each.

This cell was then replicated an infinite times in every directions. So, by describing one cell, all the space is covered, and boundary effects are cancelled. This technique is called "periodic boundary conditions". A typical cell is showed on figure 2.12.

With this technique, the polymer material properties could be simulated with the best accuracy possible.

3.2.2 Running the simulation

After the construction of the simulation box, the structure need to be equilibrated prior of the calculation. This first step is called equilibration step, contrary to the second step which is called the production step.

In order to achieve a good and quick relaxation of the system, the simulation box has to be heated well above its glass transition temperature, to provide the maximum molecular mobility. So the first relaxation step is a 300 ps molecular dynamics run
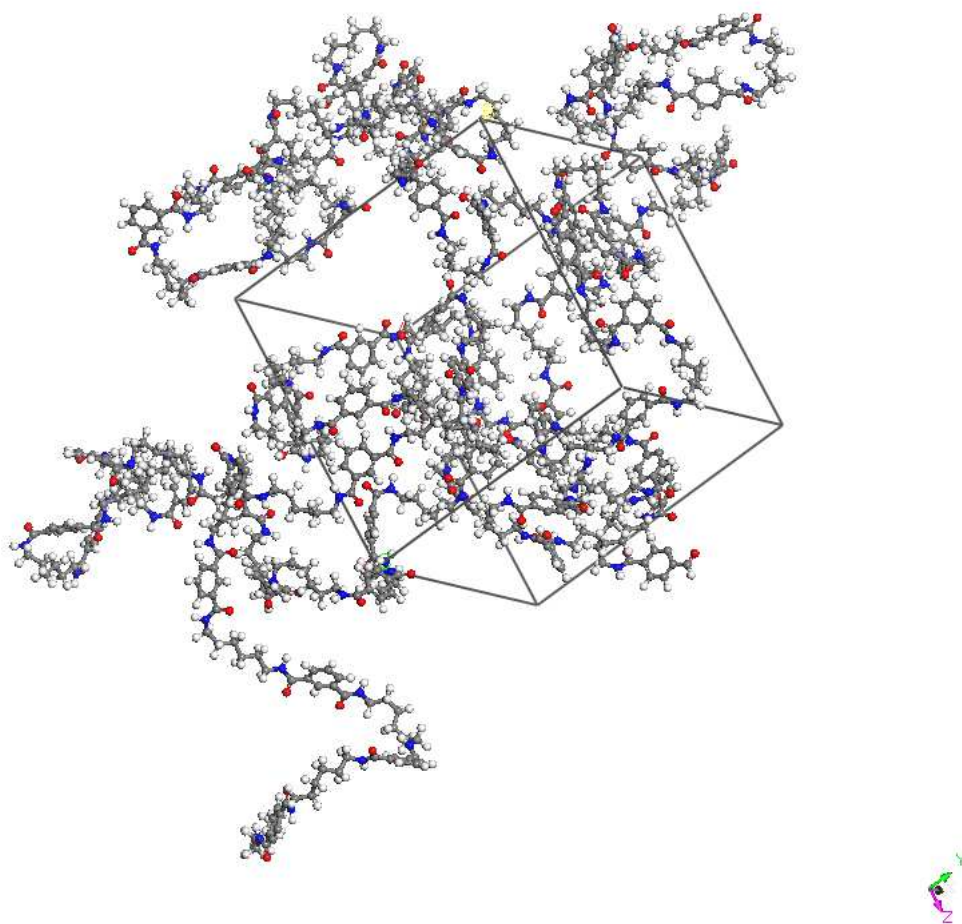
Figure 2.12: 3 chains of PA 6-I_{80}/6-T_{20} packed in a cell.

at 500 K (227°C, so more than 100°C above the expected glass transition). The first 100 ps dynamics were carried out in the NVT ensemble (isochoric) in order to quickly equilibrate the temperature, then the next 200 ps were carried out in the NPT ensemble (isobaric) to let the system relax.

After this relaxation step, the production of data could start. The principle of the simulation consists of a succession of several MD steps of 300 ps, while decreasing the temperature. During the first 100 ps, the temperature is regulated with a velocity-scale thermostat (temperature difference maximum of 10 K). This thermostat leads to a quick change of the temperature and is efficient to reach the system's equilibrium. For the following 200 ps, a Nosé-Hoover thermostat (see appendix A) is used (Q ratio of 1). This thermostat is better suited for the production of a stable and realistic structure and so for the production of data. At the end of these 200 ps, the temperature is decreased by 10 K and the MD cycle starts again (a 10 K decrease in 100 ps means a decrease at 10^{11} K/min).

This procedure is applied until the temperature has reached a desired value, which is usually the room temperature, or 50 K below the glass transition. This protocol is displayed on Figure 2.13
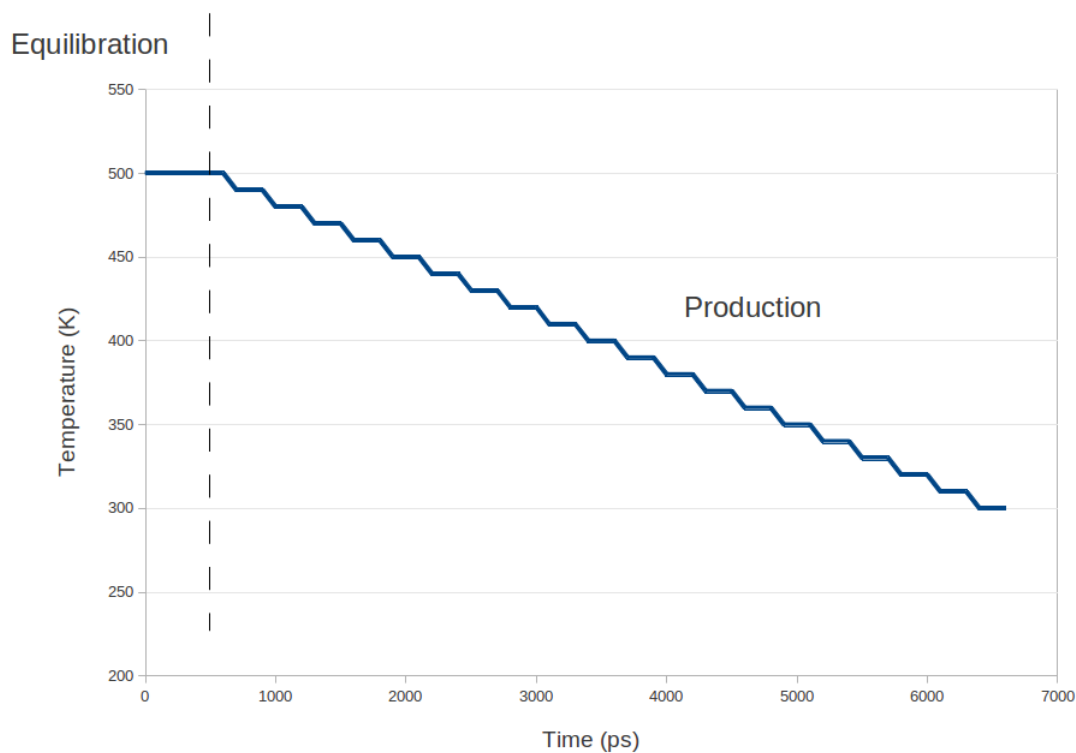
Figure 2.13: Protocol of the molecular dynamics simulations

During the simulation, different parameters were calculated at each time step of 1 femto second (1 iteration). Every 1250 steps (1.25 ps), a frame was saved. This frame contains the coordinates, velocities and forces applied to every atom of the system. The software used these 1250 iterations to calculate the density and temperature of the frame.

3.2.3   Extracting results

At the end of the simulation, the density as a function of the simulation time (a frame being the time step) is obtained. With a comparison with the setpoint temperature with regards to the simulation steps, it is possible to obtain a density vs. setpoint temperature study table. For each temperature step, the density is averaged over the 200 ps of the production step. Finally an average density as a function of the temperature chart (as shown on figure 2.14) is obtained.
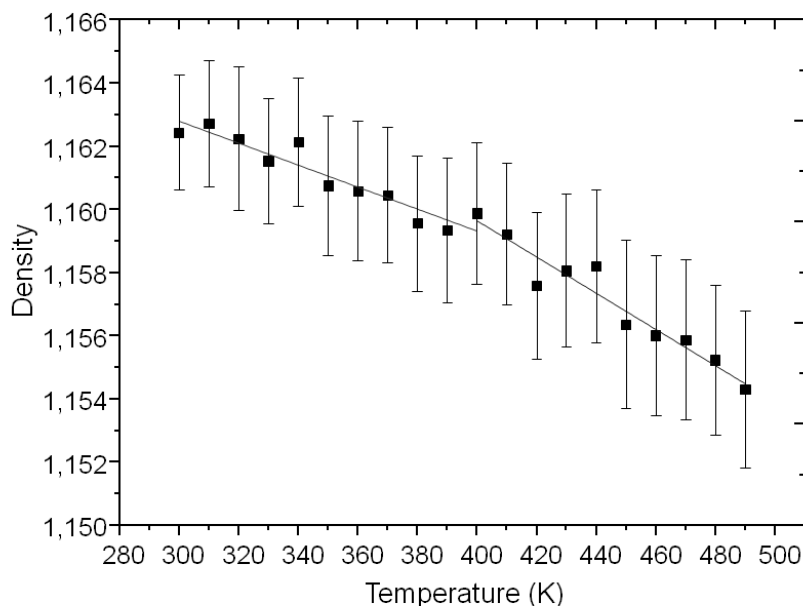
Figure 2.14: Typical density vs temperature chart.

The glass transition is observed at the intersection of the linear regression of the two parts of the chart. These two parts correspond to the two states of the polymer material: glassy at low temperature and molten or rubber-like state at higher temperature. The change of the slope of the linear regression is explained by a change of the thermal expansion coefficient of the material through the glass transition.

An averaging on a few simulations with different starting configurations is necessary, in order to get rid of special configurations (chains trapped, interweaving, ...) that could change the local mobility of the chains and so the result of the simulation.

3.2.4 Presentation of the modelled PPA

The simulation procedure above, in addition to QSPR, was used to model a series of PPA based on petroleum monomers such as terephthalic acid, isophthalic acid and HMDA. The composition of this PA 6-T/6-I series is shown on table 2.2. The counterpart of these diacids is pure hexamethylene diamine.

Simulation	TPA (mol %)	IPA (mol %)
1	0	100
2	10	90
3	20	80
4	30	70
5	40	60
6	50	50
7	100	0

Table 2.2: Molar composition of the simulated polyphthalamides by MD

From experiments it is known that these copolymers became semi-crystalline as soon as more than 50 % of the diacid part is composed of terephthalic acid. And since the modelling of the crystallization phenomena is not possible by MD simulations, only PPA with 0-50 % of TPA were modelled. The 100 % terephthalic polymer is only for comparison with literature data.

For the QSPR simulations, all copolymers ranging from 0 to 100 % of terephthalic acid ratio where modelled (10 % steps) with a molar mass of 20000 g/mol. In these simulations too, only amorphous polymers can be modelled.

4   Results

The first observations that could be done on the polyphthalamides that were synthesized is that they are all transparent, light yellowish, materials. The fact that these materials are optically transparent led us to suppose that they were amorphous. Pictures of these materials are displayed in Appendix B

4.1   Chemical characterizations

4.1.1   Viscosimetry

Results of the solution viscosimetry analysis are presented in table 2.3. In this table, the reduced viscosity (calculated from equation (2.1)) and intrinsec viscosity (calculated from equation (2.5)) of the PA 6-I$_x$/6-T$_y$ co-polyphthalamides is displayed.

Composition (Isophthalic/Terephthalic)	η_{red} (mL/g)	$[\eta]$ (dL/g)
100 / 0	125	1.057
90 / 10	87	0.769
80 / 20	130	1.092
70 / 30	106	0.918
60 / 40	163	1.324

Table 2.3: Reduced viscosities of PA 6-I$_x$/6-T$_y$ copolyhthalamides

All polymers were synthesized with the same protocol but exhibits different reduced viscosities. However, this variation cannot be correlated with the increase of the terephthalic acid ratio. This effect was noticed during the different synthesis and in particular during the reproduction of syntheses with the same compositions of monomers that gave very different reduced viscosities. This shows the poor reproducibility of this type of synthesis with this set-up. This may be caused by the non-homogeneity of the temperature in the reactor during the bulk synthesis of the PPA and by the poor control of the reaction parameters in the type of devices that we used.

4.1.2   NMR

The proton NMR analysis was used to confirm the composition of the different synthesized copolyamides. The spectrum of a PA 6-T$_{80}$/6-I$_{20}$ is presented in figures 2.15 and 2.16. In the figure 2.16, a zoom over the aromatic protons zone is shown

and the peak identification is presented. The chemical shifts for all protons are shown in table 2.4.
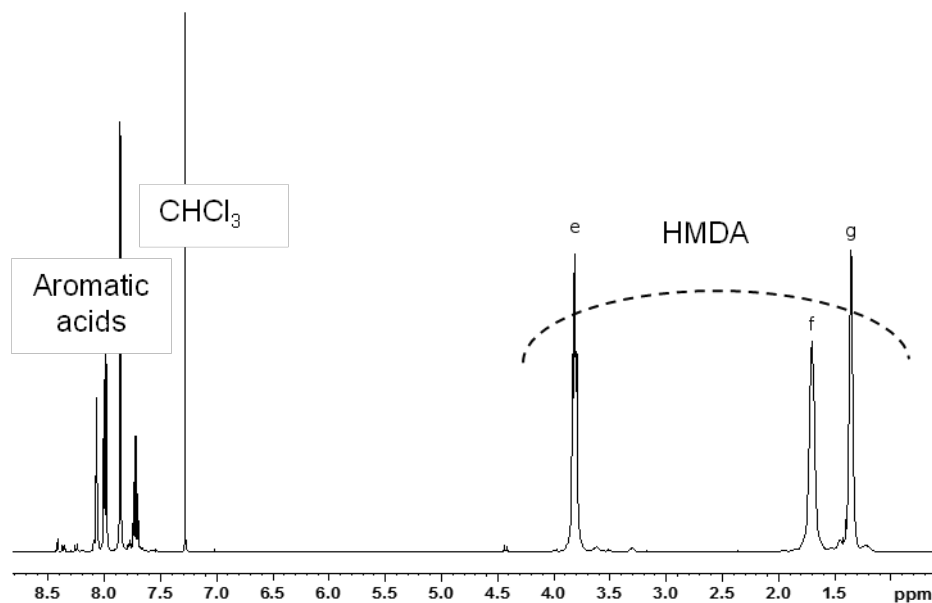
Figure 2.15: ^{1}H NMR, 400MHz, CDCl$_3$ with TFAA, copolymer PA 6-I/6-T

The isophthalic/terephthalic acids ratio is accessible through the calculation of the different integrals with the following equation:

$$\frac{terephthalic}{isophthalic + terephthalic} = \frac{I_d}{I_a + I_b + I_c + I_d} \tag{2.7}$$

where I_i is the integral of the corresponding "i" peak.

The results of the NMR characterization showed that in all synthesized polymer the TPA/IPA composition of the copolymers corresponds to the feeding ratio of the reactor.
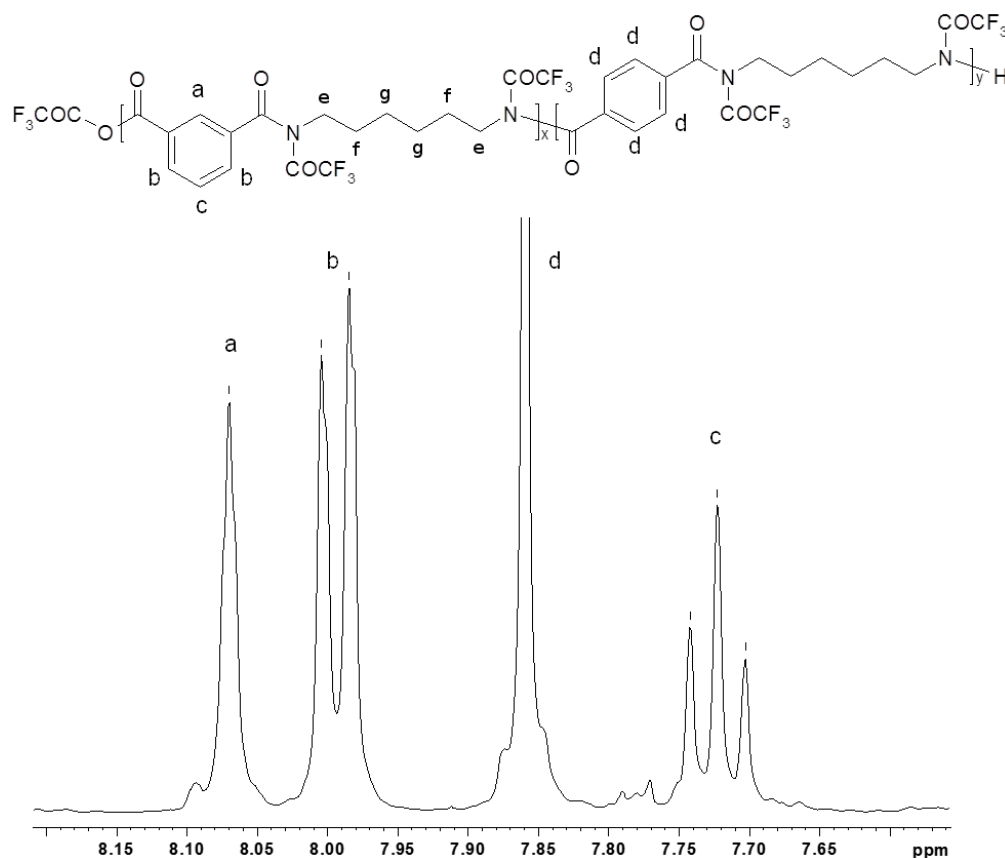
Figure 2.16: ^{1}H NMR, 400MHz, CDCl$_3$ with TFAA, copolymer PA 6-I/6-T, 7.5-8.2 ppm range
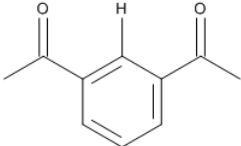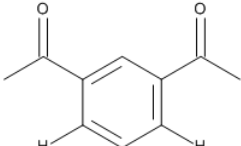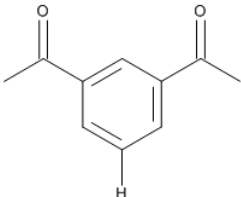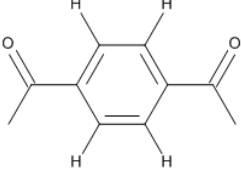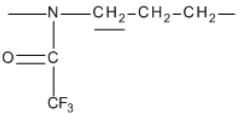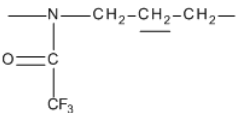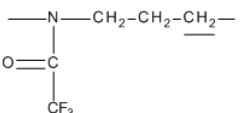
Proton	Group	Chemical shift (ppm)
a		8.07
b		8.00
c		7.72
d		7.86
e		3.80
f		1.70
g		1.35

Table 2.4: Chemical shifts (CDCl$_3$/TFAA) of PA 6-I_{80}/6-T_{20}

4.1.3 SEC

The results of the size-exclusion chromatography on modified PPA , in comparison with solution viscosimetry results, are presented in table 2.5. All presented molar mass are recalculated to take into account the modification due to derivatization and are the "real" mass.

NMR	SEC				Viscosimetry	
Composition (Isophthalic/Terephthalic)	DPn	$\bar{M}_n$ (g/mol)	$\bar{M}_w$ (g/mol)	$\bar{M}_w$ / $\bar{M}_n$	η_{red} (mL/g)	$[\eta]$ (dL/g)
100 / 0	63.8	15700	33100	2.1	125	1.057
90 / 10	34.1	8400	20000	2.4	87	0.769
80 / 20	65.8	16200	31000	1.9	130	1.092
70 / 30	51.2	12600	29100	2.3	106	0.918
60 / 40	54.5	13400	38900	2.9	163	1.324

Table 2.5: Molar mass and reduced viscosity of synthesized polyamides

The first comment that could be done from the data shown in this table, is the confirmation of the correlation between molar mass by SEC and the reduced viscosities of the polymers. Indeed when the reduced viscosity of the PPA (easily measured) is plotted as a function of the molar mass measured by SEC as showed on the figures 2.17 and 2.18, this correlation seemed obvious. It was especially true for the weight average molar mass, which is more closely related to the hydrodynamical volume than the number average molar mass.

Equation	y = a + b*x		
		Value	Standard E
ln eta	Intercept	-4,543	1,75575
	Slope	0,9055	0,17042
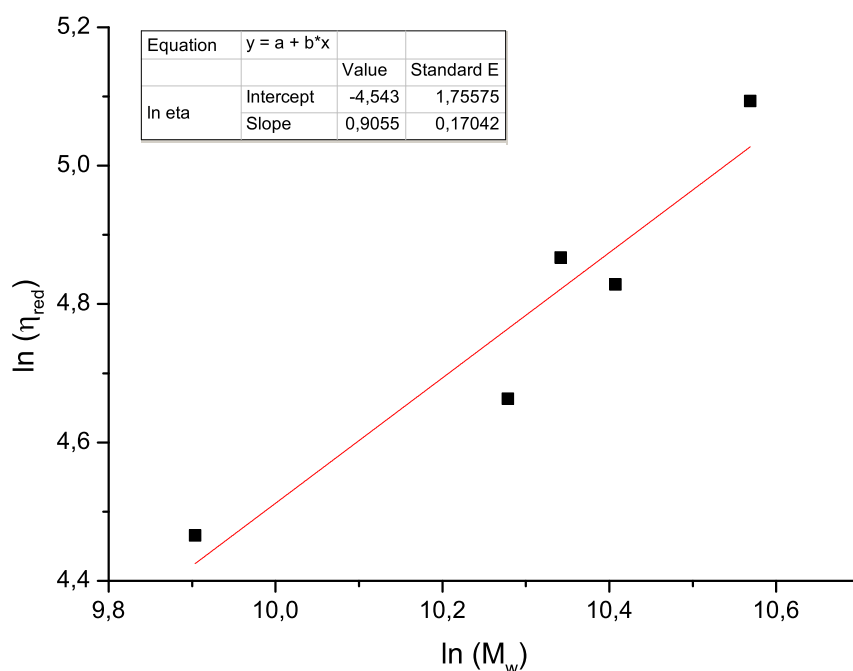
Figure 2.17: Reduced viscosity as a function of $\bar{M}_w$ (by SEC)

These empiric master curves linking the reduced viscosity to the molar mass could help us to make quick assumptions of the molar mass order of magnitude.

The value that deviates from the fitted line in the $\bar{M}_n$ plot is the PPA with the 60/40 (TPA/IPA) composition. For this polymer the polydispersity, $I_p = 2.9$, deviates from its normal value of 2 for polymer obtained by polycondensation. This increase in the dispersity of the chain lengths could be explained by the increase of the terephthalic content in the composition, which imposes a higher reaction temperature. This high temperature (300°C) promotes side reactions, as explained in paragraph 2.1.2.

The different copolymers exhibit number average molar mass around 12000 g/mol, corresponding to an average degree of polymerization of 50. These mass are typical
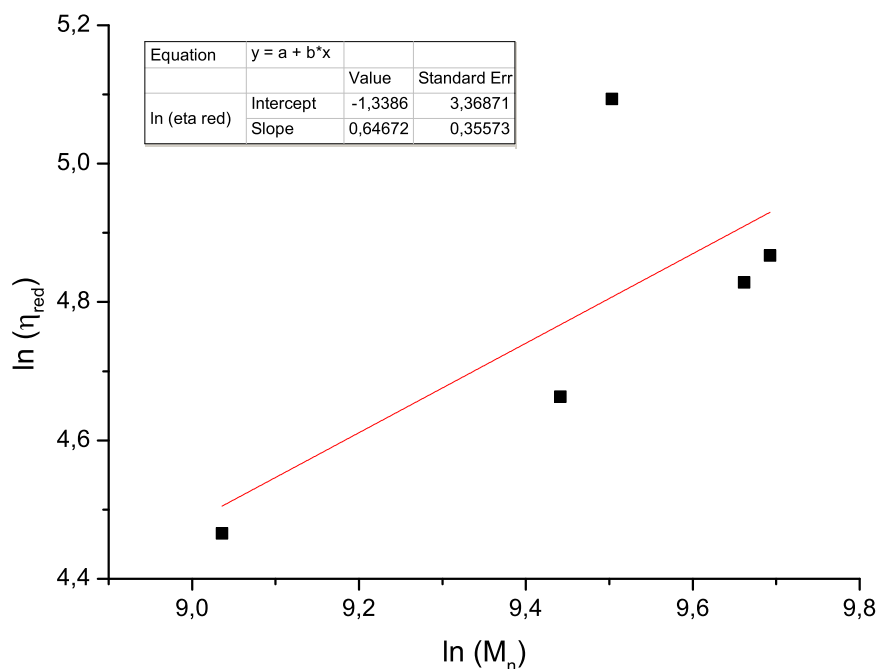
Figure 2.18: Reduced viscosity as a function of $\bar{M}_n$ (by SEC)

for polyphthalamides made with direct polycondensation techniques as they are in a range between 12000 and 16000 g/mol. Also a variation of the molar mass of the synthesized PA is observed between different compositions. However, this variation cannot be correlated with the increase of the terephthalic acid ratio. This effect was also noticed on the reduced viscosities and as explained previously, it may be caused by the poor reproducibility of the syntheses due to the inhomogeneity of the reaction mixture with our set-up.

The Mark-Houwink "type" relationship (Equation (2.9)) was an inspiration for establishing correlations between molar mass and solution viscosity even if we cannot called them Mark-Houwink because we have copolymers and not homopolymers.

$$[\eta] = K M_v^a \tag{2.8}$$

It is possible to draw a graph linking the intrinsic viscosity of our copolymers with the molar mass measured by SEC in order to extract Mark-Houwink type parameters (Figure 2.19)

On this plot, it is the natural logarithm of the intrinsic viscosity that is plotted as a function of the molar mass, in order to extract from the graph "Mark-Houwink" like parameters. Indeed the Mark-Houwink equation is presented in equation 2.9.
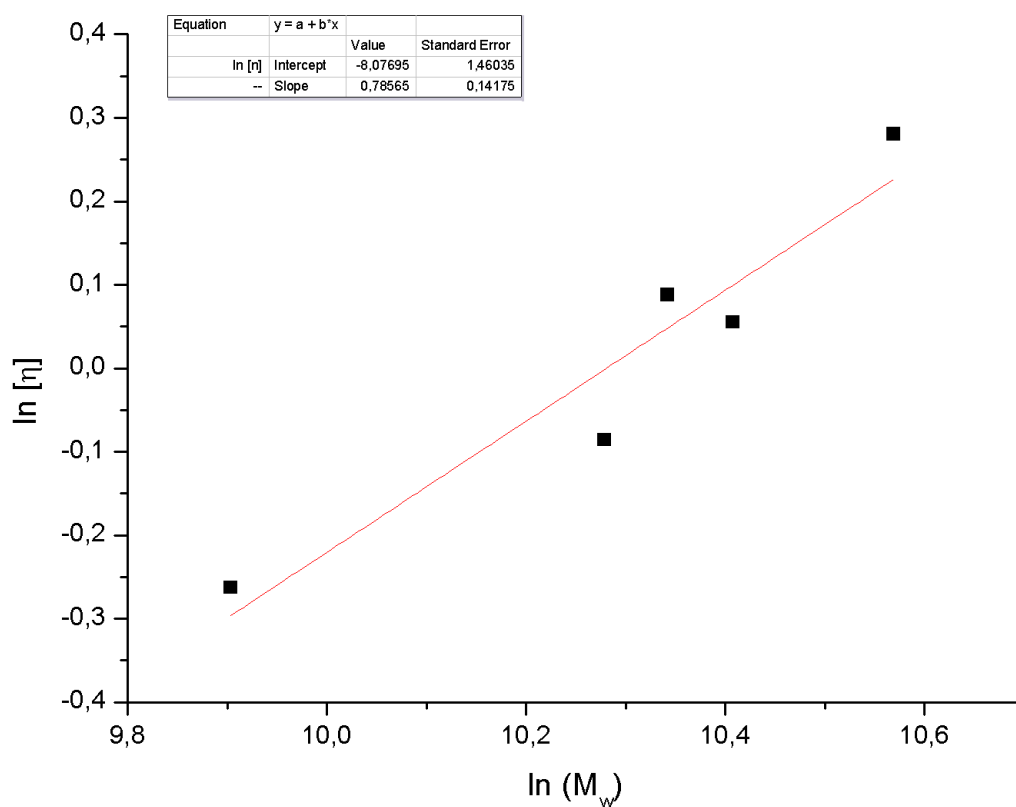
Figure 2.19: Intrinsic viscosty as a function of $\bar{M}_w$ (by SEC)

By taking the nature logarithm of this expression, we could obtain the equation 2.10.

$$[\eta] = K'M^{a'} \tag{2.9}$$

$$\ln[\eta] = \ln K' + a' \ln M \tag{2.10}$$

Here the same mathematical operation was done and from the chart we could directly extract the "Mark-Houwink"-like parameters where K' is the intercept of the linear fit with the y axis and a' is the slope of this linear fit. Here the weight average molar mass was taken for the Mark-Houwink type equation instead of the viscosimetric average molar mass $\bar{M}_v$ which is normally used in the Mark-Houwink equation. The $\bar{M}_w$ was easier to measured (by SEC) and is closer to the viscosimetric average molar mass compared to the number average molar mass $\bar{M}_n$.

It is said that for flexible polymers $0.5 \leq a' \leq 0.8$ and for semi-flexible polymers $a' \geq 0.8$. In our case $a' = 0.79$, which is coherent with the semi-flexible nature of the semi-aromatic PPA (Figure 2.17). In our case $K' = 31.3$ mL/g.

4.2 Thermal properties

4.2.1 DSC

The different synthesized copolymers were characterized by Differential Scanning Calorimetry to study their thermophysical properties and the influence of the terephthalic acid content. All thermograms are presented in Appendix D. No melting or crystallization peak was present in the temperature range of the analysis between 25°C and 330°C, but a glass transition was observed at 124°C in the case of PA 6-I (Figure 2.20). This thermogram shows that the PA 6-I is an amorphous polymer. The other synthesized PPA exhibit the same behavior, with only a change in the value of the Tg. The glass transition temperatures for the various synthesized PPA are displayed on table 2.6.

Terephthalic acid ratio	Glass transition temperature (°C)
0	122
10	123
20	124
30	124
40	125
100	140* [21]

Table 2.6: Glass transition temperatures for the synthesized copolyphthalamides
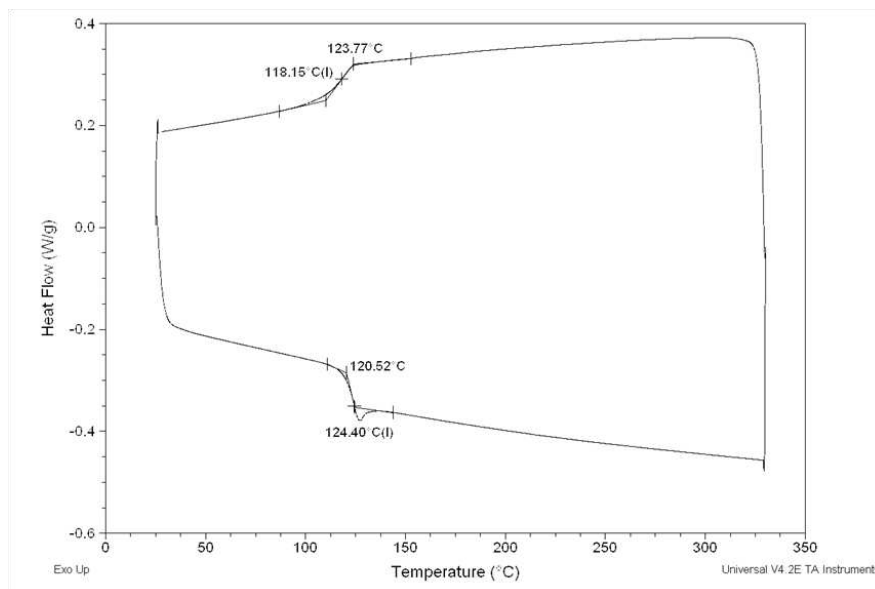
Figure 2.20: Thermogram of a PA 6-I by Differential Scanning Calorimetry

The introduction of a fraction of terephthalic acid in the polymer mainly composed of isophthalic acid and HMDA leads to a change in the glass transitions of the copolymers. A chart displaying the variation of the glass transition temperature as a function of the terephthalic content is shown in Figure 2.21.

The Tg of the copolymers varies between 122 and 140°C from pure PA 6-I to pure PA 6-T respectively. As explained previously, we did not synthesized any PPA with higher content of terephthalic acid because the polymers become semi-crystalline and we have to face experimental problems with our traditional laboratory glassware.

The slight increase in Tg that we noticed is in agreement with some published data on pure PA 6-I, PA 6-T and their copolymers [23]. This moderate increase is related to the positions of the carboxylic acid functions on the aromatic ring on terephthalic and isophthalic acids. Indeed the 1,4 positions of the TPA produce a monomer that is symmetric (180° between the two functions) with a very rigid body (benzene ring), whereas the 1,3 positions of the isophthalic acid give a non-flat angle. This leads to very straight and rigid PA 6-T chains, with a reduced mobility and then a higher Tg than PA 6-I, which has more torsions between neighboring monomers and more flexibility.

The result for PA 6-T found in the literature showed that its Tg was equal to 140°C [21]. It is much higher than the expected value (129°C) if the increase of the glass transition temperature was linear with the increase of terephthalic acid ratio. This could be explained by the semi-crystalline behaviour of this polymer. Indeed, the amorphous chains trapped between crystalline domains have much less
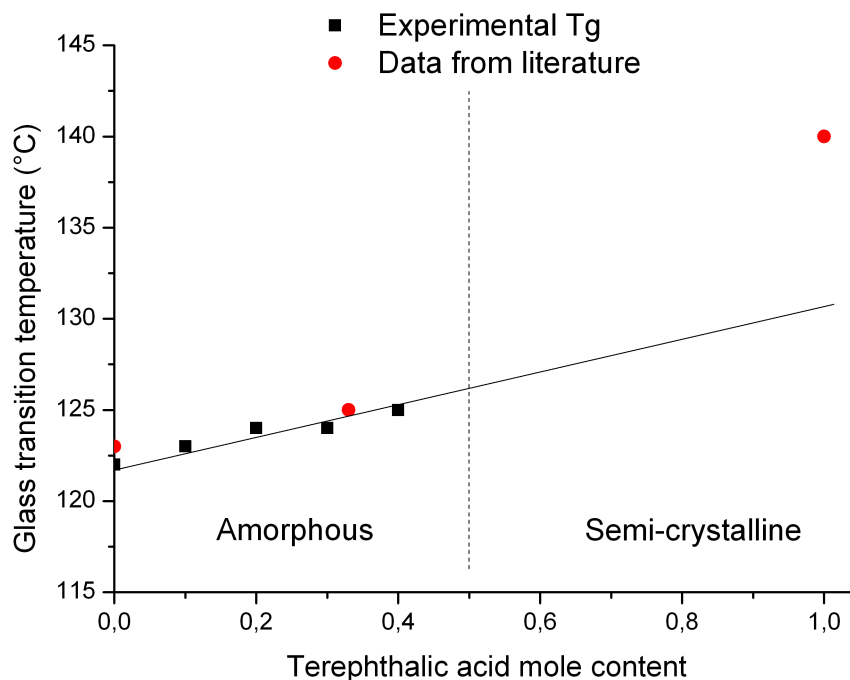
Figure 2.21: Evolution of the glass transition temperature as a function of the terephthalic acid mole content (literature from ref [21, 22])

mobility and free volume than the chains in a fully amorphous polymer, which increases the glass transition temperature. Another factor of this increase is related to the measurement technique, because DMA analysis gives higher glass transition temperature measurement compared to DSC (usually 10°C per decade of frequency). The combination of these two factors could explain the significantly higher value of Tg of the pure PA 6-T compared to the copolyamides with a majority of isophthalic acid.

4.2.2 TGA

Thermogravimetric analyses were performed on the various model synthesized PPA. A typical example of a PPA analysis is shown on figure 2.22. Its degrades in a single step process. The TGA analysis of other PPA are presented in Appendx C.

All the polyphthalamides synthesized showed a good resistance to thermal decomposition. Indeed, a 5 % weight loss was observed at approximately 400°C and a 50 % weight loss at 450°C for all PPA. There is no significant influence of the amount of terephthalic acid used for the synthesis. All PPA behave in the same way This features, in combination with high glass transition temperature, makes
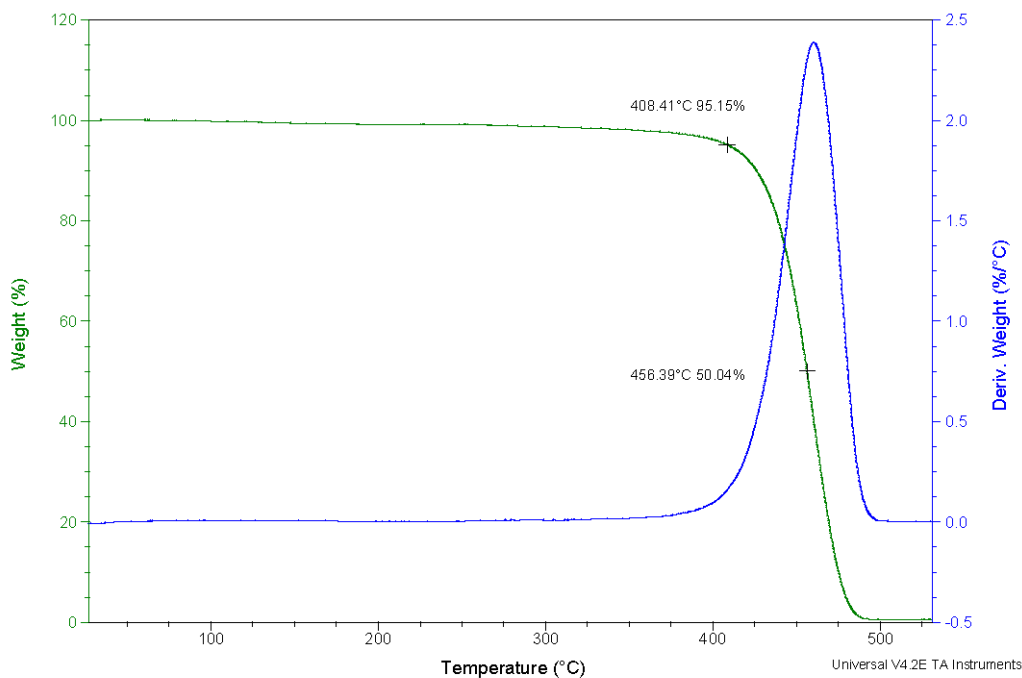
Figure 2.22: Typical thermogravimetric analysis thermogram (under N_2)

the PPA suitable materials for high temperature uses.

4.3   Simulation results

The results of the simulation protocol of QSPR and MD with the intersection method are displayed in the table 2.7. The results presented are an average over 3-5 simulations form different starting conformations. The standard deviation of the MD simulations was calculated as the square root of the variance of the glass transition temperatures calculated by MD over the 3-5 simulations for each composition.

All the calculated glass transitions are in the range between 130 and 190 °C. These values are coherent and realistic on a physical point of view (classical PPA T_g range between 100 and 180 °C). The general trend that could be extracted from this table is that the glass transition temperature of the copolymers increases as the amount of TPA increases (from 135 °C for pure PA 6-I to 162 for the pure PA 6-T by MD results).

Another observation that could be made is that the QSPR modelling give results that are approximately 20 degrees higher than MD simulation and with a higher standard deviation (7 % of the absolute temperature), when compared to MD simulations. Indeed the MD simulations standard deviation is approx. 15 °C,

TPA ratio	QSPR		MD	
	T_g (°C)	Standard deviation	T_g (°C)	Standard deviation
0	155	30	135	15
10	158	30	136	15
20	161	30	142	19
30	165	31	140	13
40	168	31	142	16
50	171	31	–	–
60	175	31	–	–
70	178	32	–	–
80	182	32	–	–
90	185	32	–	–
100	188	32	162	15

Table 2.7: Glass transition temperature of a series of polyphthalamide by MD studies

which may seems high but actually this variation is only about 4 % of the absolute temperature (in Kelvin). In order to increase the accuracy of the MD simulations, we could increase the number of steps in the protocol, i.e. calculate the density every 5°C instead of 10°C, or we could also increase the duration of each step (for example 500 ps with 200 ps of equilibration and 300 ps of production of data) in order to let the system reach its equilibrium. A last technique could be the averaging over more than 3 to 5 different starting configurations, however all these methods to increase the accuracy have a big cost in terms of calculation times.

4.4 Comparison with synthesized PPA

The goal of these simulations was to develop a protocol that could match with a certain precision to experimentally prepared materials. The comparison between the simulations and prepared materials' glass transition temperature is presented in figure 2.23.

On this chart, the glass transitions temperature of PPA with various terephthalic acid content, either measured by DSC for experimentally prepared materials or calculated by MD protocol or the group contribution technique, are presented. The first observation that could be made is that both the experimental and modelling data exhibit the same trend: an increase in the glass transition temperature with the increasing amount of terephthalic acid in the copolymers. The T_g calculated by the QSPR method is significantly higher than the experimental one, while the
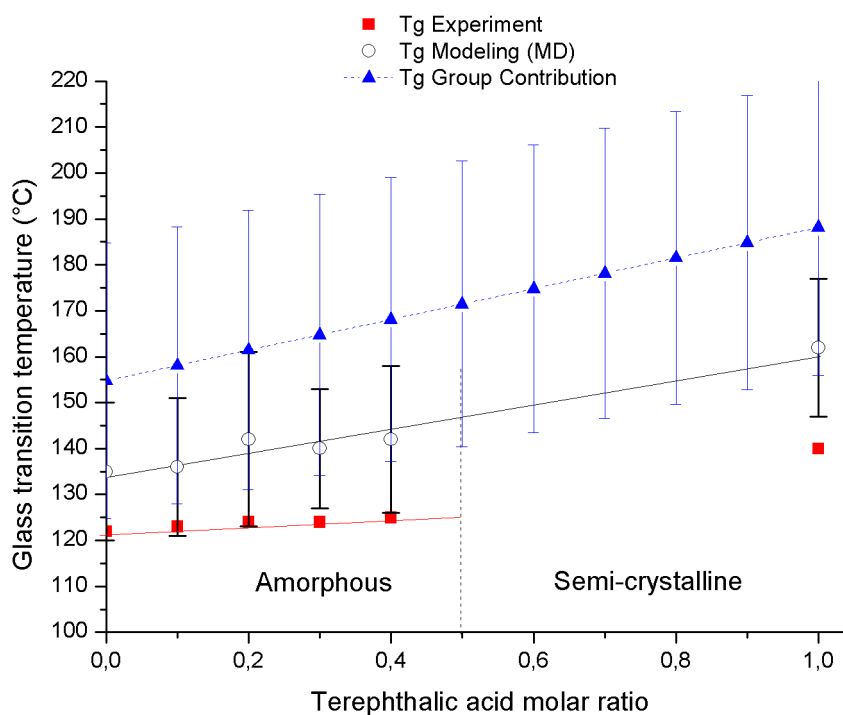
Figure 2.23: Glass transition temperatures as a function of the TPA content in PA 6-I_x/6-T_y copolyphthalamides measured by DSC and calculated with simulations.

MD calculated glass transitions are also higher than experiments but much closer to reality.

The Quantitative Struture-Properties Relationships method also did not take into account the crystallization effects. Indeed, the increase in T_g is linear from pure PA 6-I to PA 6-T. So this method gives a quick but not very accurate estimation of the glass transition temperature of these PPA if the micro-structure of these polymers is not known, especially is they are semi-crystalline.

The MD results are much closer to reality. There is only a 20 K difference between modelled and experimental results. This difference may come from two main phenomena. The first one is the polydispersity. Indeed the modelled polymer material is a monodisperse one, whereas the real PPA has a PDI of approximately 2. This dispersion of the molar mass may lead to a decrease or a broader T_g since the smaller chains could act as plasticizers for the longer ones. The second argument may be the glass transition temperature dependence on kinetics effects. Indeed the time-scales involved in a MD simulation and a DSC experiment are very different. During a DSC experiment, the sample is cooled at a 10°C/min rate, while in a MD experiment a change of 10 °C is obtained in 50 ps. This extremely quick cooling of the material could lead to an early vitrification of the polyphthalamide and then to a higher measured glass transition temperature.

5   Conclusion

In this chapter, a series of polyphthalamide materials were synthesized by condensation between terephthalic and isophthalic acid with hexamethylene diamine. The synthesized materials were characterized by several methods (NMR, DSC, TGA, ...). Their structure was characterized by NMR. It was found that the amount and ratio of the mixture of acids introduced in the reactor were conserved during polymerization. The molar mass of the synthesized PPA were measured by viscosimetry and SEC. It was found that the PPA we synthesized had molar mass and polydispersity index typical for PPA made by melt polycondensation. Their thermal properties where measured by DSC and TGA. It was found that the glass transition temperature of the copolyphthalamides only slighty increases with the amount of terephthalic acid introduced, while the degradation temperatures were not impacted by the terephthalic acid addition.

In a second part, different molecular modelling techniques were used. The Quantitative Structure-Properties Relationships method is based on the relations between the chemical structure of a chemical (or polymer) and the properties ensuing. This

method is very quick (small computation time required) and easy, but the results are not accurate and reliable enough to be used as a prediction tool. However this technique could be used for the large screening of materials and for pointing out major trends.

On the other hand, a molecular dynamics protocol was developed in order to model with a good precision the glass transition temperatures of several polyphthalamides. The polymer chains were built to be as close as possible to real chains and the protocol was made to estimate the glass transition temperatures of these PPA. This method successfully modelled their T_g and its increase with the amount of terephthalic acid in the copolymers. However, when compared to experimental values, modelled glass transitions temperature are on average 20°C higher. This could be explained by the differences in the cooling rates between experimental measurements and modelling protocol which leads to an early glassification of the PPA.

This MD protocol has proven to be successful [24] and could be used to study now polymers from the same class (i.e. polyphthalamides) with the incorporation of new monomers, such as bio-based 2,5-furandicarboxylic acid.

References

[1] M. Fermeglia and S. Pricl, "Multiscale modeling for polymer systems of industrial interest," *Progress in Organic Coatings*, vol. 58, no. 2-3, pp. 187–199, 2007.

[2] Y. Xiao, W. P. Luo, X. Y. Zhang, C. C. Guo, Q. Liu, G. F. Jiang, and Q. H. Li, "Aerobic Oxidation of p-Toluic Acid to Terephthalic Acid over T(p−Cl)PPMnCl/Co(OAc)$_2$ Under Moderate Conditions," *Catalysis Letters*, vol. 134, no. 1-2, pp. 155–161, Nov. 2009.

[3] X. Zuo, B. Subramaniam, and D. H. Busch, "Liquid-Phase Oxidation of Toluene and p-toluic Acid under Mild Conditions: Synergistic Effects of Cobalt, Zirconium, Ketones, and Carbon Dioxide," *Industrial and Engineering Chemistry Research*, vol. 47, no. 3, pp. 546–552, 2007.

[4] X. Zuo, F. Niu, K. Snavely, B. Subramaniam, and D. H. Busch, "Liquid phase oxidation of p-xylene to terephthalic acid at medium-high temperatures: multiple benefits of CO2-expanded liquids," *Green Chemistry*, vol. 12, no. 2, pp. 260–267, Feb. 2010.

[5] T. M. Carole, J. Pellegrino, and M. D. Paster, "Opportunities in the Industrial Biobased Products Industry," *Applied Biochemistry and Biotechnology*, vol. 115, no. 1-3, pp. 0871–0886, 2004.

[6] C. Berti, M. Colonna, M. Fiorini, G. Kannan, S. Karanam, M. Mazzacurati, I. Odeh, and M. Vannini, "Bio-based terephthlate polyesters," Patent WO 2010/078 328 A2, 2010.

[7] O. F. Solomon and I. Z. Ciută, "Détermination de la viscosité intrinsèque de solutions de polymères par une simple détermination de la viscosité," *Journal of Applied Polymer Science*, vol. 6, no. 24, pp. 683–686, 1962.

[8] V. Girardon, I. Correira, M. Tessier, and E. Marechal, "Characterization of functional aliphatic oligoamides using N-Trifluoroacetylation. I- NMR analysis," *European Polymer Journal*, vol. 34, no. 3-4, pp. 363–380, 1998.

[9] H. H. Kausch, N. Heymans, C. J. Plummer, and P. Decroly, *Matériaux Polymères: Propriétés Mécaniques et Physiques.* PPUR presses polytechniques, 2001.

[10] V. Girardon, M. Tessier, and E. Marechal, "Characterization of functional aliphatic oligoamides using N-trifluoroacetylation–II. size exclusion chromatography," *European Polymer Journal*, vol. 34, no. 9, pp. 1325–1330, Sep. 1998.

[11] P. Gramatica, "A short History of QSAR Evolution," *http://www.qsarworld.com*, 2008.

[12] C. D. Selassie, *Chap. 1 : History of Quantitative Structure-Activity Relationships. In Burger's Medicinal Chemistry and Drug Discovery.* John Wiley & Sons, Inc., 2003.

[13] D. W. van Krevelen and K. te Nijenhuis, *Properties of Polymers: Their Correlation with Chemical Structure; their Numerical Estimation and Prediction from Additive Group Contributions.* Elsevier Science, 2009.

[14] A. Askadski, *Physical Properties of Polymers: Prediction and Control*, ser. Polymer Science and Engineering Monographs. Taylor & Francis, 1996.

[15] Accelrys, "Synthia," San Fransisco (CA), 2009.

[16] J. A. Bondy and U. S. R. Murty, *Graph Theory.* New York: Springer, 2008.

[17] J. Bicerano, *Prediction of Polymer Properties*, ser. Plastics Engineering. Taylor & Francis, 2002.

[18] Accelrys, "Materials Studio V5.0, Amorphous Cell, Forcite +," San Fransisco (CA), 2009.

[19] H. Sun, "COMPASS: An ab Initio Force-Field Optimized for Condensed-Phase Applications Overview with Details on Alkane and Benzene Compounds," *The Journal of Physical Chemistry B*, vol. 102, no. 38, pp. 7338–7364, 1998.

[20] H. Sun, P. Ren, and J. Fried, "The COMPASS force field: parameterization and validation for phosphazenes," *Computational and Theoretical Polymer Science*, vol. 8, no. 1-2, pp. 229–246, 1998.

[21] M. Kohan, *Nylons Plastics Handbook*. New York: Carl Hanser Verlag, 1995.

[22] Y. S. Hu, S. Mehta, D. A. Schiraldi, A. Hiltner, and E. Baer, "Effect of water sorption on oxygen-barrier properties of aromatic polyamides," *Journal of Polymer Science Part B: Polymer Physics*, vol. 43, no. 11, pp. 1365–1381, 2005.

[23] A. Siciliano, D. Severgnini, A. Seves, T. Pedrelli, and L. Vicini, "Thermal and mechanical behavior of polyamide 6/polyamide 6i/6t blends," *Journal of Applied Polymer Science*, vol. 60, no. 10, pp. 1757–1764, 1996.

[24] T. Cousin, J. Galy, and J. Dupuy, "Molecular modelling of polyphthalamides thermal properties: Comparison between modelling and experimental results," *Polymer*, vol. 53, no. 15, pp. 3203–3210, 2012.

Chapter 3

Synthesis and properties of furan-2,5-dicarboxylic acid based polyphthalamides

Contents

125

1 Introduction

A protocol for the simulation and calculation of the glass transition temperature of polyphthalamides has been successfully developed in the previous chapter. In this chapter, we will focus on the synthesis, characterization and modelling of FDCA based polyphthalamides.

A series of polyamides made by the condensation of a mixture of isophthalic and FDCA acids with hexamethylene diamine has been synthesized. Their chemical structure and composition have been assessed by NMR, MALDI-TOF mass spectroscopy, SEC and viscosimetry techniques. Their physical properties have been measured by DSC, TGA, and tensile tests, as well as molecular simulation.

2 Experimental methods

2.1 Characterization of the FDCA

The furan-2,5-dicarboxylic acid is our main monomer used in this study. Since this monomer is not common and that the literature on its synthesis and uses is scarce and contradictory (see Chapter 1), an extensive characterization was needed.

2.1.1 Chemical characterization

The supplier claims that the FDCA we bought had a purity of 97 %. In order to verify its purity the first test that was carried was a High Performance Liquid Chromatography (HPLC) experiment. We used a Carbosep 107H column (specially dedicated to organic acids), the sample was eluated in H_2SO_4 0.001 M at 0.5 mL/min of flow rate thus giving 38-40 bars in the system. Detection was done with refractive index. The result is presented in Figure 3.1.
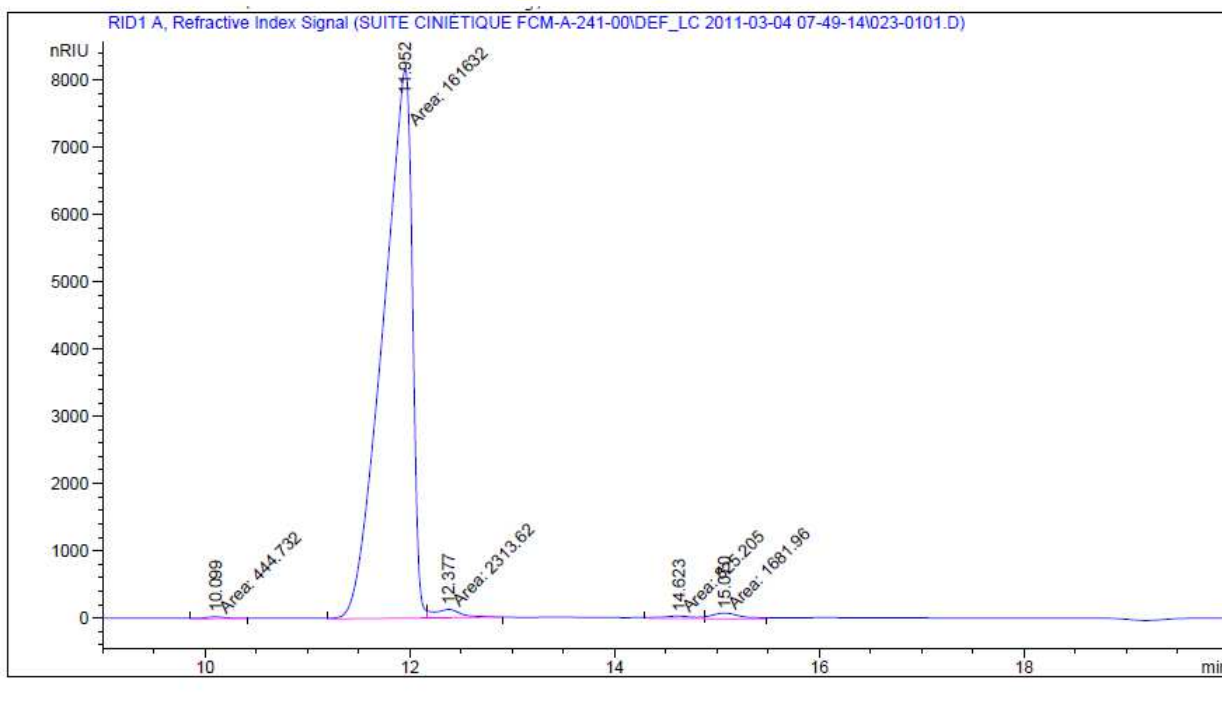
Figure 3.1: HPLC test of the FDCA on acid columns, 5µL injection volume

On this figure the main peak was attributed to the FDCA. The area under the FDCA peak represents 96.9 % of the global area, meaning that our FDCA sample was very pure.

In order to confirm this first assessment, a proton NMR experiment was carried out in DMSO-d6. The spectrum is presented in Figure 3.2.

On this spectrum, the peak corresponding to the FDCA is the one at 7.298 ppm, with his two satellites at 6.940 and 7.666 ppm. By integration of the different peaks displayed on this spectrum, the calculated purity of FDCA was about 99 %. This confirms the high purity of our monomer.
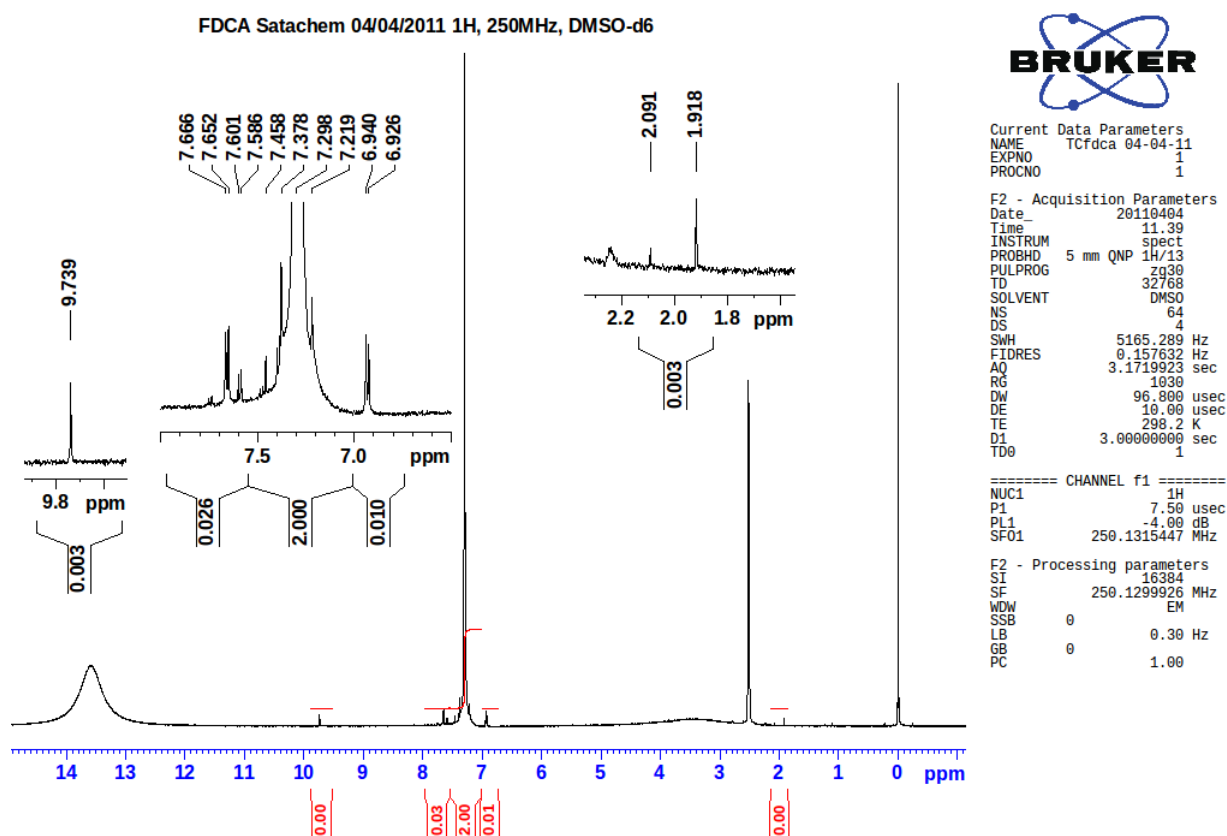
Figure 3.2: ^{1}H NMR of FDCA, in DMSO-d6

2.1.2   Thermal characterization

During the polycondensation reaction, the FDCA will be subject to high temperature conditions. So it is important to characterize the thermal properties and resistance of the furan-2,5-dicarboxylic acid. In order to study these thermal properties, DSC and TGA tests were carried.

The differential Scanning Calorimetry test was performed in an aluminum capsule, at a 10°C/min rate from 25°C to 400°C, under a nitrogen flow. The resulting thermogram is shown on figure 3.3. On the DSC thermogram, during the heating
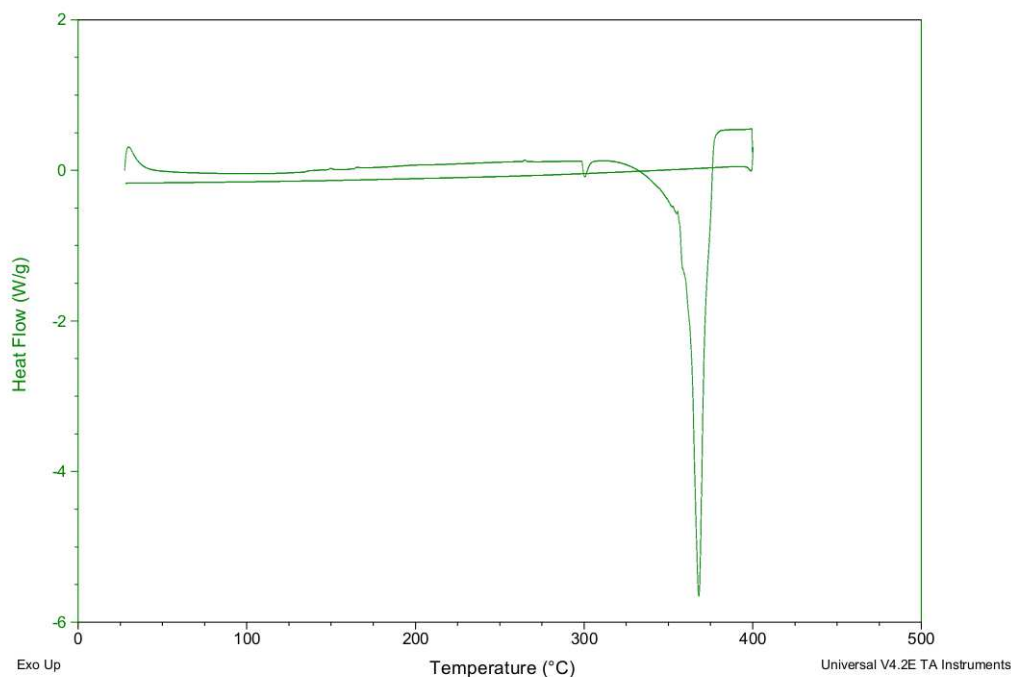
Figure 3.3: Differential Scanning Calorimetry test of FDCA

stage, an endothermic peak was observed at 375°C, whereas during the cooling stage, no change in the heat flow was observed. This endothermic peak could be the sign of a melting; however on the cooling stage no crystallization was observed. So instead of a melting, the endothermic peak is more likely a sublimation or a decomposition.

In order to confirm this decomposition, thermogravimetric analysis experiments were performed under nitrogen flow and also under air flow, as presented in figures 3.4 and 3.5.

In both cases, the degradation of the FDCA starts at 230°C, with a maximum of the first derivative of the weight loss at 310°C. Since there is no difference between this loss of the FDCA under air or nitrogen flow, and beacause the mass measured went quickly to 0, this phenomena was more likely a sublimation than a decompo-
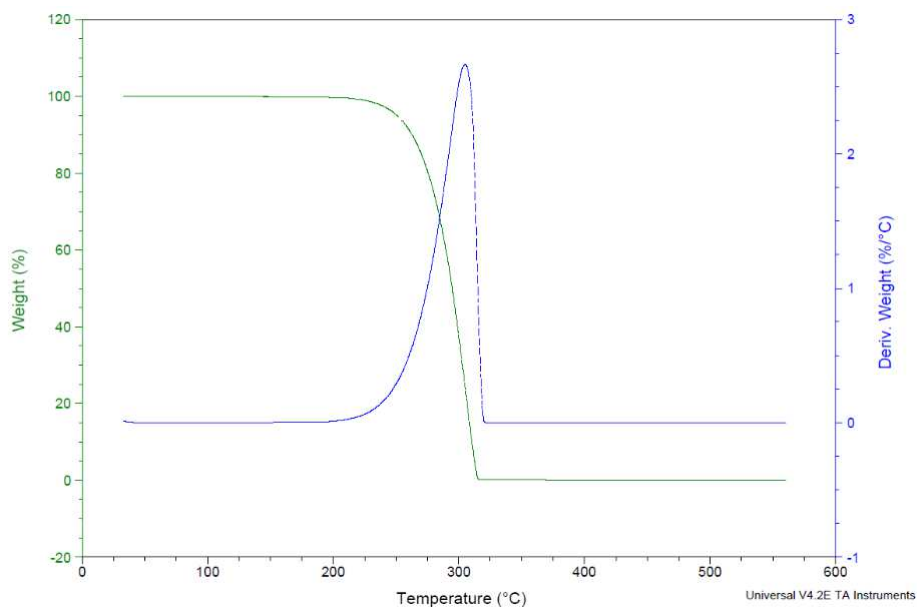
Figure 3.4: Thermogravimetric analysis under nitrogen flow
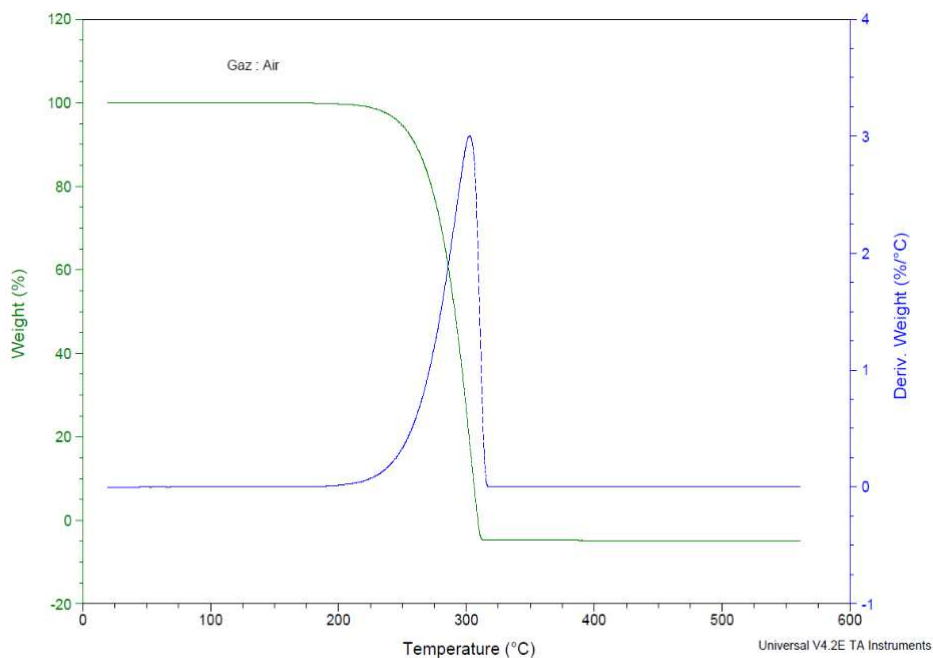
Figure 3.5: Thermogravimetric analysis under air flow

sition. This low thermal stability of the FDCA, even in the absence of oxygen, may causes problems during the synthesis of polyphthalamides, which requires reaction temperatures higher than 230°C.

2.1.3   Conclusion

The FDCA we used was very pure (99 % by NMR), however this monomer exhibits a poor thermal stability under air as well as under nitrogen flow (sublimation starting at 230°C) which may be a problem during polyphthalamides synthesis

2.2   Synthesis

2.2.1   Materials

Hexamethylene diamine 98% (HMDA) was obtained from Sigma-Aldrich, France; 2,5-furandicarboxylic acid 99% (FDCA) was obtained from Satachem CO., China; and isophthalic 99+% (IPA) acid was obtained from BP Chemicals. Additives used in this study were antioxidant (Irganox® 1098, BASF), antifoam (Rhodorsil 411, Rhodia) ans phosphoric acid (Sigma-Aldrich, France). All chemicals were used without further purification.

The FDCA used in this study was not from a biomass origin, but from oil source since the biobased FDCA is still very expensive and the process for its production is only at a pilot-scale. However we expect the two monomers to be identical and the biobased one to be soon available at a reasonable price.

2.2.2   Protocol

In the previous chapter, we synthesized polyphthalamides in traditional laboratory glassware. We found the syntheses to be not reproducible, so in order to improve this, a pilot-scale reactor was used.

The melt condensation polymerization was performed in a high-temperature pilot-scale polyamide reactor (1L, 350°C, 50 bars). This reactor is fully instrumented in order to control the temperature and pressure (Figure 3.6).

The use of a pilot-scale reactor requires the use of additional chemicals such as an antifoam product. Antifoam was needed in order to prevent the formation of a foam composed of a polyamide salt solution that could be deposited on the stirring mechanism. In each synthesis, 200 mg of Rhodorsill 411 antifoam were used. Moreover, we used an antioxydant (Irganox) to improve the FDCA thermal stability as well as prevent theirdegradation of polymers during melt polycondensation.
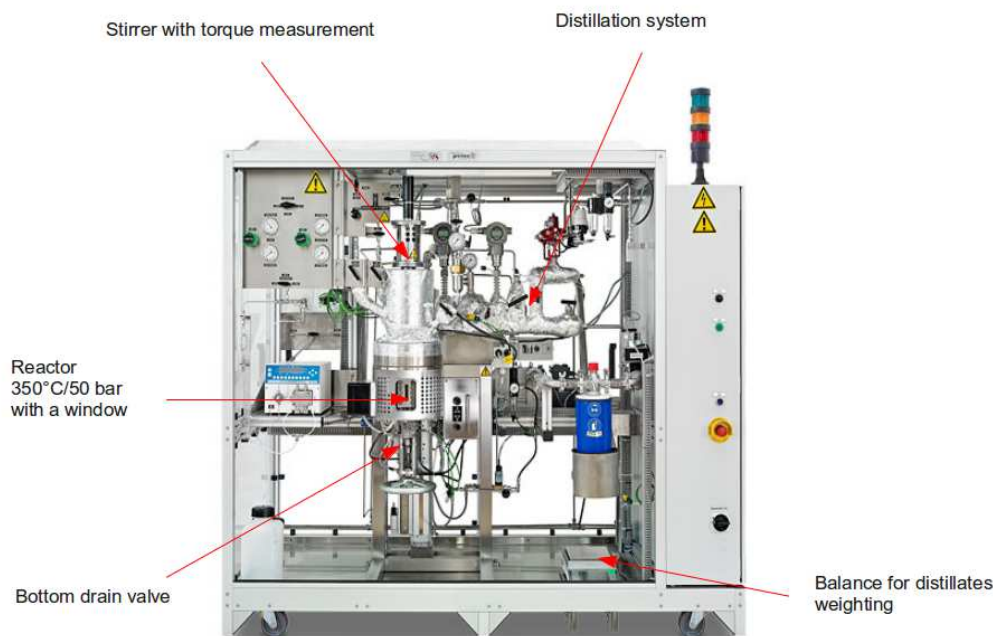
Figure 3.6: Polyamide pilote-scale reactor

Approximately 1.5 g of antioxydant was used in every synthesis. Finally, the last additive was phosphoric acid. It is known to be a catalyst for the polyamide synthesis (approximately 0.5 mol % per synthesis).

The polymerization process is composed of four main steps: water boiling (1), high pressure stage (2), depressurization (3) and a final stage under vacuum (4), as shown on Figure 3.7. The diacid monomers were introduced as powders into the reactor, then the solution of diamine (50 wt % in water) was added. The total water amount added in the reaction mixture was about 50 wt % (approximately 150 to 180 g) in order to help the homogenization of the reactants and the formation of a polyamide salt solution.

The first step corresponds to the polyamide salt solution formation, as explained in the first chapter. Indeed, in this step the monomers were mixed altogether with water and the mixture was heated at 140°C.

The pressure was set to 0.6 bar (relative pressure), and the excess water that was added for the homogenization of the reaction mixture was distilled. At the end of this step, the monomers were in the form of a salt aqueous solution at a concentration equal to 75 wt %. In the second step, the temperature was increased up to 180°C at 10°C/min and followed by 30 minutes stages at 180, 200 and 220°C.
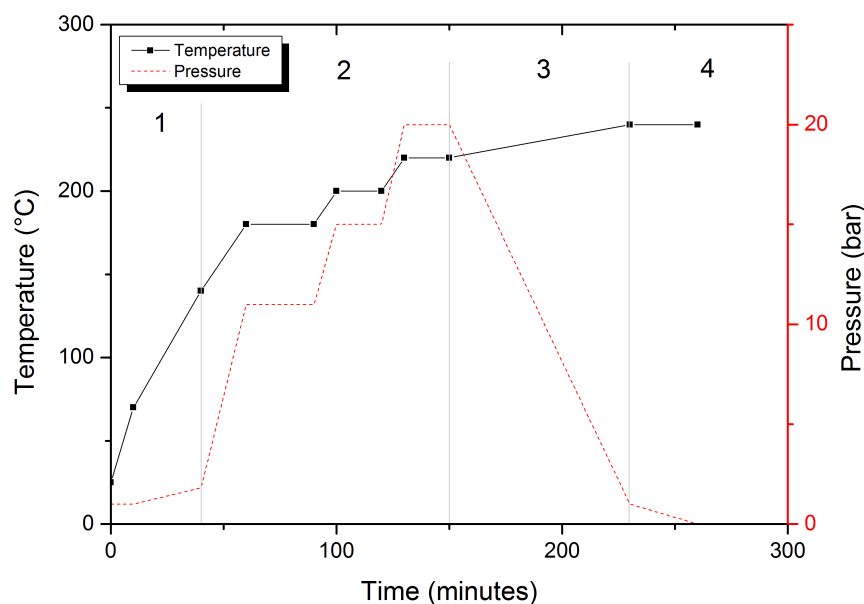
Figure 3.7: Furan-2,5-dicarboxylic acid based polyamides pilot-scale polymerization process

During these stages the system is closed and the pressure generated by the water boiling rised up to 18-20 bar. Closing the reactor prevents the loss of diamine. In the third step, the pressure was slowly released (0.5 bar/min) to the atmospheric pressure and the temperature increased to 240°C (1°C/min). In the last step, the reactor pressure was decreased to less than 0.1 mbar (absolute pressure) at a rate of 0.5 mbar/min by using a vacuum device, in order to remove water made by the polycondensation reaction (equilibrium displacement). During this step, the stirring torque was monitored and at the desired torque (2 N.m), the polymer material was extruded through the bottom drain valve into a cooling bath and then granulated. Approximately 250 g of polymer pellets were obtained per batch.

With this protocol, a series of copolyphthalamides were synthesized. They were all based on the condensation of a mixture of isophthalic and FDCA acids with HMDA (see Figure 3.8).
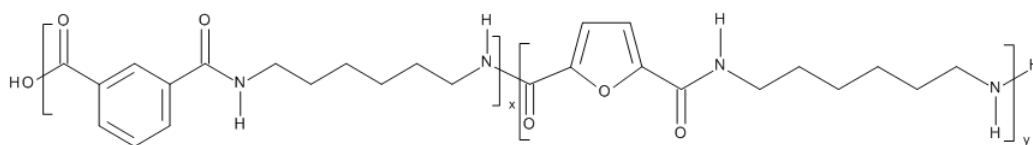
Figure 3.8: Copolymers synthesized PA 6I(x)-co-6F(y)

The nomenclature adopted in this study is the following: PA 6-I$_{(x)}$/6-F$_{(y)}$, where x and y represent the molar proportions of isophthalic and 2,5-furadicarboxylic acids respectively, condensed with hexamethylene diamine (6). The polymers synthesized in this study range from pure PA 6-I to pure PA 6-F with intermediates compositions of 10, 20, 30, 40 and 50 mol % of FDCA in the copolymers.

2.3   Characterization techniques

2.3.1   NMR

NMR experiments were carried out in order to fully characterize the structure and composition of the synthesized polymer, especially for the PA6F. All NMR experiments were performed on the synthesized polymer materials dissolved at room temperature in a 1/1 weight mixture of 1,1,1,3,3,3-Hexafluoro-2-propanol (HFIP) and CDCl$_3$. The spectra were collected at 300 K on an Avance III Bruker 400 MHz spectrometer. ^{1}H, ^{13}C NMR experiments were performed as well as 2D NMR techniques such as COSY (Correlation spectroscopy), HSQC (Heteronuclear Single-Quantum Correlation spectroscopy) and HMBC (Heteronuclear Multiple-Bond Correlation Spectroscopy).

2.3.2   MALDI-TOF mass spectrometry

In order to characterize the structure of PA 6-F polymer chains, matrix-assisted laser desorption/ionisation – time of flight (MALDI-TOF) mass spectrometry analyses were carried out. To this end, a polymer solution at 10mg/mL in HFIP was mixed to a matrix (dithranol) solution at 10mg/mL in HFIP (45/5 v/v). The mixture was spotted on the MALDI sample plate and air-dried.

2.3.3   Viscosimetry

Polymer solutions at a concentration of 5 g/L in a mixture of phenol and 1,2-dichlorobenzene (50/50 wt %) were analyzed in an Ubbelohde viscosimeter device at 25°C. In order to solubilize the materials, the mixture containing the polymer and the solvent were heated at 135°C and stirred for 1 hour. Reduced viscosity of the polymer was calculated by using the solvent and the polymer solution flow times in the viscosimeter, Eq. (3.1):

$$\eta_{red} = \frac{t - t_0}{t_0 C}(mL/g) \tag{3.1}$$

where η_{red} is the reduced viscosity of the polymer in mL/g, t is the polymer solution flow time, t_0 the solvent flow time and C the polymer solution concentration (g/mL).

By using the equation of Solomon and Ciuta [1], it was also possible to calculate the intrinsec viscosity of the polymer using the equation (3.2):

$$[\eta] = \frac{1}{c}\sqrt{2(\frac{t - t_0}{t_0} - \ln(\frac{t}{t_0}))} \tag{3.2}$$

2.3.4   SEC

The polymer molar mass was assessed by size exclusion chromatography (SEC) in HFIP. Samples of 1 g/L were eluted at a flow rate of 0.75 mL/min. The signals were then detected with a RI detector (Agilent-RI-1100a). The average molar mass (Mn and Mw) were determined with a calibration method using polymethylmethacrylate standards

2.3.5   DSC

Differential scanning calorimetry tests were performed on a Thermal Analysis (TA) Q20 instrument, at a heating/cooling rate of 10°C/min, under nitrogen gas flow (50 mL/min). Samples were heated at 280°C, cooled to 0°C and then heated again to 280°C. The glass transition temperatures were measured at the onset during the second cooling cycle.

2.3.6   TGA

Thermogravimetrical analyses were performed on a TA TGA Q500 instrument. Approximately 5 mg of sample were weighted and heated (20°C/min) from room temperature to 600°C, under nitrogen gas flow (90 mL/min).

2.3.7   Water Uptake

Several dogbone shape tensile specimens were obtained by using a DSM micro 15 extruder, and dogbone shape (ISO 527) mold. The extruder was set to 260°C and the mold was heated to 80°C. These samples were vacuum dried in an oven at 80°C overnight, weighted and immersed in a thermostated water bath at 25°C. The samples were taken out from the bath and weighted again at different time intervals. The increase in the mass of the sample, corresponding to the water uptake was calculated.

2.3.8   Mechanical Properties

Tensile tests were performed on several copolyphthalamides materials. Samples were injected with a DSM micro 15 extruder as dogbone shape (ISO 527). The extruder was set to 260°C and the mold was heated to 80°C. Specimens were tested after being dried overnight at 80°C under vacuum. Young modulus, strain and stress at break could then be measured for dried materials. The tensile tests were performed on a MTS 10 kN uni-axial tensile machine at a 10 mm/min speed up to the breaking of the specimen.

2.3.9   Molecular modelling technique

Two different molecular modeling techniques were used in this study, in order to point out trends in comparison with experimental data.

The first technique used was QSPR simulation (Quantitative Structure-Property Relationships). This method allows a quick screen of chemicals for a wide range of properties. In this study, the program used for these simulations is called Synthia [2] and is provided by the Accelrys company. This program is based on the work of Pr Bicerano [3] on the improvements of the QSPR method with the use of topological information – specifically connectivity indices derived from graph theory – and so essentially based upon individual atoms and bonds. Then with no database of functional group contributions required, properties can be predicted for polymer composed of the nine elements : carbon, hydrogen, silicon, sulfur, fluorine, chlorine and bromine. The major drawback of this technique is a certain lack of accuracy when predicting properties, but this a balanced by the very little time needed for the calculation (of the order of 1 s).

The second technique that was used was molecular dynamics (MD). All the simulations were performed using Materials Studio [4] , with the COMPASS force-field [5, 6] and according to the protocol developed and validated in our previous work [7]. This MD technique allows a more precise and realistic prediction for the glass transition temperatures of amorphous polyphthalamides.

3   Results and discussion

Poly(hexamethylene isophthalamide) (PA 6-I) and poly(hexamethylene-2,5-furandicarboxylamide) (PA 6-F)-based copolymers were successfully synthesized via bulk melt polycondensation with different compositions, ranging from pure PA 6-I to the PA 6-I$_{50}$/6-F$_{50}$ (with 90/10, 80/20, 70/30 and 60/40 mol % intermediate compositions) and also PA 6-F homopolymers. The first observation that could be done is a visual inspection of the synthesized materials. Pictures of these materials are presented in Appendix B. On these pictures, it is clear that the PPA based on FDCA are transparent and more orange/red as the amount of FDCA increases.

Their compositions have been extensively characterized as well as some of their physical properties.

3.1   Copolyamides Composition

In this part of the study, the focus was put on understanding the different phenomena and reactions that occur during the synthesis of FDCA-rich polyphthalamides and especially the PA 6-F. The PA 6-F synthesized has been extensively characterized with NMR, MALDI-TOF and SEC techniques.

3.1.1   NMR results

[1]**H NMR**   Various NMR techniques were used to characterized the chemical composition of the synthesized copolyphthalamides. The first goal was to measure the difference between the ratio of acids added in the reactor and the one actually in the polymer materials. In order to do this, ^{1}H NMR experiments were carried. A typical spectrum of a polyamide synthesized with an acid molar ratio IPA/FDCA equal to 70/30 is shown on Figure 3.9, with the peak attribution showed on table 3.1.
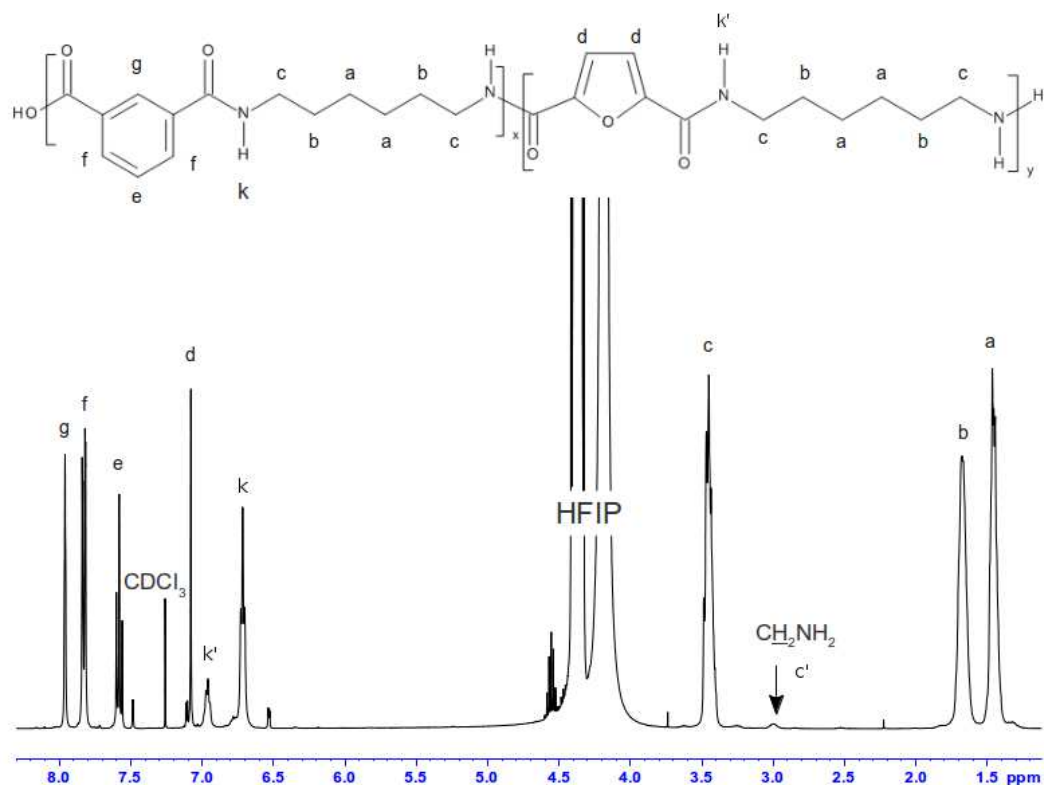
Figure 3.9: ^1H NMR spectrum of PA 6-I$_{70}$/6-F$_{30}$
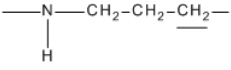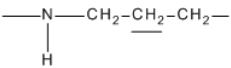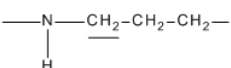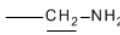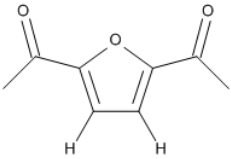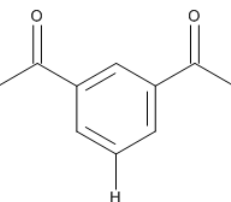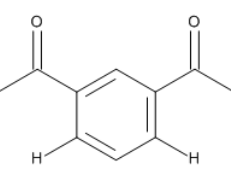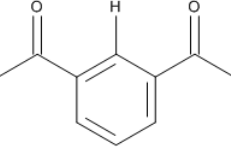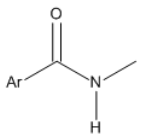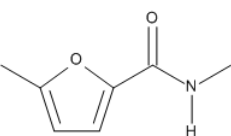
Proton	Group	Chemical shift (ppm)
a	—N(H)—CH₂–CH₂–$\underline{CH_2}$—	1.46
b	—N(H)—CH₂–$\underline{CH_2}$–CH₂—	1.68
c	—N(H)—$\underline{CH_2}$–CH₂–CH₂—	3.46
c'	—$\underline{CH_2}$–NH₂	2.96
d	2,5-diacetylfuran ring protons (H at 3,4 positions)	7.08
e	3,5-diacetylbenzene, H (para)	7.58
f	1,4-diacetylbenzene-type ring protons (H)	7.84
g	1,3-diacetylbenzene, H between acetyl groups	7.96
k	Ar—C(=O)—N(H)—CH₃	6.77
k'	5-methylfuran-2-carboxamide, C(=O)—N(H)—CH₃	6.96

Table 3.1: Chemical shifts ($CDCl_3$/HFIP) of PA 6-I_{70}/6-F_{30}

With this spectrum, it was possible to calculate the acid repartition in the poly-

mer chains. This ratio can be calculated by the Equation (3.3):

$$\frac{FDCA}{FDCA + Isophthalic} = \frac{\frac{I_d}{2}}{I_g + \frac{I_d}{2}} \tag{3.3}$$

where I_d is the integral at 7.08 ppm, corresponding to the furan ring, and I_g the integral at 7.96 ppm, corresponding to the proton attached to the carbon in position 2 of the isophthalic acid.

It was found that all synthesized polymers have the same amount of the two acids in their chains as in the feeding ratio in the reactor. However several unexpected peaks appeared between 6,5 and 7,5 ppm; moreover the more FDCA was introduced in the polymers, the more the integrals of these peaks (h, k, i, j) became important as showed on Figure 3.10:
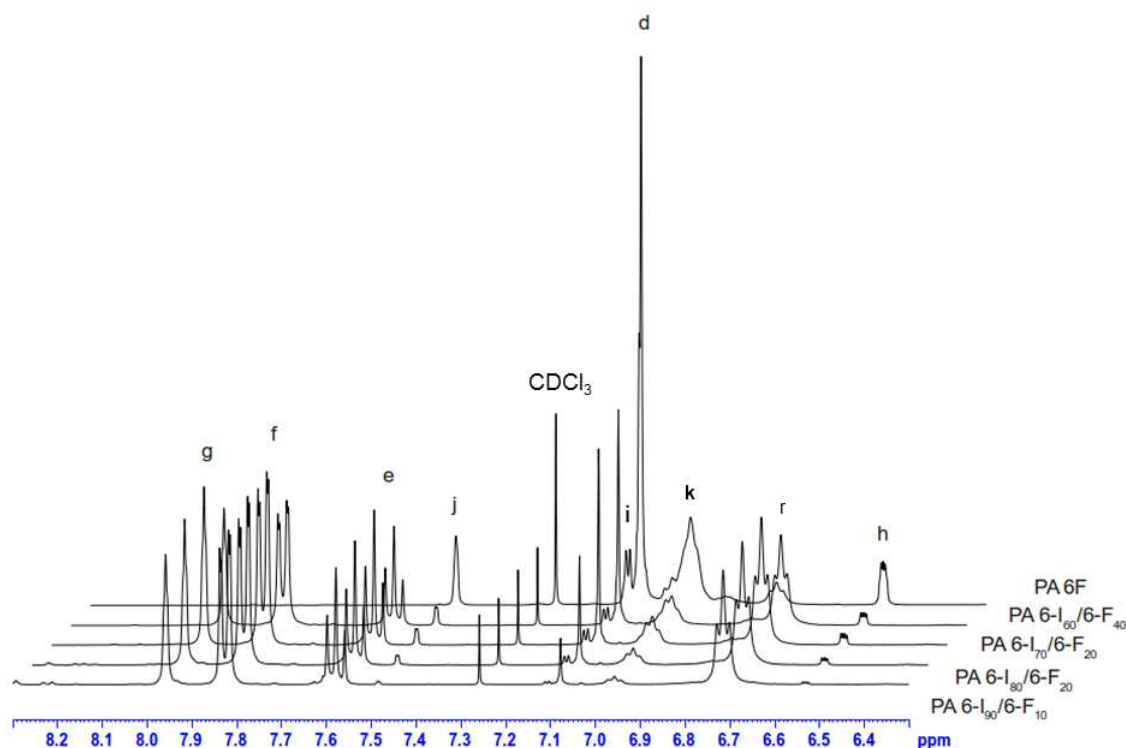
Figure 3.10: 1 H NMR spectrum of PA 6-I$_{(x)}$/6-F$_{(y)}$ in HFIP/CDCl$_3$ (50/50)

2D-NMR   In order to propose assignments to those peaks, it was necessary to perform 2D NMR experiments. These experiments were carried out on the PA 6-F

polymer, in which these unknown peaks were the more intense. 2D COSY, HMBC and HSQC NMR experiments were conducted to make unambiguous assignments.

The Correlation Spectroscopy (COSY) technique describes the coupling between protons located on different carbon atoms. The couplings are evidenced by the off-diagonal spots on the NMR spectra. Figure 3.11 shows that the k and k' protons only correlate to the c proton, which is an aliphatic CH_2 proton, the one in alpha of the amide function and not with other aliphatic or aromatic protons. The only solution that could explained this feature is that the k and k' protons are the protons of the amide function (bonded to the nitrogen). The fact that we have two different chemical shifts for an amide function means that we have two amide functions in a different electronic environment.
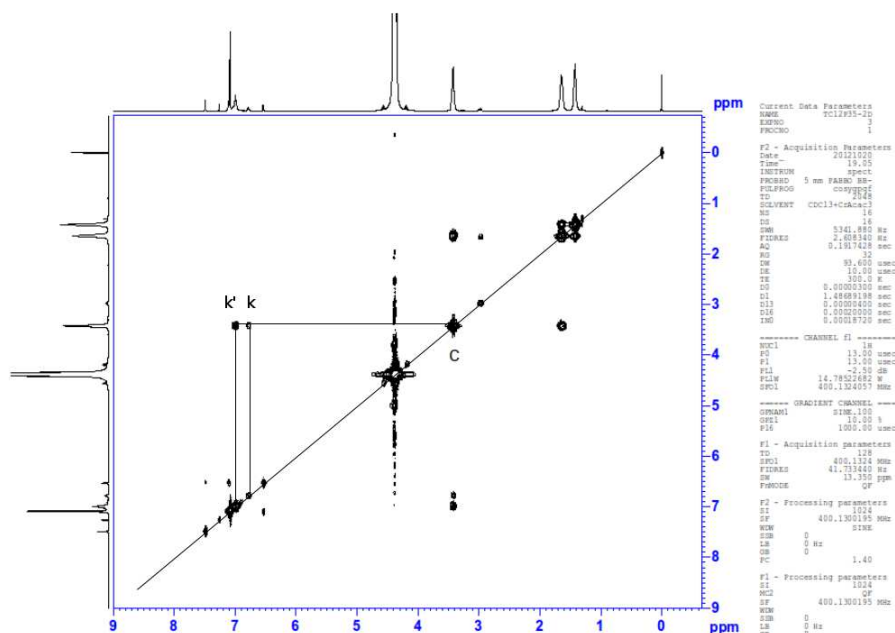
Figure 3.11: 2D Correlation spectroscopy (COSY) NMR spectra of PA 6-F in HFIP/CDCl$_3$ (50/50)

By looking to Figure 3.12, which is a zoom over the 6-8 ppm range, it is clear that the labeled proton j is located next to the labeled proton h and that the labeled proton i is situated next to the h proton as well, but i and j are not situated close to one another. They should be on each side of the h proton. So these three protons should be carried by a carbon that is in a structure close to the furan one (proton d at 7.1 ppm).

With the Heteronuclear Single-Quantum Correlation Spectroscopy (HSQC), it is possible to see the correlations between protons and carbons on which they are
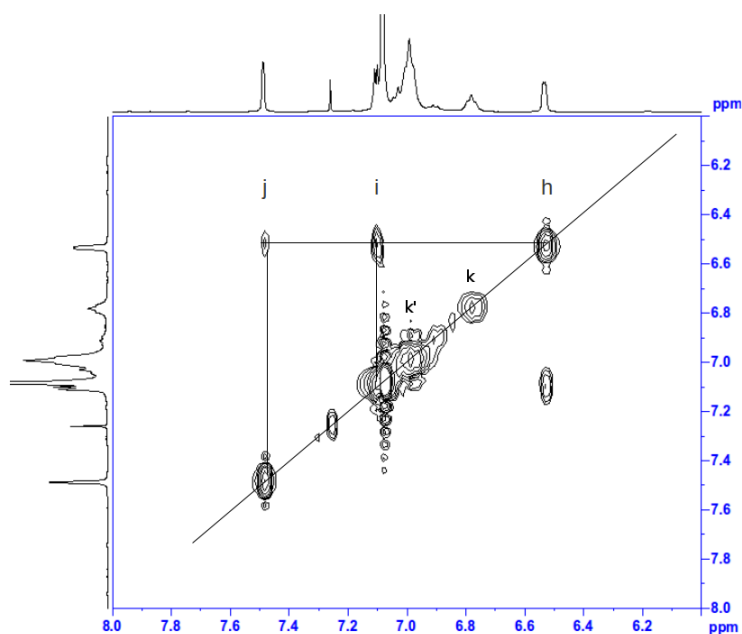
Figure 3.12: 2D Correlation spectroscopy (COSY) NMR spectra of PA 6-F in HFIP/CDCl$_3$ (50/50), 6-8 ppm range.

located. The 2D-HSQC spectrum is displayed on the Figure 3.13 and 3.14, which is a zoom over the proton 6-8 ppm range. By making correlations between the previously identified protons and the carbons they are supported on, several information can be obtained. For instance the j proton (at 7.5 ppm) is supported on a carbon next to a carbonyl function, whereas the I (at 7.1ppm) and h (at 6.55 ppm) protons are supported by furan carbons.

The last 2D-NMR technique that was used was Heteronuclear Multiple-Bond Correlation Spectroscopy (HMBC), which makes possible the study of interactions between protons and carbons several bonds apart from each others (J3, J4 and J5). A Spectrum of the PA 6-F HMBC is displayed on Figure 3.15.

With all these 2D-NMR studies, we were able to point out the chemical structure of the PA 6-F synthesized and to propose a chemical structure explaining the appearance of 4 peaks in the ^{1}H NMR spectra as soon as FDCA was introduced in the synthesis. Indeed, all these results showed the presence of a decarboxylated furan at one chain end of the polymer, the other chain end being an amine, as showed on Figure 3.16.

Figure 3.13: 2D Heteronuclear Single-Quantum Correlation Spectroscopy (HSQC) NMR spectra of PA 6-F in HFIP/CDCl$_3$ (50/50).

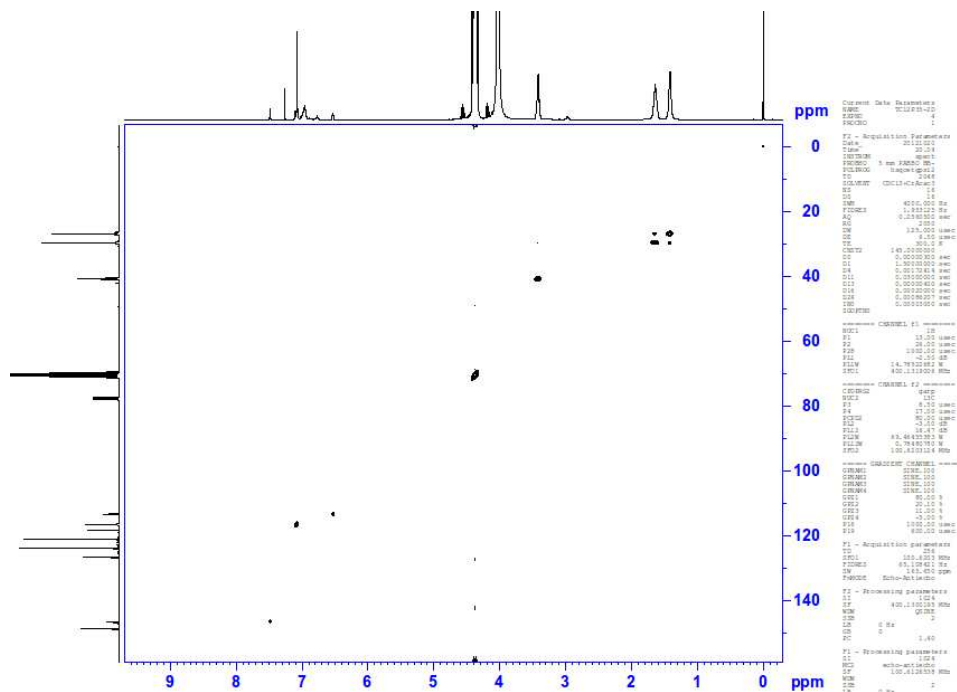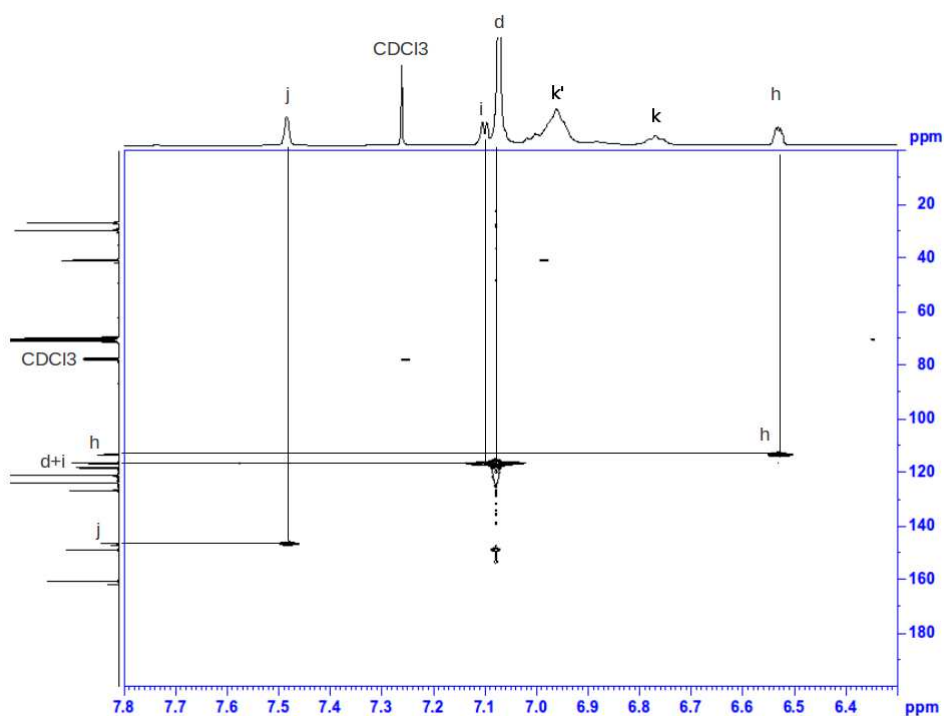Figure 3.14: 2D Heteronuclear Single-Quantum Correlation Spectroscopy (HSQC) NMR spectra of PA 6-F in HFIP/CDCl$_3$ (50/50), 6-8 ppm range.
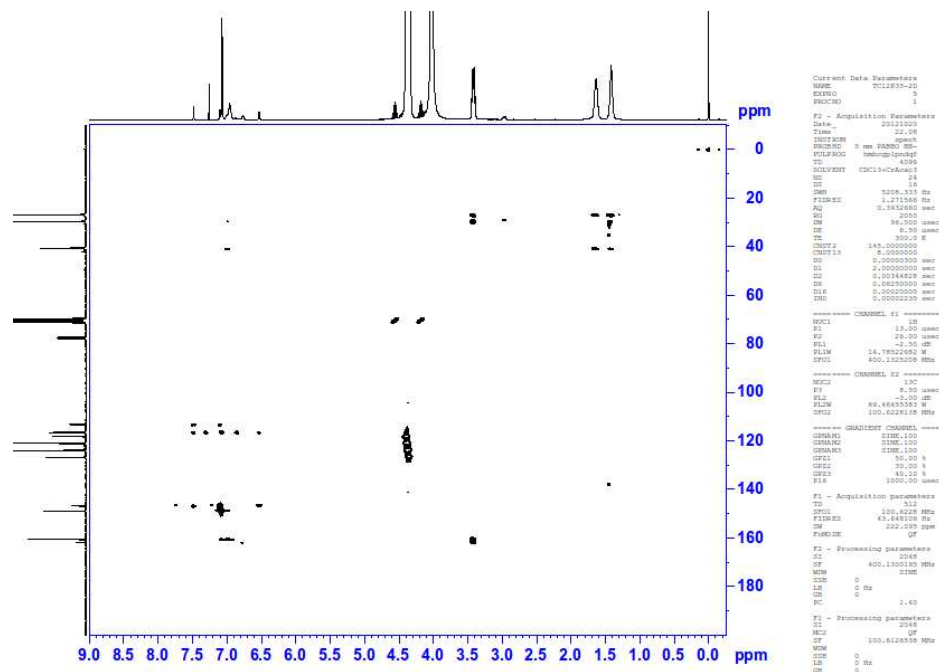
Figure 3.15: Heteronuclear Multiple-Bond Correlation Spectroscopy (HMBC) of PA 6-F in HFIP/CDCl$_3$ (50/50).
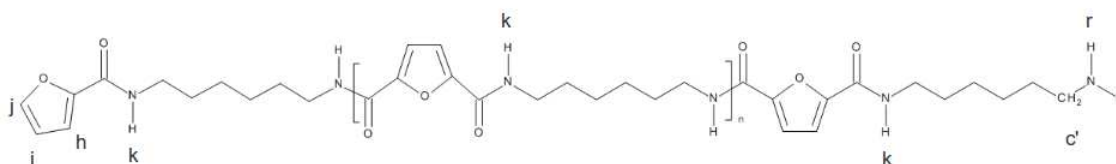
Figure 3.16: Chemical structure of the PA 6-F with furan and amino end groups.

Following the identification of the furan chain end (h, i, j) and also the amine chain end (k), we were able to calculate the proportions of both chain ends and to deduce the molar mass of the PA 6-F polymer.

With these NMR spectra (Figure 3.10) it was possible to calculate the DPn of the PA 6-F with the following formula (Eq. (3.4)):

$$DPn = 2\frac{H_{FT} + nH_{CH2cent} + nH_{FC} + 1H_{CH2-NH2}}{1H_{FT} + 1H_{CH2-NH2}} \qquad (3.4)$$

where H_{FT} is the integral corresponding to an hydrogen of a terminal furan group, nH_{CH_2cent} is the integral corresponding to the CH_2 in alpha of the amide in the polymer (CH_2 in the polymer substracting the CH_2 close to the CH_2-NH_2 chain end at 2.9 ppm), nH_{FC} the integral of the hydrogen of the furan in the polymer and $H_{CH2-NH2}$ the hydrogen corresponding to the terminal amine function. These integral can be calculated with the following formulas (Eq. (3.5), (3.6), (3.7) and (3.8)):

$$1H_{FT} = I_h \qquad (3.5)$$

$$nH_{CH_2cent} = \frac{I_c - I_{c'}}{4} \qquad (3.6)$$

$$nH_{FC} = \frac{I_d}{2} \qquad (3.7)$$

$$1H_{CH2-NH2} = \frac{I_{c'}}{2} \qquad (3.8)$$

By introducing these equations in the equation (3.4) we were able to calculate the DPn with the equation (3.9):

$$DPn = \frac{4I_h + I_c + 2I_d + I_{c'}}{2I_h + I_{c'}} \qquad (3.9)$$

By doing this calculation, we found that the DPn for the PA 6-F synthesized is equal to 9, corresponding to a mean number of repetitive units in the polymer of 3.5, corresponding to a molar mass Mn = 1036 g/mol.

It is also possible to calculate the ratio between the different terminations. The PA 6-F synthesized has 65 % of decarboxylated furan terminations and 35 % of amine terminations. The fact that we are far from the theoretical 50/50 repartition of chain ends in polycondensation clearly indicates that there was a deviation from the stoichiometry equilibrium during the synthesis. This deviation was probably caused by the decarboxylation of the FDCA, preventing it from reacting.

^{13}C NMR　^{13}C NMR experiments were also carried in order to further confirm the structure of the PA 6-F. The ^{13}C NMR spectrum of PA 6-F is presented in Figure 3.17 and a zoom over the 110-165 ppm zone is displayed in Figure 3.18.
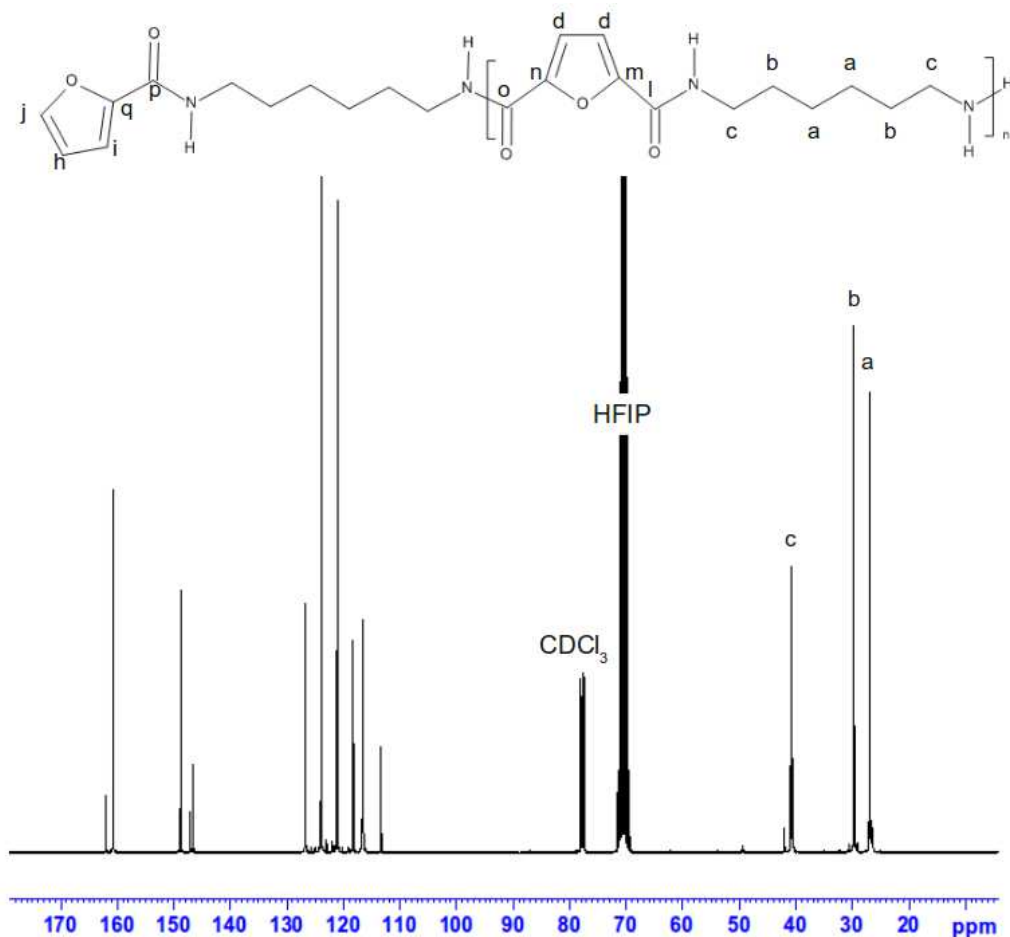
Figure 3.17: ^{13}C NMR spectrum of PA 6-F (HFIP/CDCl$_3$)

On these ^{13}C NMR spectra the same structure that the one found with ^{1}H NMR was obtained. However other information could be obtained with the ^{13}C spectrum. Indeed, only two types of C=O species were found on this spectrum: the one corresponding to the amide function in the polymer and the amide function of the decarboxylated furan chain end. No carboxylic acid C=O was found on this ^{13}C spectrum. This means that all furan in chain ends are decarboxylated. This feature is in contradiction with the paper by Hopff and Kroeger [8], which claimed that the decomposition temperature of the FDCA is 271°C and the decomposition temperature of the FDCA hexamethylene diammonium salt is 228°C. Indeed in our synthesis, the temperature never exceeds 240°C and when salt is present the temperature never get above 220°C. One explanation could be that the monomers
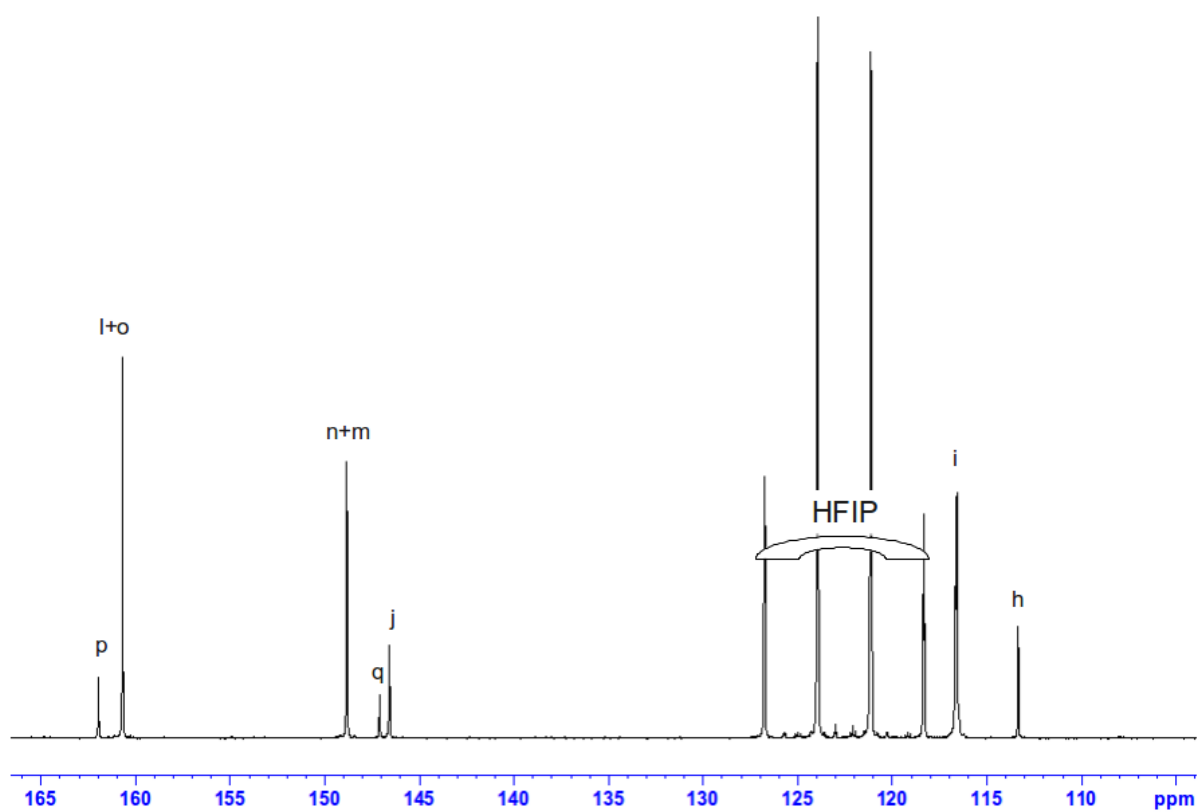
Figure 3.18: ^{13}C NMR spectrum of PA 6-F, zoom in the 100-170 ppm range

and polymer were heated below their expected decomposition temperature during a long time, so nevertheless they could still be decomposed in these conditions.

3.1.2 MALDI-TOF mass spectroscopy

In order to obtain more information on the molar mass and structures of the synthesized PA 6-F, MALDI-TOF experiments were performed. The mass spectrum is presented in Figure 3.19.
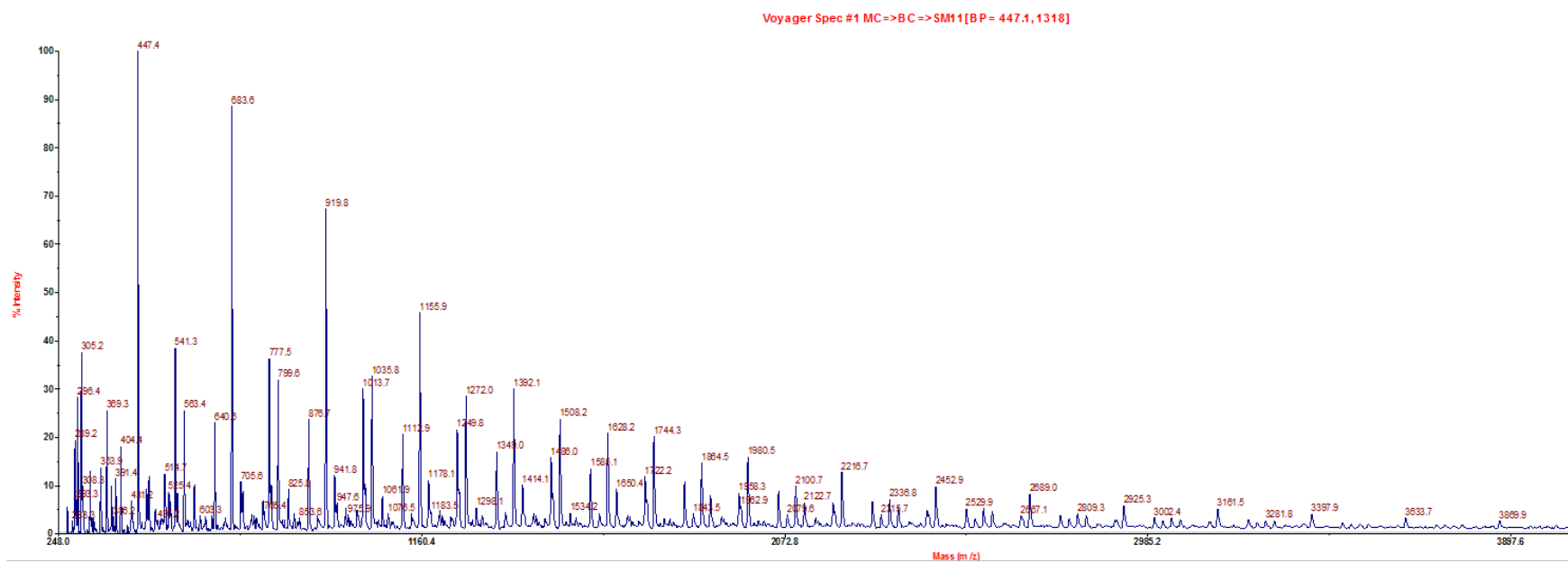
Figure 3.19: MALDI-TOF mass spectrum of PA 6-F (linear mode, dithranol matrix)

This mass spectrum reveals several peaks corresponding to different chain populations. The main population was assigned to the PA 6-F polymer with different degrees of polymerization (n) and having a furan decarboxylated chain end as shown on Figure **??**.

Indeed, the main population has a molar mass of 209 (furan end-group, $C_{11}H_{17}N_2O_2$) + 1 (H end-group) + n(236) g/mol which corresponds to this formula. Therefore, this MALDI-TOF analysis experiments confirms our NMR results.

The analysis in reflectron mode confirms the assignment of main population (i.e., "M" in figure 3.20). This population is cationized by H^+ ($[M+H]^+$ at 919.4 m/z) and Na^+ ($[M+Na]^+$ at 941.4 m/z). A second population "N"($[N+H]^+$ at 1013.4 m/z
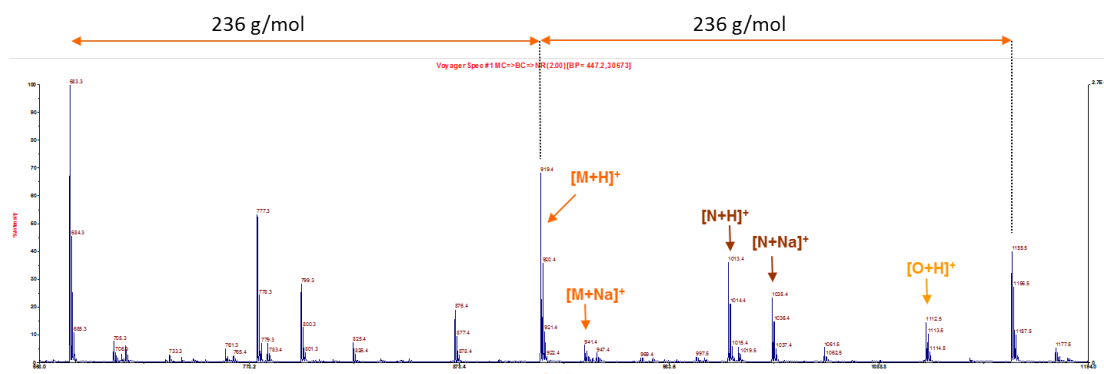
Figure 3.20: MALDI-TOF mass spectrum of the PA 6-F (reflectron mode, dithranol matrix)

and $[N+Na]^+$ at 1035.4 m/z) exists in the mass spectrum. This population could be assigned to another decarboxylated furan chain end versus M population. This population also has a n times 236.11 g/mol periodicity but at a 95 g/mol higher molar mass. This population is shown on Figure 3.20. On this figure, the "M" population corresponds to the main population of PA 6-F and the "N" to this second population. This added mass corresponds to another decarboxylated furan chain end. So this second population has both two chain ends capped with decarboxylated furans (Figure 3.21). These chain ends prevent the growth of the chains as these furan moieties cannot react further. This is one of the explanation for the low molar mass observed for this polymer. The MALDI-TOF mass spectrum of PA 6-F showed an additional distribution (named "O" on Figure 3.20). However, we were not able to assign this distribution to any expected structures.
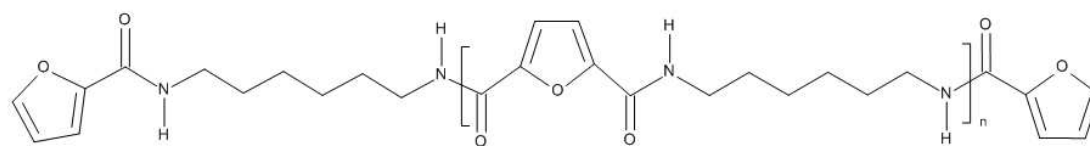
Figure 3.21: "n" PA 6-F with both chain ends capped with decarboxylated furans

3.1.3 Molar mass and reduced viscosity

The last techniques used for the characterization of the molar mass distribution of the synthesized copolyphthalamides were Size-Exclusion Chromatography and solution viscosimetry techniques.

SEC spectrum of PA 6-I$_{90}$/6-F$_{10}$ (Figure 3.22) and PA 6-F (Figure 3.23) are displayed below.
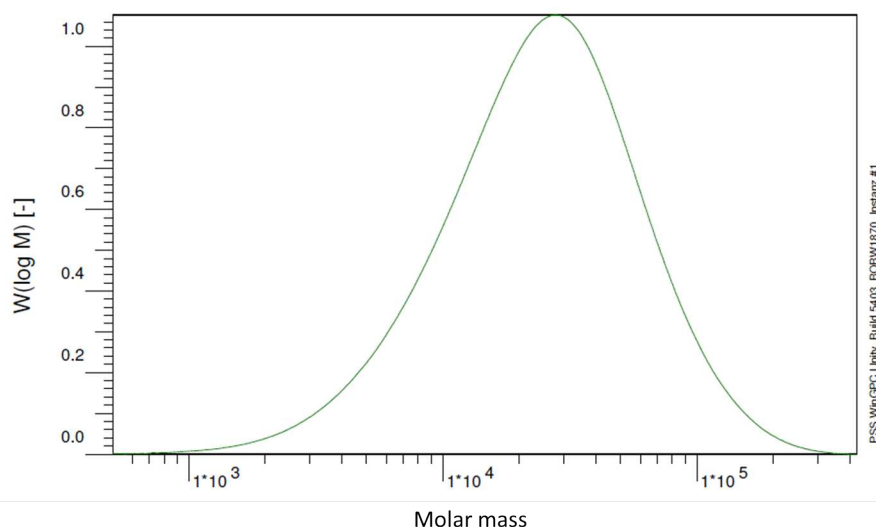
Figure 3.22: SEC spectrum of PA 6-I$_{90}$/6-F$_{10}$ in HFIP, PMMA standards

These two SEC experiments have been carried out in HFIP with PMMA standards. By looking at the two SEC experiments, it is clear that the PA 6-I$_{90}$/6-F$_{10}$ has a higher molar mass than the PA 6-F (SEC peak centred around 20000 g/mol vs. 5000 g/mol for PA 6-F). Moreover, the dispersion of the molar mass is much broader for the PA 6-F, with the apparition of a shoulder at the low molar mass.

The results of SEC and viscosimetry for all PPA compositions are presented in the Table 3.2:

It is clear that there is an influence of the amount of FDCA used in the PA synthesis on the molar mass obtained. For a content of FDCA below 30 mol %, the molar mass obtained were in the same range. For a content of FDCA higher than
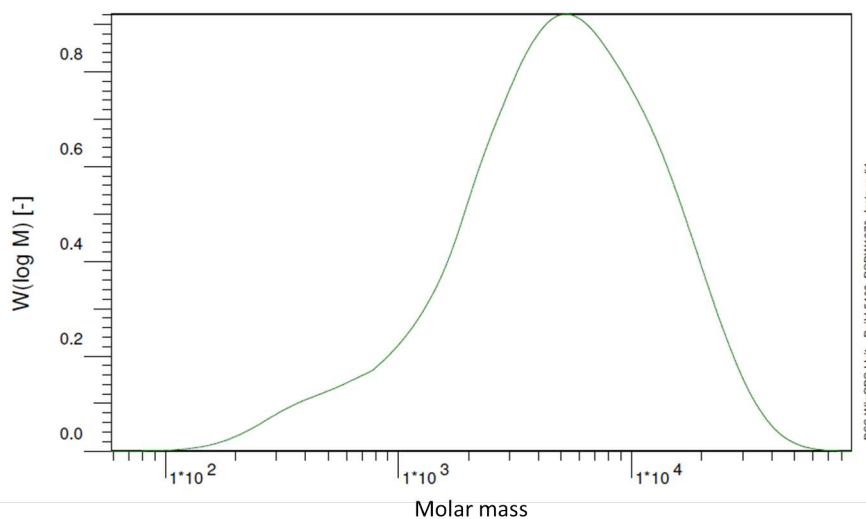
Figure 3.23: SEC spectrum of PA 6-F in HFIP, PMMA standards

Composition	SEC*			Viscosimetry	
	Mn (g/mol)	Mw (g/mol)	PDI	η_{red} (mL/g)	$[\eta]$ (dL/g)
PA 6-I	15700	33100	2.10	75.0	0.679
PA 6-I$_{90}$/6-F$_{10}$	15300	32700	2.14	67.5	0.611
PA 6-I$_{80}$/6-F$_{20}$	15400	35200	2.29	64.3	0.585
PA 6-I$_{70}$/6-F$_{30}$	14700	32550	2.22	56.4	0.520
PA 6-I$_{60}$/6-F$_{40}$	12150	31400	2.58	46.4	0.432
PA 6-I$_{50}$/6-F$_{50}$	12000	32100	2.68	46.3	0.432
PA 6-F	2400	7300	3.03	15.0	0.147

Table 3.2: SEC and relative viscosity results of PA 6-I$_{(x)}$/6-F$_{(y)}$. * SEC in HFIP, PMMA standards

30 mol %, a decrease of the molar mass is observed: the more FDCA was added, the lower the molar mass were. Finally, the polymer synthesized only from FDCA and HMDA has a very low molar mass as already underlined from the NMR and MALDI-TOF experiments.

Moreover, the polydispersity index increases as well with the FDCA content. The PDI for PA 6-I is 2.10, which is in agreement with the theoretical value of 2 for linear polycondensates. However, the PDI increases up to 3 for the PA 6-F. This is caused by the decarboxylation of furan, leading to end capping of both chain ends and to short chains. These short chains are broadening the molar mass dispersion and this is the reason of the increase of the polydispersity index.

When comparing the SEC ($Mn = 2400$ g/mol) and viscosimetry results with molar mass calculated by NMR ($Mn = 1036$ g/mol), we found different results. This difference may come from the PMMA calibration of the SEC, which should have a very different hydrodynamic volume than our PPA.

With these three techniques, we have characterized the chemical structure and molar mass of the several synthesized polyphthalamides, and in particular the PA 6-F. In a second part, we will focus on their thermal, mechanical and physical properties.

3.2 Copolyamides properties

3.2.1 Thermal properties

The different synthesized PPA were characterized by Differential Scanning Calorimetry to study the influence of the FDCA on their glass transitions and thermal behavior. The DSC thermograms are presented in Appendix D.

The glass transition temperature was measured during the cooling step of the second cycle, in order to match the modelling protocol, where the glass transition was also measured during a very fast cooling of the material. The synthesized copolyphthalamides were amorphous as no crystallization or melting peaks were observed in the whole range of experiment (from 25 to 330°C), but only glass transitions were clearly observed (94°C for the PA 6-F, see Figure 3.24).

In order to confirm this amorphous behavior several other tests were performed. The objective of these tests was to be in the most favorable experimental conditions to lead to the eventual crystallization of the polymer. The first one carried out, was to take a PA 6-F sample and to heat it in an oven under vacuum at a temperature 10-20°C above its glass transition temperature, during 48 h. After this thermal treatment, DSC test was run again and no melting peak was observed, meaning
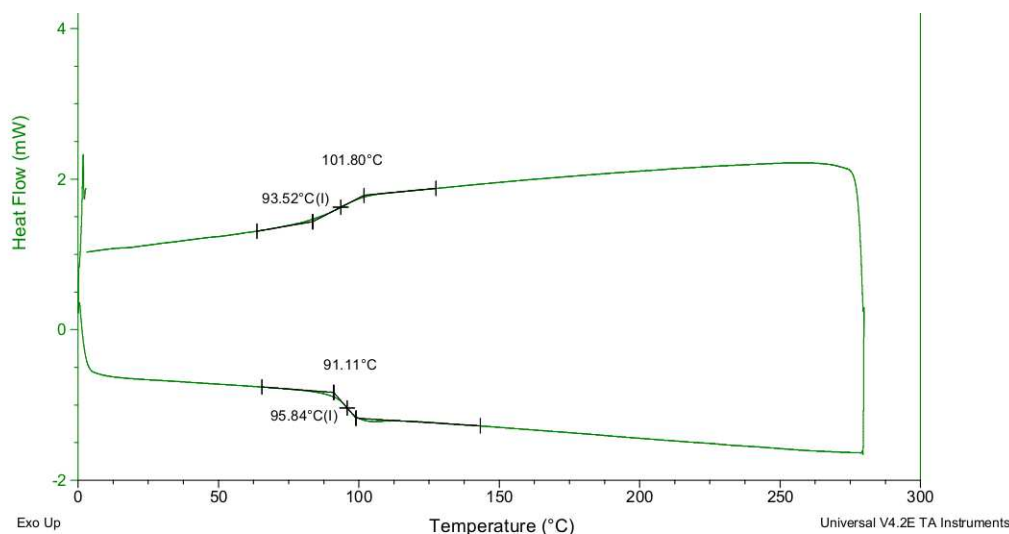
Figure 3.24: DSC thermogram of a PA 6-F

that even with a very long time with a high molecular mobility this PA 6-F was not able to crystallize. This amorphous feature has been previously observed in several studies [9, 10] whereas in other studies, similar polymers (or with different diamine chain length) were found to be semi-crystalline [11–13].

Another test was carried out in order to confirm the amorphous characteristic of the PA 6-F. A polymer solution at a 10 wt % in HFIP was prepared. This solution was poured in a petri dish, and the solvent was slowly evaporated at room temperature (HFIP boiling point is 58.2°C). This procedure should allow even more mobility to the chains than the oven method above, however no crystallization was observed by DSC.

The fact that the PA 6-F we synthesized was not able to crystallize may come from its very low molar mass. Indeed, with short polymer chains, the chain ends concentration in the material is very important and these chain ends are a source of a lot of free volume, acting as defaults in the crystalline structure and then preventing the formation of crystals.

Concerning the influence of the FDCA on the glass transition temperature of the copolyamides, its addition leads to a decrease in the glass transition temperature of the material, as shown on Figure 3.25 and 3.26.

This decrease ranges from 129°C for 10 mol% of FDCA to 95°C for pure PA 6-F. The structural parameters that play a role on the variation of the Tg are the molar mass and the molecular structure of the polymer. Even if the decrease of the molar mass of the copolymer is small, it may contribute for a part to the decrease of Tg. However, the main contribution to the decrease of Tg is more likely due to the
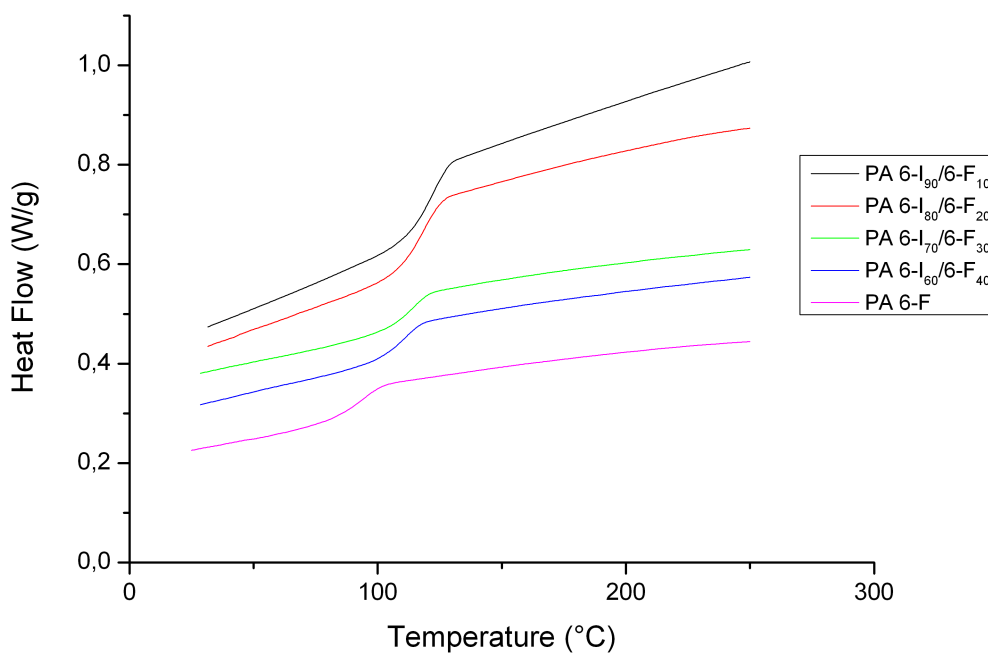
Figure 3.25: Glass transition of copolyamides in function of the FDCA amount.
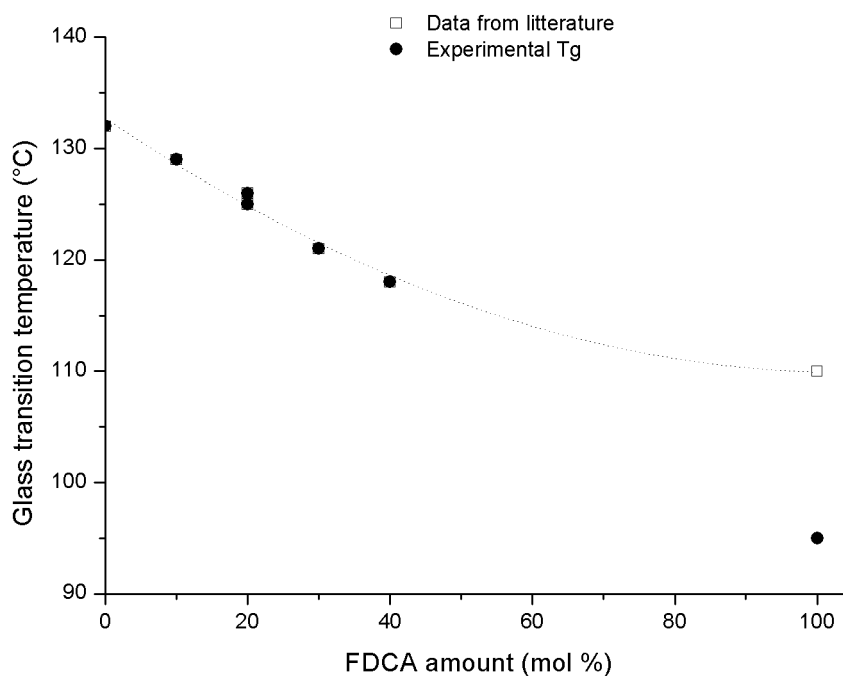
Figure 3.26: Glass transition of copolyamides in function of the FDCA amount. □ data from literature [9]

decrease of the intermolecular interactions between polymer chains when more and more FDCA is introduced in the chain. The polymer becomes less cohesive, because hydrogen bonding cannot be established so easily in the presence of FDCA. The PA 6-F polymer must be treated differently because its molar mass is particularly low and in this case this very low value contributes to the low Tg as we can see when comparing our results with Tg from literature [9].

Molecular modelling simulations were carried out in order to compare the experimental results of Tg with computer experiments by following the previously established protocol for polyphthalamides. The calculation of the glass transition temperature based on the topological theory was done using the Synthia module of the Materials Studio software. These materials were random copolymers with a molar mass of 20 000 g/mol.

No significant difference was observed between the different simulated Tg of the copolymers (Figure 3.27), since the error of the calculation is about 6 % of the temperature [2]. So the QSPR method may not be as relevant for the calculation of PA 6-I and PA 6-F as it was done in our previous work for PA 6-I/6-T, where a decrease of Tg was clearly observed when the amount of isophthalic acid was increased.
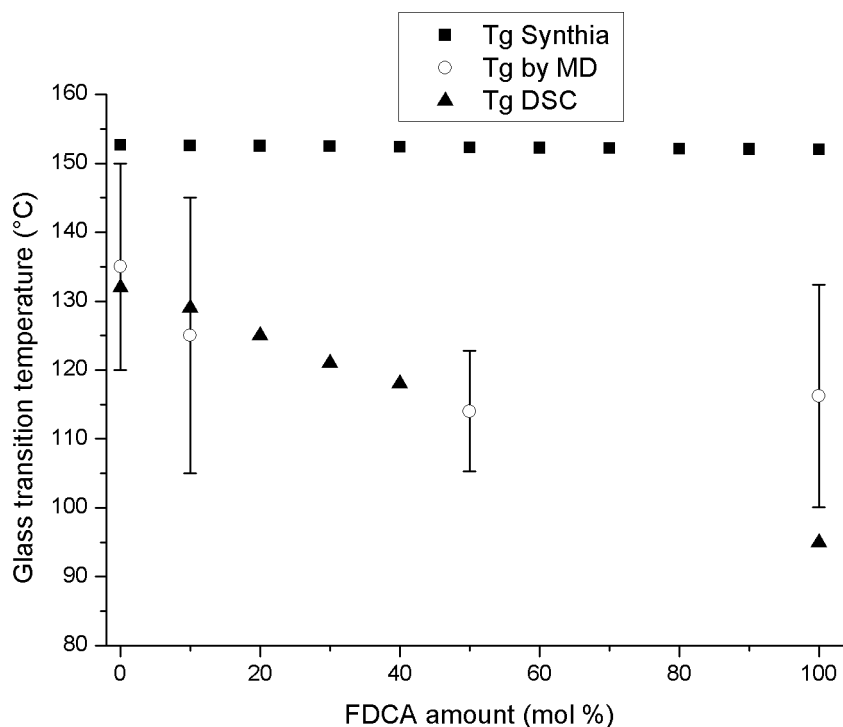
Figure 3.27: Glass transition temperature as a function of the FDCA amount calculated by modeling or measured by DSC

The glass transition of several PA 6-I/6-F copolymers were also calculated with a molecular dynamics method described in the Chapter 2. These calculations showed a decrease in the glass transition temperatures of the copolymers as the amount of FDCA in the chain was increased, from 135°C for pure PA 6-I to 116°C for pure PA 6-F (Figure 3.27). The first observation that can be made is that these values are coherent and realistic from a physical point of view. We can also observed that the standard variation for this calculation method is high (10 to 20°C). This error could be reduced with longer calculation times and more precise calculations, but this would exponentially increase the computation time.

The two simulation methods showed very different results. The QSPR pointed out the likeness of the isophthalic and 2,5-furandicarboxylic acids, whereas the MD simulation showed that the PA 6-I and PA 6-F polymers have very different glass transition temperatures. The QSPR method is by nature calculating the chemical structure impact on the properties of the polymer, and on this point of view the two monomers have similarities. However when polymerizing it with hexamethylene diamine, and studying the resulting polymers by MD, which is sensitive to cohesive energies, hydrogen bonding and chain mobility, the results are different.

When comparing the modeling results with actual experimental data, one can notice that up to 50 mol % of FDCA in the polymer, the MD simulations have the same trends than experiments (a decrease in Tg as the FDCA amount increases). However above this value, the MD results for PA6-I$_{50}$/6-F$_{50}$ and PA 6F are almost the same (114°C for PA6-I$_{50}$/6-F$_{50}$ and 116°C for PA6-F), leading to a slowing in the decreasing slope, or even a "plateau". The origin of this effect could be that the actually synthesized materials have lower Tg that they should have, due to low molar mass and high polydispersity index arising from difficulties during the polymerization as well as side reactions, while in molecular modelling, all polymers studied have the same molar mass. MD results for PA 6-F are close to the data taken from literature (Tg of PA 6-F by MD is 116°C and the one from literature is 110°C [9]). This confirms the fact that the low glass transition temperature of our PA 6-F was mainly due to its low molar mass.

TGA experiments were carried out and the results of the temperature corresponding to 5 % and 50 % weight loss under nitrogen flow are presented in Figure 3.28 and table 3.3 (all thermograms are presented in Appendix C).

On this table, it is clear that up to a composition of 50 % of FDCA in the copolymer, the temperatures of decomposition are not really impacted. Whereas the PA6F exhibits decomposition temperatures about 20°C lower than the others copolyamides (380°C for 5 % weight loss and 435°C for 50 % weight loss). The difference of the structure between the benzene and furan rings seems to have only
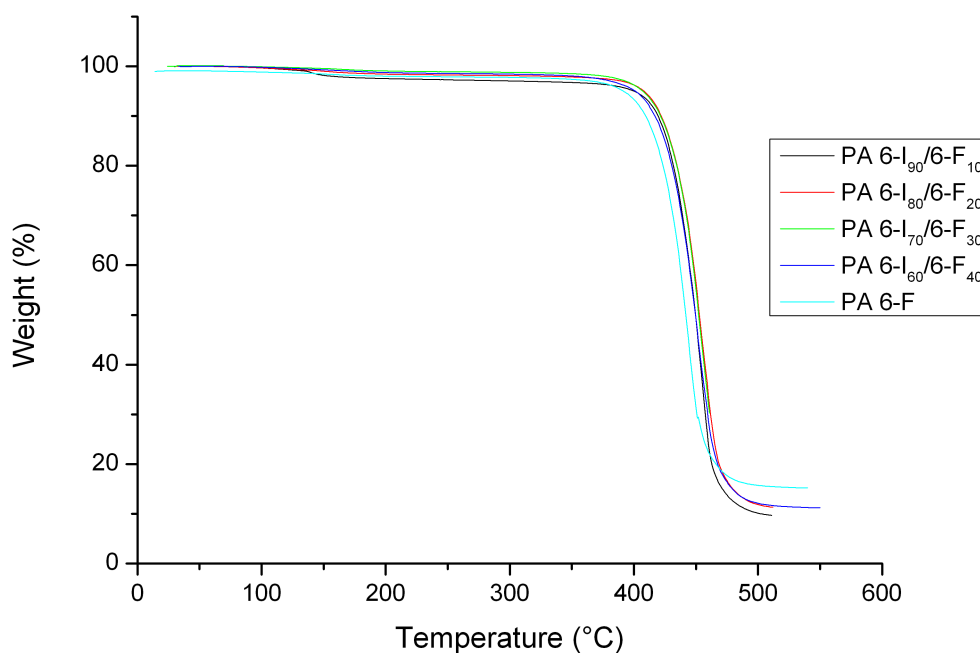
Figure 3.28: Thermogravimetrical Analysis of PA 6-I$_{(x)}$/6-F$_{(y)}$

Polymer	Glass transition temperature (°C)	Temperature of decomposition (°C)	
		5 % weight loss	50 % weight loss
PA 6-I	132	409	455
PA 6-I$_{90}$/6-F$_{10}$	129	400	450
PA 6-I$_{80}$/6-F$_{20}$	125	408	453
PA 6-I$_{70}$/6-F$_{30}$	121	407	452
PA 6-I$_{60}$/6-F$_{40}$	118	401	446
PA 6-I$_{50}$/6-F$_{50}$	-	400	442
PA 6-F	95	380	435

Table 3.3: Glass transition temperature and temperatures of decomposition (5 and 50 %) of PA 6-I$_{(x)}$/6-F$_{(y)}$

little impact on the degradation temperature even if the FDCA monomer is much less stable than the isophthalic one (the FDCA decarboxylation temperature is 278°C [8], whereas the isophthalic acid overtook no degradation up to its melting point at 347°C). The lower degradation temperature for PA 6-F may arise from the high amount of chain ends, decarboxylated furan, evidenced by NMR and MALDI-TOF. The stability of these groups is lower than the not decarboxylated ones.

3.2.2 Mechanical properties and water uptake

Mechanical properties of the synthesized copolyamides were studied. The tensile test curves of two specimens of PA 6-I$_{90}$/6-F$_{10}$ are displayed in Figure 3.29.
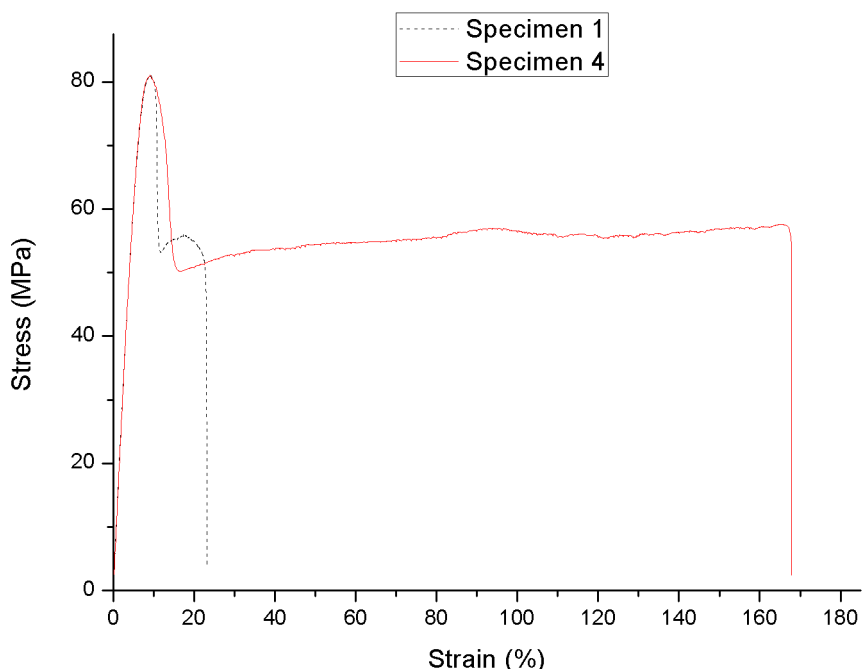
Figure 3.29: Tensile test curves of PA 6-I$_{90}$/6-F$_{10}$

On these curves, we can see that the polyphthalamides made of 90 % of isophthalic acid may have an important elongation at break (up to 160 %) with a yielding phenomena (yield stress = 81 MPa, and elongation at yield point = 9.15 %), but this plastic behaviour is not observed in all samples. Other samples showed brittle behaviour. From these tensile test curves, it is possible to calculate the tensile modulus (Young modulus) of these PPA. The results of these tensile tests are displayed on the table 3.4.

The tensile tests carried out on PPA containing more FDCA are displayed on the Figure 3.30
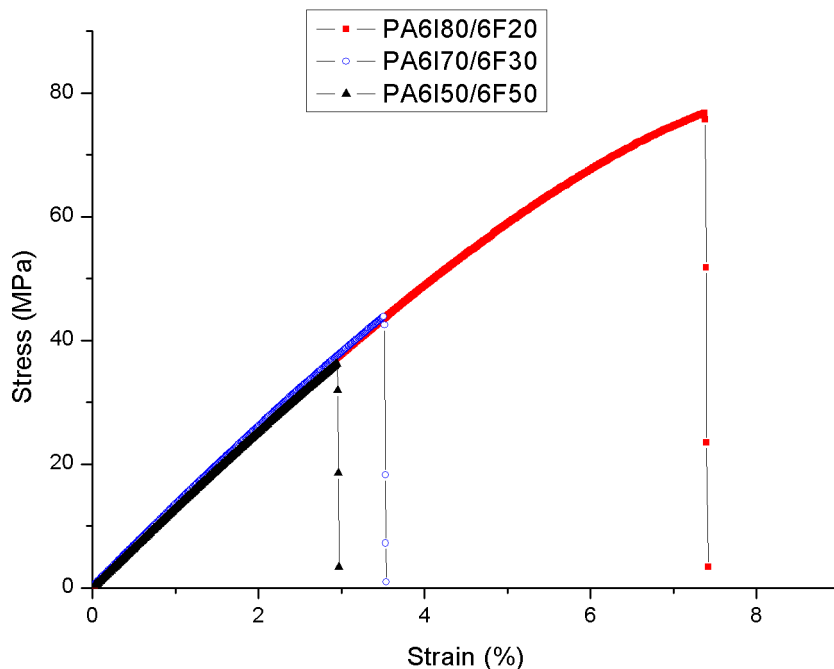
Figure 3.30: Tensile test curves of PA 6-I$_{(x)}$/6-F$_{(y)}$

From these tensile test curves, it is clear that adding more FDCA, makes the PPA more fragile (elongation at break smaller as the amount of FDCA is increased).

PA	Tensile Modulus (MPa)	Stress at break (MPa)	Strain at break (%)
PA 6-I [14]	3000	-	55
PA 6-I$_{90}$/6-F$_{10}$	1364	62.8	34.4
PA 6-I$_{80}$/6-F$_{20}$	1323	70.1	6.6
PA 6-I$_{70}$/6-F$_{30}$	1343	42.7	3.4
PA 6-I$_{50}$/6-F$_{50}$	1313	35.1	2.8

Table 3.4: Mechanical properties measured by tensile tests of PA 6-I$_{(x)}$/6-F$_{(y)}$

Except PA 6-I, the tensile modulus of all copolymers are in the same range taken into account the experimental errors. On the Figure 3.31, the strain at break

is displayed as a function of the FDCA amount in the copolyamides. On this chart it is clear that this property decreases as the amount of FDCA increases in the copolyamide. Indeed the strain at break goes from 94 % for pure PA 6I (data from literature [14]) to 2,8 % for PA 6-I$_{50}$/6-F$_{50}$. Moreover, the stress at break decreases as well with the FDCA ratio from 62 MPa for PA 6-I$_{90}$/6-F$_{10}$ to 35 MPa for PA 6-I$_{50}$/6-F$_{50}$. With these results, it is clear that adding FDCA in the PPA material makes it more brittle.
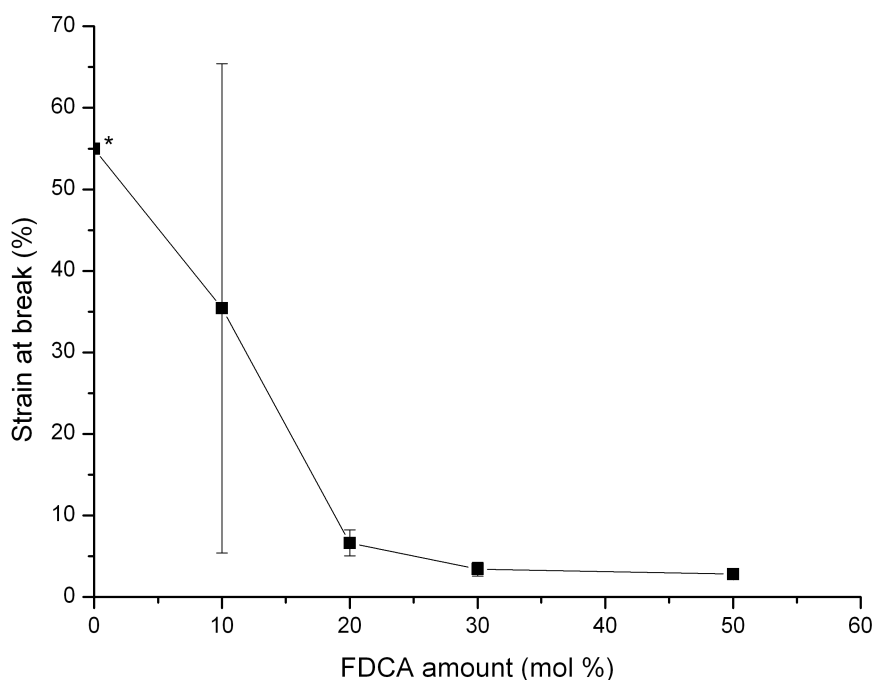
Figure 3.31: Strain at break of PPA in function of the amount of FDCA. * value is taken from literature [14]

There may be two causes for this weakening of the mechanical properties of the copolyphthalamides. The first one may be the intrinsic differences between the furan and the benzene ring. It is expected that the benzene ring will make tougher materials, because of its aromaticity and pi-stacking phenomena. The second reason is the decrease in the molar mass. Indeed with smaller molar mass, the number of chain entanglements decreases and so the mechanical properties decrease as well.

It is well known that mechanical properties of polyamides are greatly influenced by the amount of water they adsorb. Indeed, the amide group being strongly polar, it can bounds with water through hydrogen bonds and then the molecules of water act as plasticizer for the material [15, 16]. Generally polyamides absorb 1-4 % of

water at room temperature and 50 % of relative humidity (standard conditions), and PA 6I absorbs 2 % of water in these conditions. However when the humidity rate is higher, the absorption could rise up to almost 10 % for PA 6 at 100 % RH.

In order to study the influence of water on our partially (biobased) PPA, injected tensile test specimens were immersed in water at 25°C up to the saturation of the material. The amount of water that was retained in the material in function of the immersion time is showed in Figure 3.32.
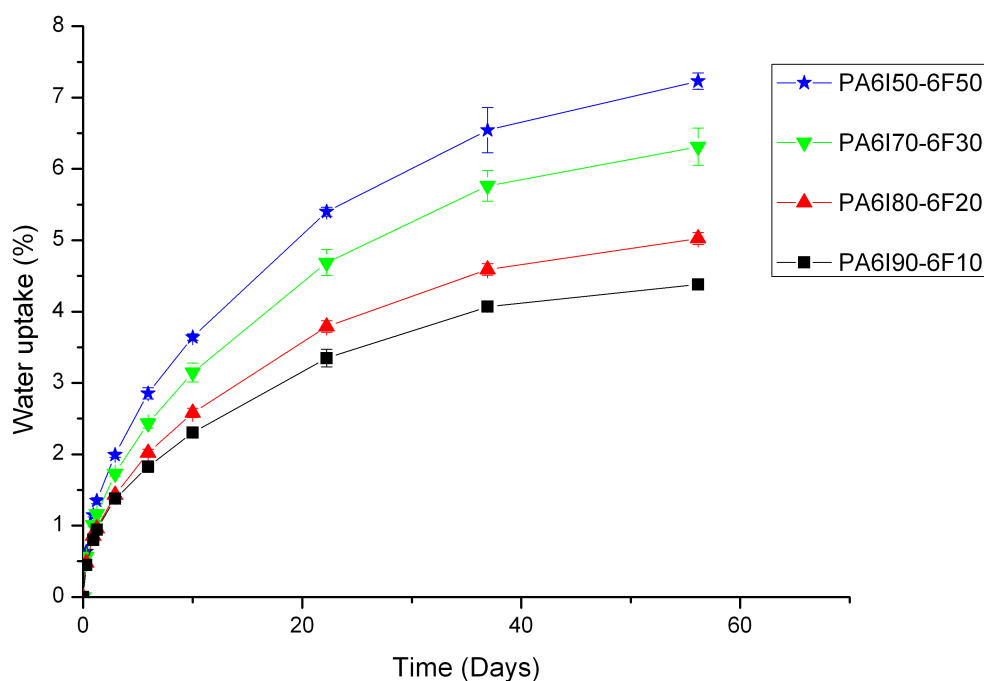
Figure 3.32: Water uptake for PA 6-I$_{(x)}$/6-F$_{(y)}$

In this figure, it is clear that the more FDCA is present in the copolymer, the more water the material absorbs. The values of water absorbed after 60 days are displayed in the table 3.5.

PA	wt % of water
PA 6-I$_{90}$/6-F$_{10}$	4.38
PA 6-I$_{80}$/6-F$_{20}$	5.02
PA 6-I$_{70}$/6-F$_{30}$	6.31
PA 6-I$_{50}$/6-F$_{50}$	7.23

Table 3.5: Percentage of water absorbed by PA 6-I$_{(x)}$/6-F$_{(y)}$ copolyamides after 60 days immersed at 25°C

This may be caused by the replacement of benzene rings, which are highly hydrophobic, by a furan ring containing an oxygen atom and then more polar and hydrophilic. Moreover, having shorter polymer chains may also increase the water uptake since with shorter chains more chain ends are found in the material, the hygroscopic behavior is strengthened.

However, even in the worst case, the amount of water absorbed by the copolymer remains lower that the amount of water absorbed by several aliphatic polyamides, such as the PA 6-6 which absorbs up to 8.5% of water at saturation. So the relatively hydrophobic behavior of the classical polyphthalamides is decreased by adding FDCA in the copolymers but these materials still perform better than several aliphatic polyamides.

4   Conclusion

Different copolyamides based on isophthalic acid and hexamethylene diamine as well as on a biobased monomer: the 2,5-furandicarboxylic acid were synthesized in a pilot-scale reactor. These materials composition and molar mass were characterized using NMR, viscosimetry, SEC; their thermal properties were studied by using DSC and TGA and their mechanical properties were also tested with a tensile machine. Moreover, two molecular modeling techniques were used in order to study the glass transition temperatures of these copolyphthalamides.

The composition of these polyamides was assessed by NMR and their molar mass were found to be on the order 15 000 g/mol for copolymers to 3 000 g/mol for PA 6F. It was difficult to synthesized PA 6F due to a poor stability of the FDCA monomer and a lack of reactivity with respect to polyamidation, leading to side-reactions and mainly decarboxylation of the furanic diacid. Indeed when synthesizing PA 6-F, only low molar mass were obtained and with a majority of the polymer chains terminated by decarboxylated furans as pointed out by NMR and MALDI-TOF experiments.

It was also found that the glass transition temperature of the copolymers decreases as the amount of FDCA in the polymer increases. This was confirmed by molecular dynamics results, however the MD showed less decrease than the actual one. In addition, it was observed that the copolymers became more brittle and more hygroscopic when the amount of FDCA in the copolymers was increased.

References

[1] O. F. Solomon and I. Z. Ciută, "Détermination de la viscosité intrinsèque de solutions de polymères par une simple détermination de la viscosité," *Journal of Applied Polymer Science*, vol. 6, no. 24, pp. 683–686, 1962.

[2] Accelrys, "Synthia," San Fransisco (CA), 2009.

[3] J. Bicerano, *Prediction of Polymer Properties*, ser. Plastics Engineering. Taylor & Francis, 2002.

[4] Accelrys, "Materials Studio V5.0, Amorphous Cell, Forcite +," San Fransisco (CA), 2009.

[5] H. Sun, "COMPASS: An ab Initio Force-Field Optimized for Condensed-Phase Applications Overview with Details on Alkane and Benzene Compounds," *The Journal of Physical Chemistry B*, vol. 102, no. 38, pp. 7338–7364, 1998.

[6] H. Sun, P. Ren, and J. Fried, "The COMPASS force field: parameterization and validation for phosphazenes," *Computational and Theoretical Polymer Science*, vol. 8, no. 1-2, pp. 229–246, 1998.

[7] T. Cousin, J. Galy, and J. Dupuy, "Molecular modelling of polyphthalamides thermal properties: Comparison between modelling and experimental results," *Polymer*, vol. 53, no. 15, pp. 3203–3210, 2012.

[8] H. Hopff and A. Krieger, "Über Decarboxylierung und Dissoziation heterocyclischer Dicarbonsäuren," *Helvetica Chimica Acta*, vol. 44, no. 4, pp. 1058–1063, 1961.

[9] O. Grosshardt, U. Fehrencacher, K. Kowollik, B. Tübke, N. Dingenouts, and M. Wilhem, "Synthese und Characterisierung von Polyestern und Polyamiden auf der Basis von Furan-2,5-dicarbonsäure," *Chemie Ingenieur Technik*, vol. 11, p. 81, 2009.

[10] K. Yutaka, T. Miura, K. Matsuda, and T. Komuro, "Polyamide compound and molded article thereof," Patent Application WO 2012/132 792 A1, 2012.

[11] P. M. Heertjes and G. J. Kok, "Polycondensation products of 2,5-furandicarboxylic acid," *Delft Progress Report Series A*, vol. 1, pp. 59–63, 1974.

[12] J. A. Moore and W. W. Bunting, "Polyesters and polyamides containing isomeric furan dicarboxylic acids," *Polymer science and technology*, vol. 31, pp. 51–91.

[13] H. Hopff and A. Kreiger, *Makromolecular Chemie*, vol. 47, p. 93, 1961.

[14] M. Kohan, *Nylons Plastics Handbook*. New York: Carl Hanser Verlag, 1995.

[15] B. Sillion, "Aromatic and Heterocyclic Polymers - What Future?" *High Performance Polymers*, vol. 11, no. 4, pp. 417–436, 1999.

[16] B. Guerin, "Polyamides," *Les Techniques de l'Ingénieur*, 1994.

Conclusion

The aim of this study was to synthesize and simulate through molecular modelling a series of biobased polyamides, based on furan-2,5-dicarboxylic acid (FDCA). This monomer is especially interesting because recently it became available from renewable resources. Its similarity of chemical structure with isophthalic acid lets us suppose that PA with the same range of properties could be synthesized.

In order to achieve this goal, the first step was to develop a molecular modelling simulation protocol that was able to predict the glass transition temperatures of polyphthalamides. In order to do this, it was necessary to synthesize a series of polyphthalamides, made from the condensation of a mixture of isophthalic and terephthalic acids with hexamethylene diamine. The PPA were synthesized in a specific set-up, with reasonable molar mass (10000-15000 g/mol) and polydispersity index ranging from 1.9 to 2.9. It was proven by NMR spectroscopy that the acid ratio in the polymer chains was the same as the one introduced in the reactor.

The molecular dynamics protocol was developed to simulate a density vs temperature chart. This MD simulation was composed of several steps. The first step was the construction of the polymer chain. The second step was the packing of several polymer chains in a cell with periodic boundaries, and finally the last step was the molecular dynamics protocol itself. Results of this technique showed that the glass transition of the PA 6-I/6-T copolymers increases as the amount of terephthalic acid was increased in the system. The same trend was observed with the synthesized PPA by DSC, however the modelled Tg were 20°C higher than the experimentally measured ones. This difference was attributed to the polydispersity of the actual specimens and also to the difference of cooling rate during the measurement of the glass transition.

Despite this difference, the molecular modelling protocol for the simulation of the glass transition temperature of polyphthalamides was validated.

The second part of this thesis was dedicated to the simulation and synthesis of the potentially biobased polyphthalamides based on FDCA. The molecular dynamics protocol showed that the glass transition of the PA 6-I/6-F copolymers should

167

decrease as the amount of FDCA increases. In order to confirm this prediction, a series of PA 6-I/6-F copolyamides where synthesized in a pilot-scale reactor. Their chemical structure and composition were studied by NMR, SEC and viscosimetry. It was found that the molar mass of PA 6-F was very low and that several unexpected peaks appeared on the NMR spectra. Therefore NMR (^{13}C, COSY, HMBC, HSQC) and mass spectroscopy (MALDI-TOF) studies were carried out to explain this phenomena. A decarboxylation of the FDCA was pointed out, preventing the chain growth of the PA 6-F and so explaining its very low molar mass.

The thermal and mechanical properties of the PA 6-I/6-F copolymers decreases as the amount of FDCA increases, making the material more brittle, with a lower Tg, and lower resistance to thermal decomposition. All these facts could have two main causes: the very low molar mass of the PA 6-F and/or the influence of the furan heterocycle, which is less rigid and more hydrophilic than the benzene ring of the isophthalic acid.

Within this thesis, we achieve the synthesis of an unusual and potentially biobased polyamide, based on FDCA. However, the molar mass of this polymer were so low that its properties were profoundly affected by that feature. To solve this problem different approaches could be envisaged: It would be interesting to study in the future in a more detailed way the reactivity and stability of this monomer. Indeed, ab-initio simulations of the polymerization reaction of this monomer could provide us with important information, as well as a kinetic study.

In order to increase the molar mass of the PA 6-F, the use of a polymerization catalyst would also be helpful. We studied a few catalysts (phosphoric acid, titanium butoxide, ...) however results were not satisfactory. Another idea would be to improve the protocol of synthesis in the pilote-scale reactor. Indeed, we started the study by using a protocol typical for polyphthalamides, but the FDCA turned out to be less stable than isophthalic acid. Then tailoring the protocol to match this peculiar feature would certainly help to increase of the molar mass of the polymer produced and then its physical properties.

It was also observed that several research groups achieve the synthesis of PA 6-F (or analogues) starting from the dimethyl or diethyl esters instead of the diacids with higher molar mass that we obtained. The diesters may be more thermally stablme than the diacid counterparts.

Finally, it would be interesting to copolymerize the FDCA with other monomers than isophthalic acid, in order to screen a wider range of properties, as for example the copolymerization with 11-aminoundecanoic acid to produce a semi-crystalline, more flexible and with a lower Tg, PA 11/6-F.

Appendix A

Theory in molecular dynamics simulations

1 General considerations

As soon as the notion of temperature is introduced in a simulation, the physics of the system is no longer the one of a system in its lower energy state. Indeed, the energy generated by the temperature allows the system to change from one configuration to another of higher energy. Each conformation has a probability of being adopted by the system. Then every physical or chemical properties have to be defined and calculated as average values over all the possible configurations.

It is the statistical mechanics theory that makes a link between microscopic properties of the system and macroscopic observables (temperature, pressure, etc.) possible. In order to apply statistical mechanics to a defined system, its thermodynamic state has to be defined. This state is defined by a set of parameters such as the number of particles in the system, the temperature...

In this thermodynamic state, the microscopic state of the system constituted of n particles is defined by the atomic coordinates $\mathbf{R_i}$ and by the momentums $\mathbf{p_i}$, for $i \in \{1, ..., n\}$. Together the $\mathbf{R_i}$ and $\mathbf{p_i}$ described a multidimensional space called phase space. In this phase space, a collection of microstates defined by the $(\mathbf{R_i}, \mathbf{p_i})$ couples which are representative of a particular thermodynamical state, describe a statistical ensemble. These statistical ensembles are characterized by the physical quantities that are conservative. The most important ensembles are the micro-canonical (NVE), canonical (NVT), isothermal-isobaric (NPT) and grand canonical (μVT) ensembles.

The aim of the molecular simulation is to obtain a sample of the $(\mathbf{R_i}, \mathbf{p_i})$ couples which are representative of the material which is simulated. Then an observable A

(in the statistical mechanics meaning, every measurable macroscopic property) is calculated as well as its average value $< A >$. In order to compute this average value, the principle of ergodicity is used. The underlying idea is that for certain systems the time average of their properties is equal to the average over the entire space. The Monte-Carlo simulation method provides ensemble averages whereas molecular dynamics provides time averages [1].

The molecular dynamics technique is a deterministic (no random phenomena involved) way to obtain a sample of microstates from trajectories defined through the space of phases of a collection of particles (atoms). From the interaction potential $V(\mathbf{R_i},...,\mathbf{R_M})$ of a conformation (also called forcefield), the resolution of the Newtonian equations of movement provides the evolution of this conformation. This evolution also allows the calculation of average properties of molecules. After an infinite time, the system would have visit the entire space, thus fulfilling the ergodicity hypothesis. However in reality the simulations times are never infinite and the ergodicity of the system is never achieved. Averages values of properties could still be calculated with a desired precision.

The quality of a molecular dynamics (MD) simulation is influenced by several parameters. Among them, one of the most important is the potential V, or forcefield.This forcefield contains in its mathematical expression all the physics and interactions of the system. So if this potential does not represent the reality of the system, the simulation output will be biased. The second important parameter for the accuracy of a simulation is the choice of the integrator. It is the algorithm used to solve the Newton's equations. Then a few other parameters may have an impact on the simulation, such as the thermostat or barostat.

2   Forcefield

2.1   Introduction

The potential $V(\mathbf{R_i},...,\mathbf{R_M})$, or forcefield, is composed of a set of mathematical parameters which represents the several interactions suffered or caused by particles. The particles that are being modelled in fully atomistic MD simulations are atoms, but it is also possible to model groups of atoms in the case of coarse-grained MD simulations.

For the forcefield of an organic material system such as polymers, it is convenient to split the potential into two parts: the first one representing the covalent bondings and the second part representing the non-bonding interactions.

The covalent, or intramolecular potential equation is showed on the equation A.1

$$V_{intra} = \sum_{bounds} V_{vibration} + \sum_{angles} V_{stretching} + \sum_{dihedral\ angles} V_{torsion} + \sum V_{cross-coupling}$$

$$(A.1)$$

The intermolecular interactions are all the interactions between atoms that do not interact through bonds, angles or torsion angles. This potential is also called non-bonded potential and is composed of two terms: a Van der Waals term and an electrostatic interaction term. This potential could be written as showed on the equation A.2

$$V_{inter} = \sum_{non\ bonded\ atoms} V_{Van\ der\ Waals} + \sum_{non\ bonded\ atoms} V_{Electrostatic} \qquad (A.2)$$

For this study we have chosen the COMPASS forcefield, from the company Accelrys, which is a forcefield optimized for organic molecules and polymers.

2.2 COMPASS

COMPASS stands for *Condensed-phase Optimized Molecular Potential of Atomic Simulation Studies*. This forcefield was developed by the Accelrys company [2] (ex MSI, San Diego, California). It was developed and optimized for the study of the thermo-physical properties of the condensed mater, and especially organic molecules and polymers. This optimisation was done by *ab-initio* calculation in combination with experimental values [3].

The mathematical expression of the COMPASS forcefield is shown on figure A.1

This equation could be divided into two parts: the valence terms and the non-bonding interaction terms. The valence terms represent the inner coordinates of the chemical bonds (b), angles (θ), torsion angles (ϕ) and out of-plane torsions (χ). It also represents the different cross coupling terms which are a combination of 2 or 3 of these coordinates. These coupling terms are important for the prediction of bond vibrations and all properties associated with the conformation of the molecules.

The non-bonding interaction terms is here represented by LJ-9-6 term. This term is a Lennard-Jones potential with the powers 9 and 6 [4]. It represents the Van der Waals interaction (repulsive at small distances and attractive at higher distances) [1]. The second non-bonding term is a Coulombic function that stands for the electrostatic interactions.

Every parameter of this equation is specific for an atom "type" and was calculated or measured.

$$
\begin{aligned}
E_{\text{total}} = &\sum_b [k_2(b - b_{\text{o}})^2 + k_3(b - b_{\text{o}})^3 + k_4(b - b_{\text{o}})^4] + \\
&\sum_\theta [k_2(\theta - \theta_{\text{o}})^2 + k_3(\theta - \theta_{\text{o}})^3 + k_4(\theta - \theta_{\text{o}})^4] + \\
&\sum_\phi [k_1(1 - \cos\phi) + k_2(1 - \cos 2\phi) + k_3(1 - \cos 3\phi)] + \\
&\sum_\chi k_2\chi^2 + \sum_{b,b'} k(b - b_{\text{o}})(b' - b'_{\text{o}}) + \\
&\sum_{b,\theta} k(b - b_{\text{o}})(\theta - \theta_{\text{o}}) + \sum_{b,\phi} (b - b_{\text{o}})[k_1\cos\phi + \\
&k_2\cos 2\phi + k_3\cos 3\phi] + \sum_{\theta,\phi} (\theta - \theta_{\text{o}})[k_1\cos\phi + \\
&k_2\cos 2\phi + k_3\cos 3\phi] + \sum_{b,\theta} k(\theta' - \theta_{\text{o}}')(\theta - \theta_{\text{o}}) + \\
&\sum_{\theta,\theta,\phi} k(\theta - \theta_{\text{o}})(\theta' - \theta'_{\text{o}})\cos\phi + \sum_{i,j} \frac{q_i q_j}{r_{ij}} + \\
&\sum_{i,j} \epsilon_{ij}\left[2\left(\frac{r_{ij}^{\text{o}}}{r_{ij}}\right)^9 - 3\left(\frac{r_{ij}^{\text{o}}}{r_{ij}}\right)^6\right]
\end{aligned}
$$

Figure A.1: Mathematical expression of the COMPASS forcefield.

3 Integrators

An integration algorithm should possess some essential qualities such as a good accuracy, the energy conservation, reversibility with the time, light consumption of memory and speed of calculation. It should also preserve the symplectic form on phase space. Symplectic integrators possess as a conserved quantity a Hamiltonian which is slightly perturbed from the original one. By virtue of these advantages, the SI scheme has been widely applied to the calculations of long-term evolution of chaotic Hamiltonian systems ranging from the Kepler problem to the classical and semi-classical simulations in molecular dynamics.

Among the several available integrators, the Verlet algorithm [5] is one of the simplest and more robust. An improved version of this algorithm has been developed, which is called "velocity-Verlet" [6, 7].

3.1 Verlet integrator

This algorithm is based on the Taylor decomposition up to the 4th order of the R_i position versus the time, as showed on the equations A.3 and A.4.

$$R_i(t + \Delta t) = R_i(t) + v_i(t) + \frac{F_i(t)}{2M_i}\Delta t^2 + \frac{\Delta t^3}{3}\frac{d^3 R(t)}{dt^3} + o(\Delta t^4) \qquad (A.3)$$

$$R_i(t - \Delta t) = R_i(t) - v_i(t) + \frac{F_i(t)}{2M_i}\Delta t^2 - \frac{\Delta t^3}{3}\frac{d^3 R(t)}{dt^3} + o(\Delta t^4) \qquad (A.4)$$

The Δt term is the time step of the MD simulation. Usually a time step of 1 fs (10^{-15}s) is used, which requires 1000 integrations for a 1 ps trajectory. This time step is a good compromise between calculation time and accuracy. The term $v_i(t)$ represent the velocity of the particle i and the term $F_i(t)$ its acceleration.

By adding the equations A.3 and A.4, we could obtain the following equations:

$$R_i(t + \Delta t) + R_i(t - \Delta t) = 2R_i(t) + \frac{F_i(t)}{M_i}\Delta t^2 + o(\Delta t^4) \qquad (A.5)$$

$$R_i(t + \Delta t) = 2R_i(t) - R_i(t - \Delta t) + \frac{F_i(t)}{M_i}\Delta t^2 + o(\Delta t^4) \qquad (A.6)$$

Starting from the position at the t and $t - \Delta t$ times and the acceleration at the time t, the equation A.6 gives us the position at the time $t + \Delta t$. This equation then could provide a trajectory for the particle i.

With this equation the velocity at the time t was not necessary to calculate the new position. However, for the calculation of dynamic properties, it is necessary to

know the velocity of the particles at every step of the simulation. This velocity is calculable by the finite difference method for the i particle at time t:

$$v_i(t) = \frac{R_i(t + \Delta t) - R_i(t - \Delta t)}{2\Delta t} + o(\Delta t^2) \qquad (A.7)$$

The Verlet algorithm is time-reversible and pseudo symplectic. Indeed, in the infinitely small time step limit, the algorithm conserves a pseudo hamiltonian close to the hamiltonian of the real system. As a consequence, the energy of the system drift only slightly at long simulation times, but this algorithm is not very accurate at big time steps.

In order to increase the accuracy of the integration of the velocity, two algorithms based on the Verlet integrator exist. The first one is called leapfrog Verlet, which calculates with a good accuracy the velocity but not at the same value of the time variable than the position. This feature prevents the computation of the potential and kinetic energies of the system, thus the total energy of the system in a direct way. This is the major drawback of this method. The second integrator is the velocity Verlet integrator, which is less accurate than the leapfrog one, but the velocity and position are calculated at the same value of the time variable, so its allows the calculations of energies.

3.2 Velocity Verlet algorithm

This algorithm starts with the Taylor development to the second order of the atomic coordinates:

$$R_i(t + \Delta t) = R_i(t) + v_i(t) + \frac{F_i(t)}{2M_i}\Delta t^2 \qquad (A.8)$$

Of the velocity:

$$v_i(t + \Delta t) = v_i(t) + \frac{F_i(t)}{M}\Delta t + \frac{\dot{F}_i(t)}{2M_i}\Delta t^2 \qquad (A.9)$$

And the force:

$$F_i(t + \Delta t) = F_i(t) + \dot{F}_i(t)\Delta t \qquad (A.10)$$

$$\frac{\dot{F}_i(t)\Delta t}{2M} = \frac{F_i(t + \Delta t) - F_i(t)}{2M} \qquad (A.11)$$

By incorporating the equation A.11 in the equation A.9, the velocity is calculable:

$$v_i(t + \Delta t) = v_i(t) + \frac{F_i(t + \Delta t) + F_i(t)}{M} \Delta t \qquad \text{(A.12)}$$

The equations A.8 and A.12 allow the calculation of the position and velocity of the particles at the time $t + \Delta t$. This algorithm is adapted for solving the Newton's equations of motion in MD simulations.

An addition to this algorithm could be done in order to quickly compute the non-bonding interactions. This technique is known as the Ewald summation method [8, 9]. The basic idea of this method is to replace the summation of interaction energies in real space with an equivalent summation in Fourier space. The advantage of this approach is the rapid convergence of the Fourier-space summation compared to its real-space equivalent when the real-space interactions are long-range. Because electrostatic energies consist of both short- and long-range interactions, it is maximally efficient to decompose the interaction potential into a short-range component summed in real space and a long-range component summed in Fourier space.

Generally, the use of Newton equations implies that the energy of the system is conserved. As a consequence, the statistical ensemble is similar to the microcanonical ensemble, in which the total number of particles N, the volume V and the energy E are conserved. In practical, for the study of materials, it may be convenient to work in thermodynamical conditions close to reality. With MD simulations it is possible to work with realistic ensembles such as canonical ensemble (NVT) and the isothermal-isobaric (NPT) ensembles.

In order to keep constant pressure or temperature in these ensembles, the use of thermostats or barostat is required.

4 Thermostat

In classical statistical mechanics, the equipartition theorem is a general formula that relates the temperature of a system with its average energies. The mathematical expression of the temperature is showed on the equation A.13:

$$\langle \sum_{i=1}^{N} \frac{p_i^2}{2m} \rangle = \langle K \rangle = \frac{N_{lib} kT}{2} \qquad \text{(A.13)}$$

On this equation we can see that if the total energy is conserved, fluctuations of the kinetic energy K, and the potential energy V may occur. k is the Boltzmann constant.

The thermodynamical temperature is a way to quantify the average energy associated to the different degrees of freedom of the system N_{lib}. Starting from this

equation, it is possible to calculate an instantaneous temperature T_{inst}:

$$T_{inst} = \frac{2K}{N_{lib}kT} \tag{A.14}$$

The thermodynamical temperature is obtained through averaging the instantaneous temperature.

Imposing a fixed T_{inst} is not an efficient way of controlling the temperature of the simulation because in this case we prevent these natural fluctuations of the kinetic energy, which allows conformation changes and molecular motion. In the NVT ensemble, it may be much more efficient to use other ways of control. These methods are called thermostats.

4.1   Isokinetics methods

These methods are based on the equipartition theorem. As a consequence, they may not model ensembles where the temperature has to be constant. These isokinetics methods are based on the idea of the conservation of the temperature with a fluctuating quantity of movement:

$$\sum \frac{(\lambda p_i)^2}{m} = N_{lib}k_B T \tag{A.15}$$

Several techniques are available to determine the parameterλ. The more used one is called "velocity scalling". This method calculates the velocity of the atoms v_{new} with the following constraint:

$$\left(\frac{v_{new}}{v_{old}}\right)^2 = \frac{T_{ext}}{T} \tag{A.16}$$

This equation explains the term "velocity scaling". Indeed, this thermostat applies a direct modification to all particles velocities that is equal to the ratio between the desired temperature (T_{ext}, temperature of the external heat bath) and the "measured" instantaneous temperature.

4.2   Berendsen thermostat

Another technique is called the Berendsen thermostat [10]. In this method, the system has to obey the following equation:

$$\frac{dT}{dt} = \frac{(T - T_{ext})}{\tau_T} \tag{A.17}$$

where τ_T is the time constant characterizing the frequency of the coupling of the system to the temperature bath. The solution of the equation A.17 forces velocities and positions to be scaled at every time-step by the factor χ_T:

$$\chi_T = \left(1 + \frac{dt}{\tau_T} \left(\frac{T}{T_{ext}} - 1 \right) \right)^{\frac{1}{2}} \tag{A.18}$$

These thermostats are simple but they suffer from the fact that they are not defined in a certain statistical ensemble. Consequently, there exists no Hamiltonian conserved during the MD simulation, i.e. the equations of motion are no longer time reversible. To overpass this major drawback, other thermostats algorithms have been developed.

4.3 Andersen thermostat

In the constant-temperature method proposed by Andersen [11] the system is coupled to a heat bath that imposes the desired temperature. The coupling to a heat bath is represented by stochastic impulsive forces that act occasionally on randomly selected particles. The probability of a particle to undergo this stochastic collision is $\upsilon \Delta t$, where υ is the frequency of the collisions (adjustable parameter) and Δt the time step of the simulation.

If a particle is selected to undergo this collision, it has its velocity replaced by a random velocity taken from a Gaussian distribution of velocities corresponding to the desired temperature (see equation A.19).

$$P(\vec{v}) \propto \exp\left(\frac{-mv^2}{2k_BT} \right) \tag{A.19}$$

This thermostat is efficient when only static properties are extracted from the simulation. Indeed, the stochastic collisions modify the trajectories of the particles so they become unrealistic. The calculation of all the dynamic properties from this simulation is then perturbed. This drawback may not be so severe if the frequency of collision is very small, but then the efficiency of the thermostat to control the temperature is reduced.

4.4 Nosé-Hoover thermostat

In order to constraint temperature, Nosé [12] introduced an additional degree of freedom, s, in the Lagrangian of the system. In classical mechanics the Lagrangian, L is equal to $L = K - V$, where K is the kinetic energy and V the potential energy

of the system.

The parameter s plays the role of a heat bath, whose aim is to damp out temperature deviations from the desirable level. This necessitates adding to the total energy an additional potential energy term:

$$V_s = gk_BT\ln s \tag{A.20}$$

and an additional kinetic energy term of the form:

$$K_s = \frac{Q}{2}\left(\frac{\dot{s}}{s}\right)^2 = \frac{p_s^2}{2Q} \tag{A.21}$$

In the two equations A.20 and A.21, g is the total number of degree of freedom ($g = 3N_{atoms} - N_{bonds} - 3$) with N_{atoms} and N_{bonds} standing for the total number of atoms and bonds in the system respectively), while Q and p_s represent the "effective mass" and momentum, respectively, associated with the new degree of freedom s. Then equations of motion are derived from the Lagrangian of the extended ensemble, including the degree of freedom s. Hoover worked on the formalisation of these equation as follows [13]:

$$\dot{\mathbf{r}}_i = \frac{\mathbf{p}_i}{m_i} \tag{A.22}$$

$$\dot{\mathbf{p}}_i = -\frac{\partial V}{\partial \mathbf{r}_i} - \frac{\dot{s}}{s}\mathbf{p}_i \tag{A.23}$$

$$\dot{p}_s = \frac{1}{Q}\left(\sum_{i=1}^{N}\frac{\mathbf{p}_i^2}{m_i} - gk_BT\right),\ with\ p_s = Q\frac{\dot{s}}{s} \tag{A.24}$$

This set of equations leads to a canonical distribution.

The total Hamiltonian of the system, which should be conserved during the MD simulation becomes:

$$H_{Nose-Hoover} = \sum_{i=1}^{N}\frac{\mathbf{p}_i^2}{m_i} + V(\mathbf{r}^N) + gk_BT\ln s + \frac{p_s^2}{2Q} \tag{A.25}$$

Q, which is the effective mass associated to the s virtual coordinates, controls the inertia of the heat bath. A small value of Q will correspond to a small inertia of the heat bath, leading to quick fluctuations of temperature. This impose the use of a small time step, otherwise the calculation may diverge. On the contrary, a big value a Q may lead to slow temperature fluctuations.

The use of this additional degree of freedom acts as a scale factor on all parame-

ters. A link between simulation parameters and reality could be made with the use of these equations: $t_{true} = \frac{t_{sim}}{s}$; $p_{true} = \frac{p_{sim}}{s}$; $r_{true} = r_{sim}$ and $s_{true} = s_{sim}$.

This Nosé-Hoover thermostat is an efficient MD thermostat, leading to realistic trajectories. However its Hamiltonian is not symplectic and this may lead to problems with a few particular systems.

5   Barostats

Barostats are based on the same principle that thermostats. The thermostats apply changes on the velocity of particles or on the momentum, while barostats applies changes on positions. The most common barostat used is the Berendsen one. It is based on the same kind of equations that its thermostat. The main equation that the system has to obey is the following:

$$\frac{dP}{dt} = \frac{(P - P_{ext})}{\tau_P} \tag{A.26}$$

By integration, it could be shown that all positions have to be scale by a factor χ_P, with P_{ext} the pressure of the external bath, i.e. the desired pressure:

$$\chi_P = 1 - \beta_T \frac{dt}{\tau_P}(P - P_{ext}) \tag{A.27}$$

with β_T the isothermal compressibility of the system.

These several tools, like thermostat and barostat, have to be parametrized very carefully, because they modify the equations of the model (in particular the Newton's equations) and may have a major impact on the accuracy of the simulations.

References

[1] D. Frenkel and B. Smit, *Understanding Molecular Simulation, Second Edition: From Algorithms to Applications*, 2nd ed.   Academic Press, Nov. 2001.

[2] Accelrys, "Materials Studio V5.0, Amorphous Cell, Forcite +," San Fransisco (CA), 2009.

[3] H. Sun, P. Ren, and J. Fried, "The COMPASS force field: parameterization and validation for phosphazenes," *Computational and Theoretical Polymer Science*, vol. 8, no. 1-2, pp. 229–246, 1998.

[4] A. Warshel and S. Lifson, "Consistent Force Field Calculations. II. Crystal Structures, Sublimation Energies, Molecular and Lattice Vibrations, Molecular

Conformations, and Enthalpies of Alkanes," *The Journal of Chemical Physics*, vol. 53, no. 2, pp. 582–594, 1970.

[5] L. Verlet, "Computer "Experiments" on Classical Fluids. I. Thermodynamical Properties of Lennard-Jones Molecules," *Physical Review*, vol. 159, pp. 98–103, Jul 1967.

[6] W. C. Swope, H. C. Andersen, P. H. Berens, and K. R. Wilson, "A computer simulation method for the calculation of equilibrium constants for the formation of physical clusters of molecules: Application to small water clusters," *The Journal of Chemical Physics*, vol. 76, no. 1, pp. 637–649, 1982.

[7] E. Hairer, C. Lubich, and G. Wanner, "Geometric numerical integration illustrated by the Störmer-Verlet method," *Acta Numerica*, vol. 12, pp. 399–450, 2003.

[8] P. P. Ewald, "Die Berechnung optischer und elektrostatischer Gitterpotentiale," *Annalen der Physik*, vol. 369, no. 3, pp. 253–287, 1921.

[9] T. Darden, D. York, and L. Pedersen, "Particle mesh Ewald: An N-log(N) method for Ewald sums in large systems," *The Journal of Chemical Physics*, vol. 98, no. 12, pp. 10 089–10 092, 1993.

[10] H. J. C. Berendsen, J. P. M. Postma, W. F. van Gunsteren, A. DiNola, and J. R. Haak, "Molecular dynamics with coupling to an external bath," *The Journal of Chemical Physics*, vol. 81, no. 8, pp. 3684–3690, Oct. 1984.

[11] H. C. Andersen, "Molecular dynamics simulations at constant pressure and/or temperature," *The Journal of Chemical Physics*, vol. 72, no. 4, pp. 2384–2393, 1980.

[12] S. Nose, "A unified formulation of the constant temperature molecular dynamics methods," *The Journal of Chemical Physics*, vol. 81, no. 1, pp. 511–519, 1984.

[13] W. G. Hoover, "Canonical dynamics: Equilibrium phase-space distributions," *Physical Review part A*, vol. 31, pp. 1695–1697, Mar 1985.

Appendix B

Pictures of the polyphthalamides synthesized

1 FDCA based polyphthalamides
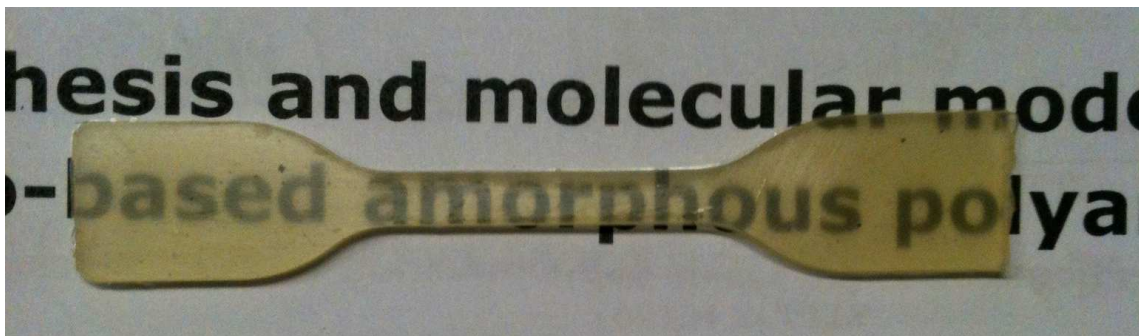
Figure B.1: Picture of a PA 6-I$_{80}$/6-F$_{20}$
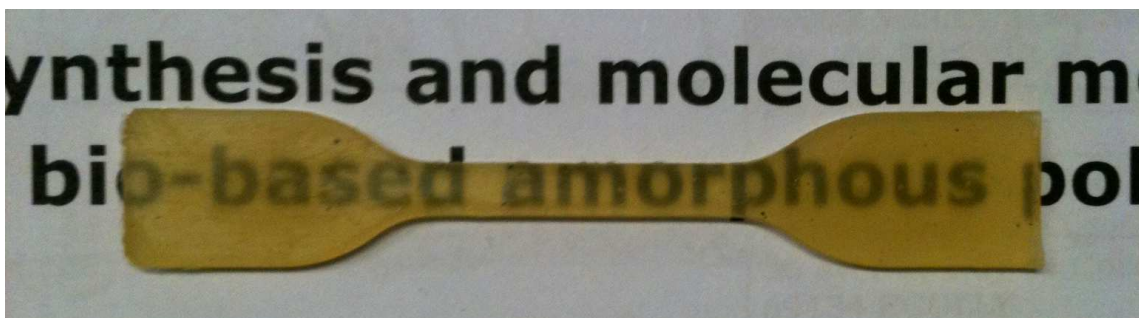
Figure B.2: Picture of a PA 6-I$_{70}$/6-F$_{30}$
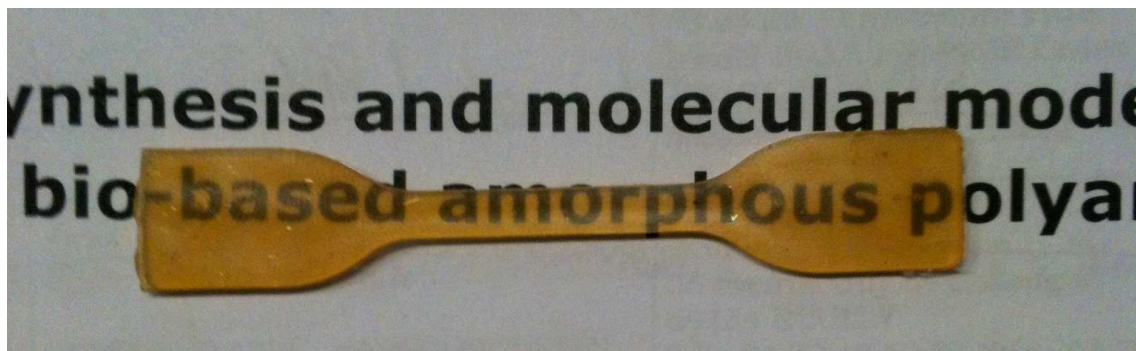
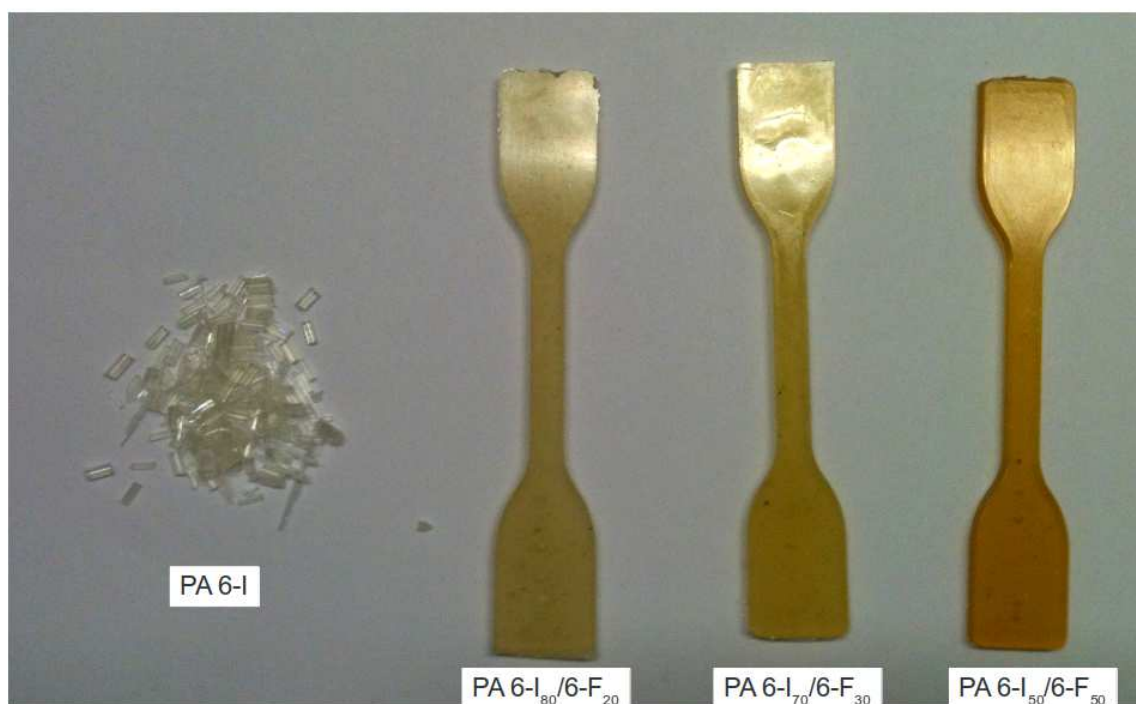Figure B.3: Picture of a PA 6-I_{50}/6-F_{50}

Figure B.4: Comparison of the colors of the synthesized PA 6-I_x/6-F_y
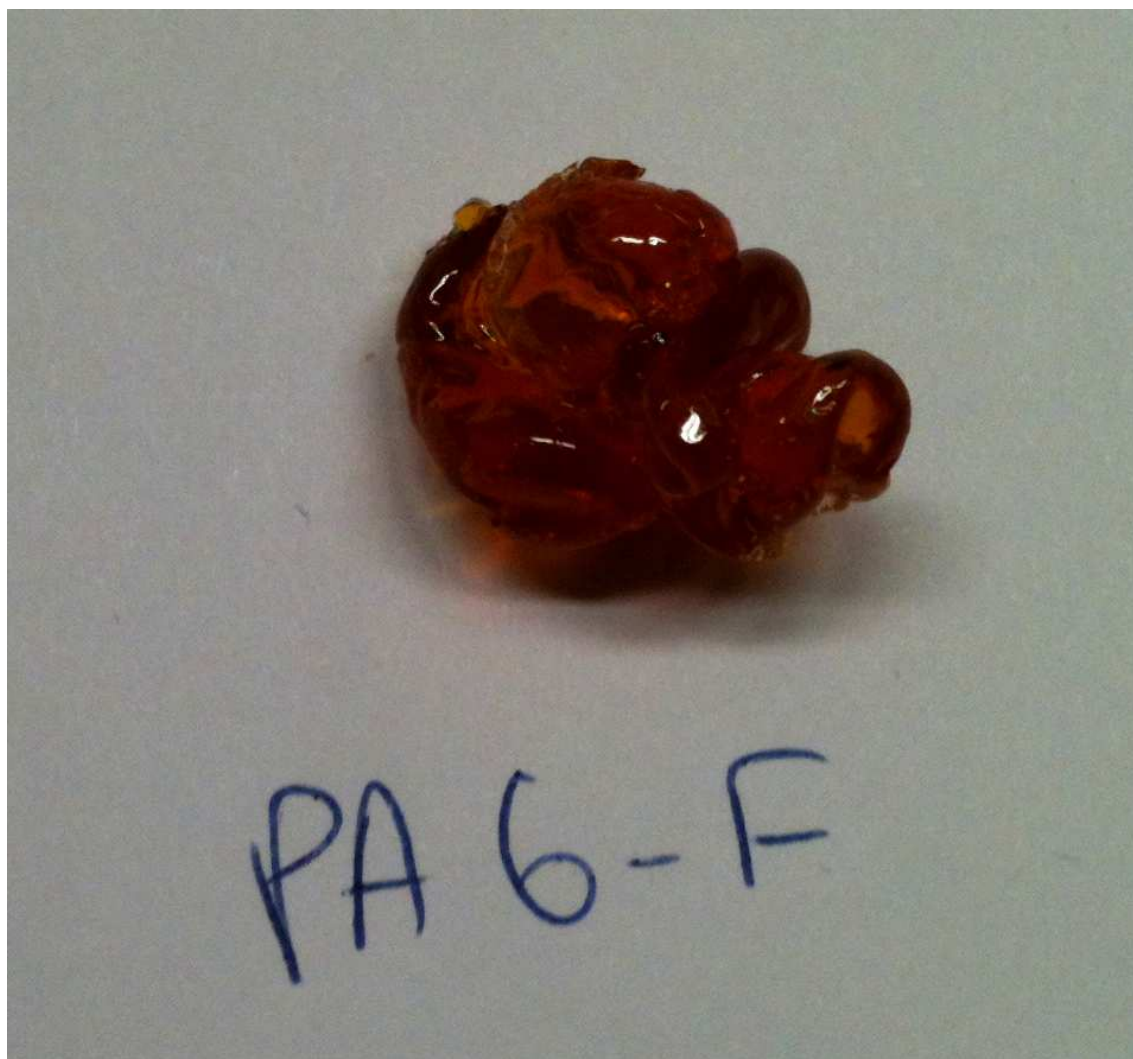
Figure B.5: Picture of a PA 6-F
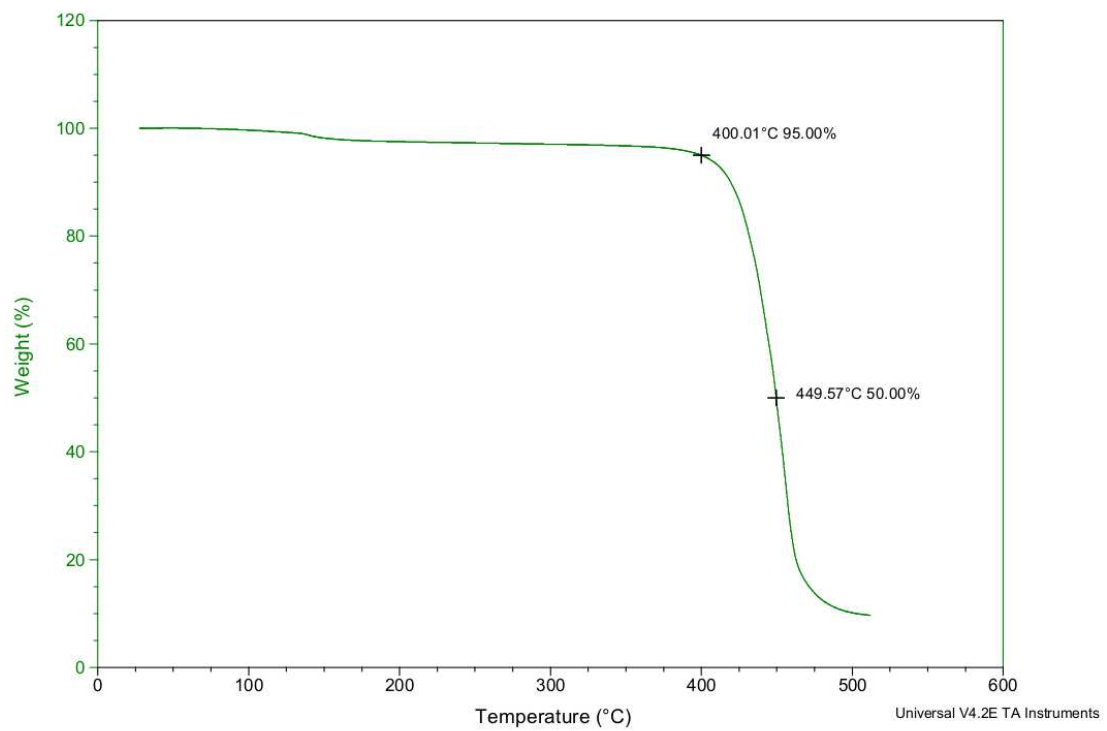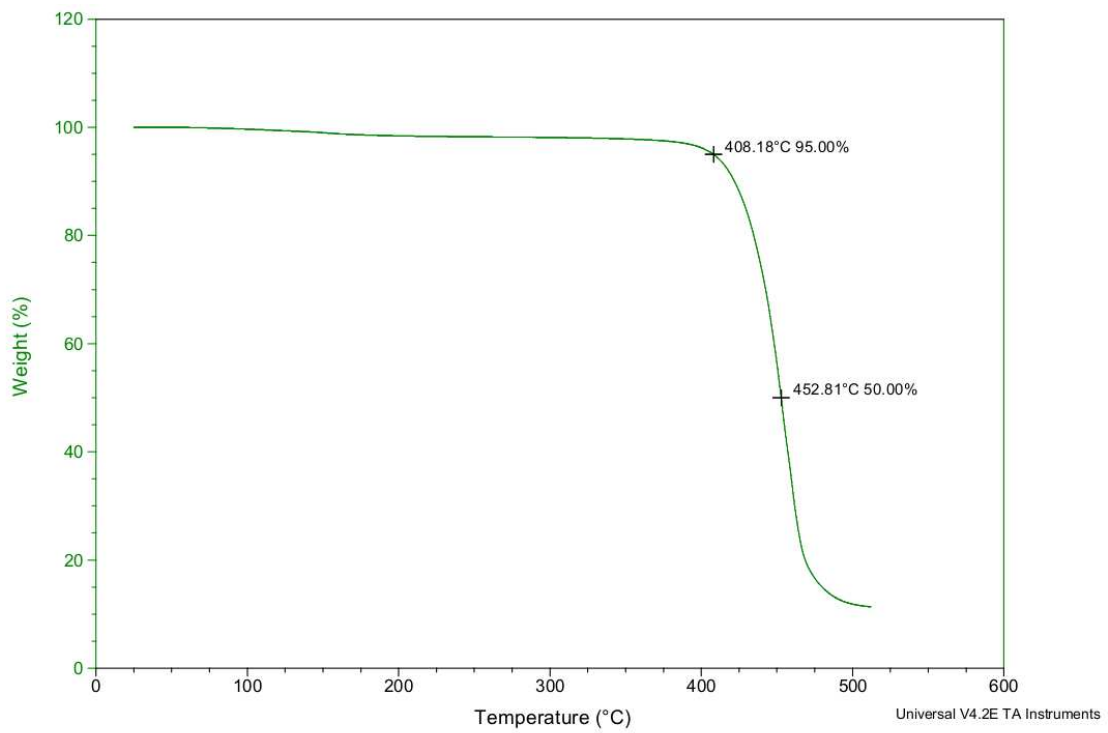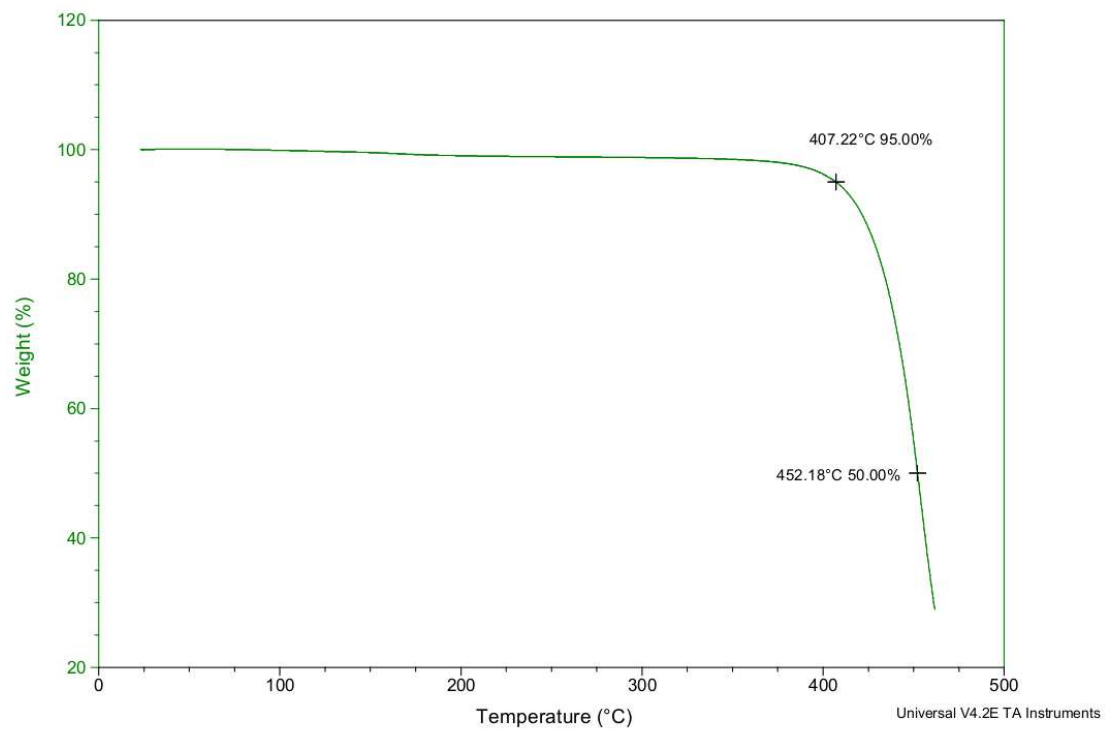
Appendix C

Thermogravimetric analysis

Figure C.1: TGA of a PA 6-I$_{90}$/6-F$_{10}$

Figure C.2: TGA of a PA 6-I$_{80}$/6-F$_{20}$

Figure C.3: TGA of a PA 6-I$_{70}$/6-F$_{30}$
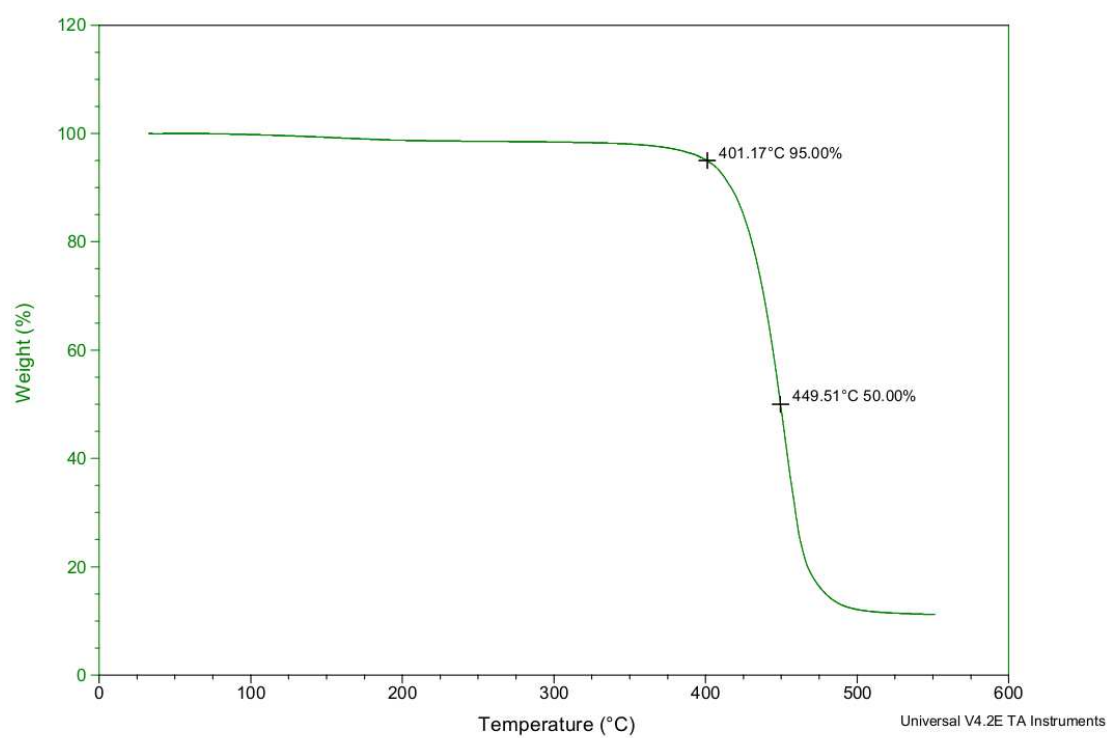
Figure C.4: TGA of a PA 6-I$_{60}$/6-F$_{40}$

Appendix D

Differential Scanning Calorimetry analysis

1 PA 6-I/6-T copolymers
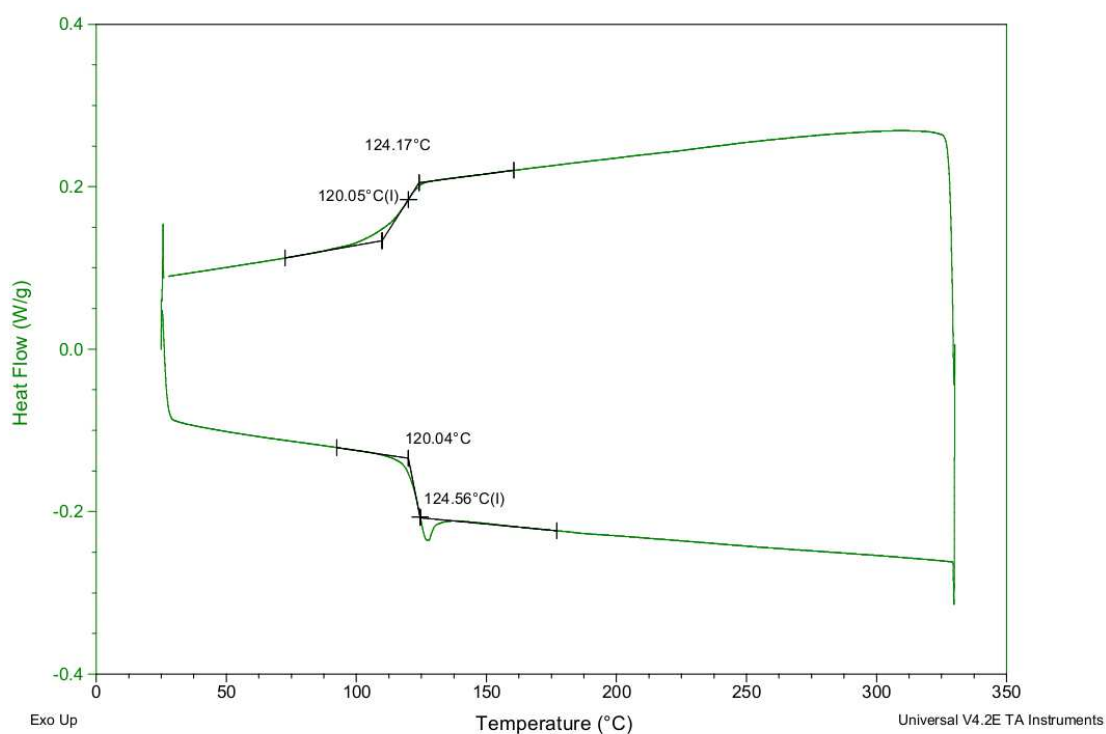
Figure D.1: DSC of a PA 6-I

189
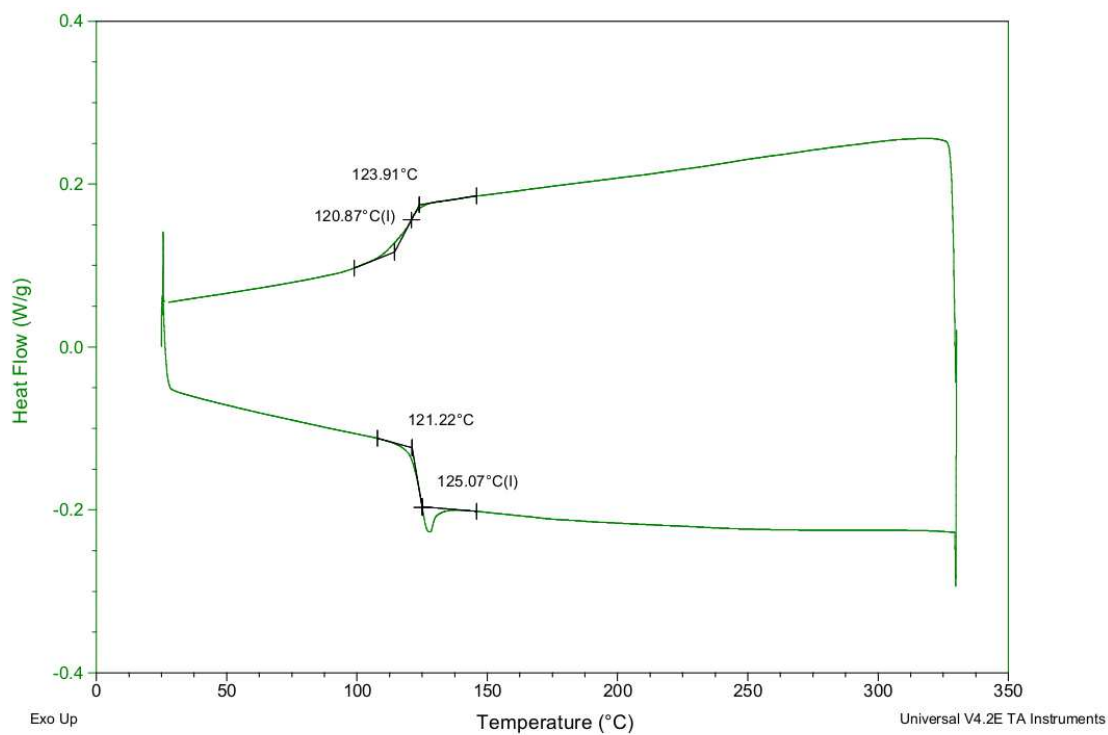
Figure D.2: DSC of a PA 6-I$_{90}$/6-T$_{10}$
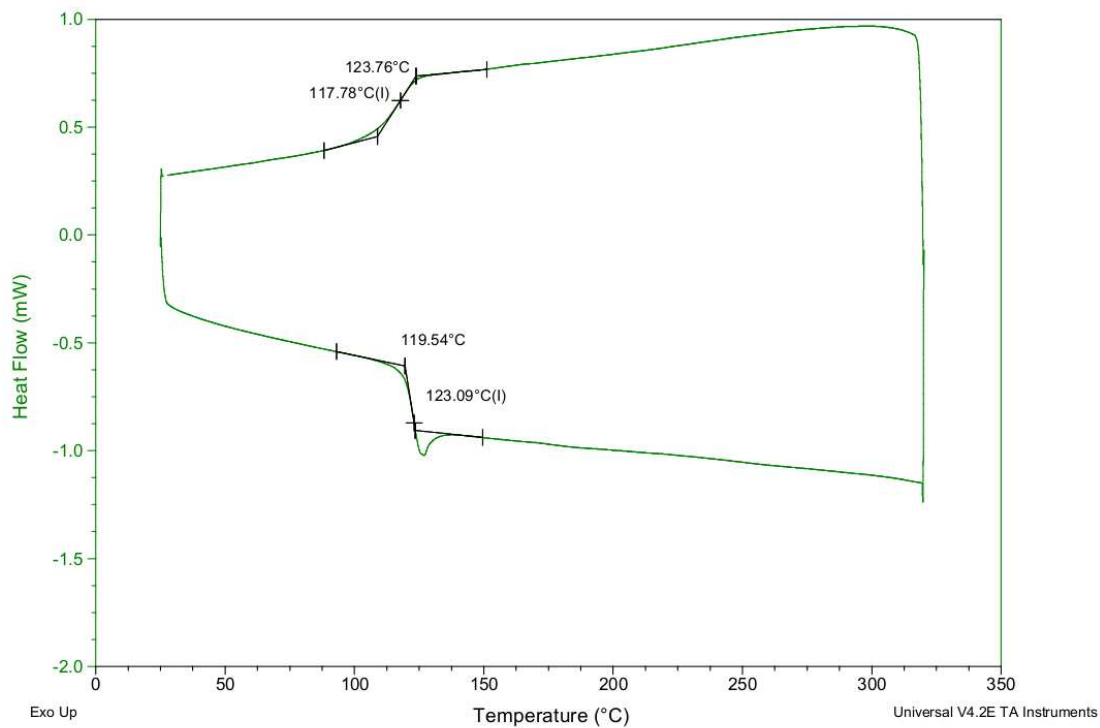
Figure D.3: DSC of a PA 6-I$_{80}$/6-T$_{20}$
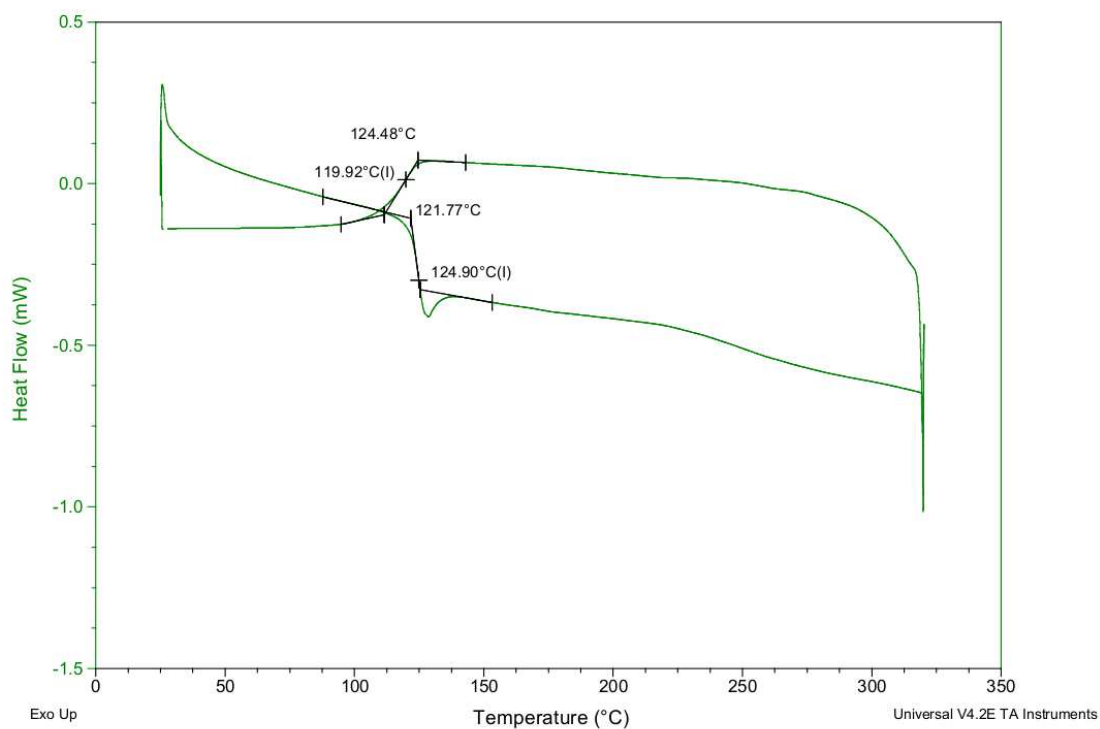
Figure D.4: DSC of a PA 6-I$_{70}$/6-T$_{30}$
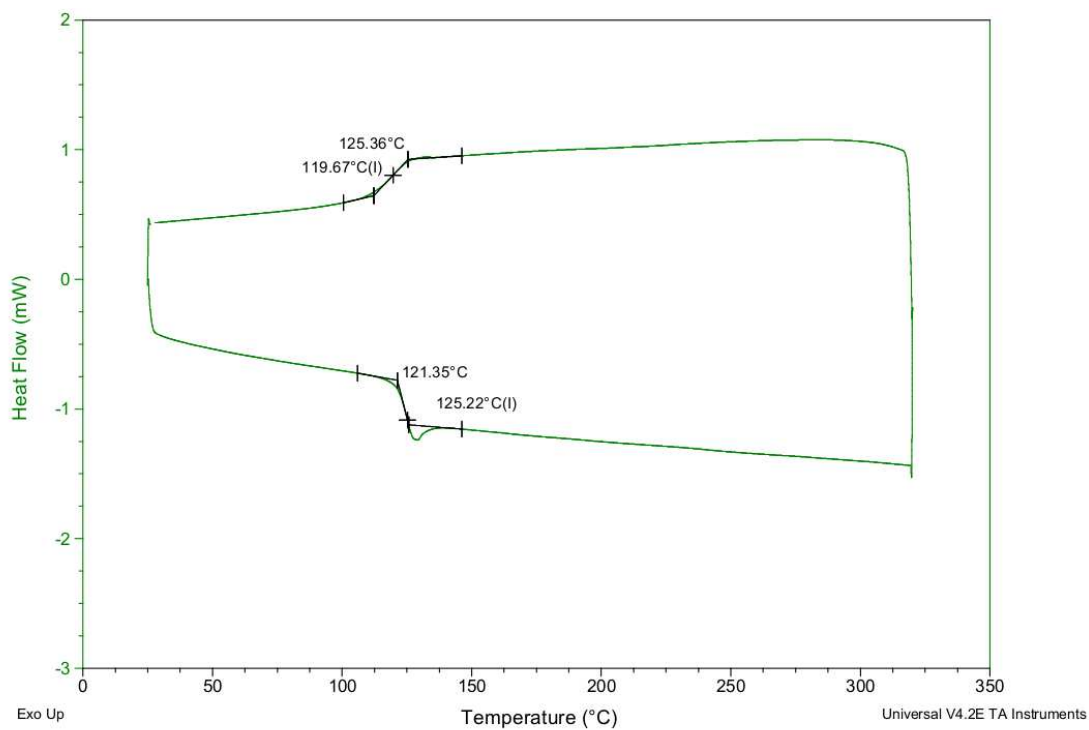
Figure D.5: DSC of a PA 6-I$_{60}$/6-T$_{40}$

2   PA 6-I/6-F copolymers
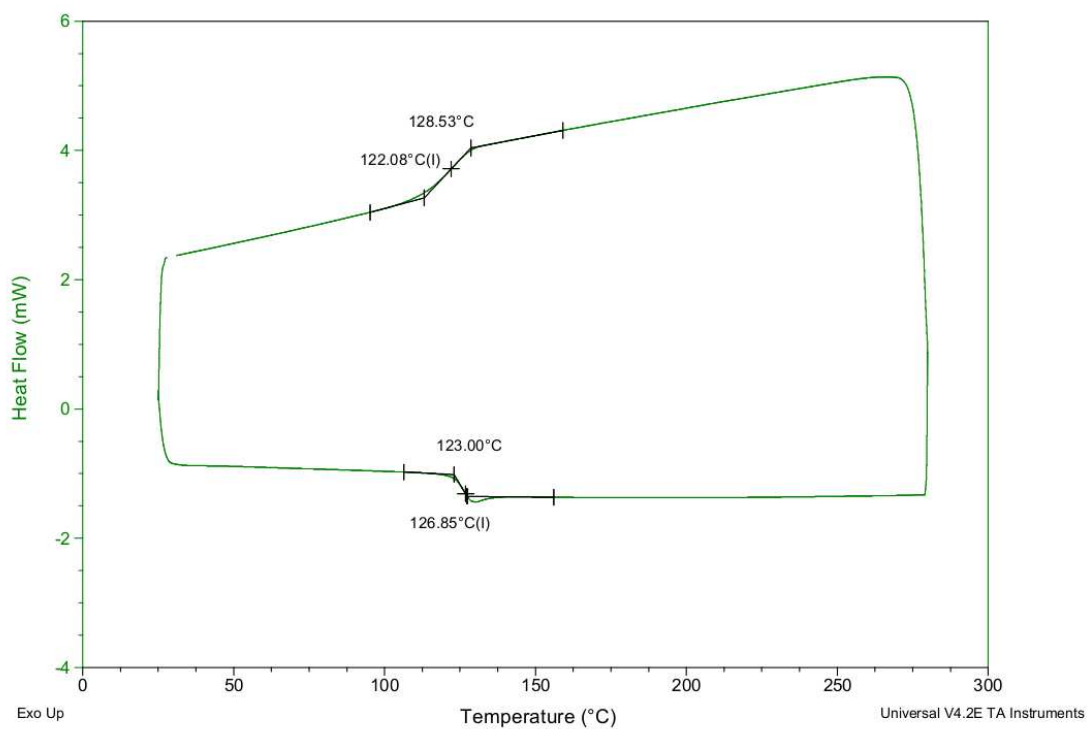
Figure D.6: DSC of a PA 6-I$_{90}$/6-F$_{10}$
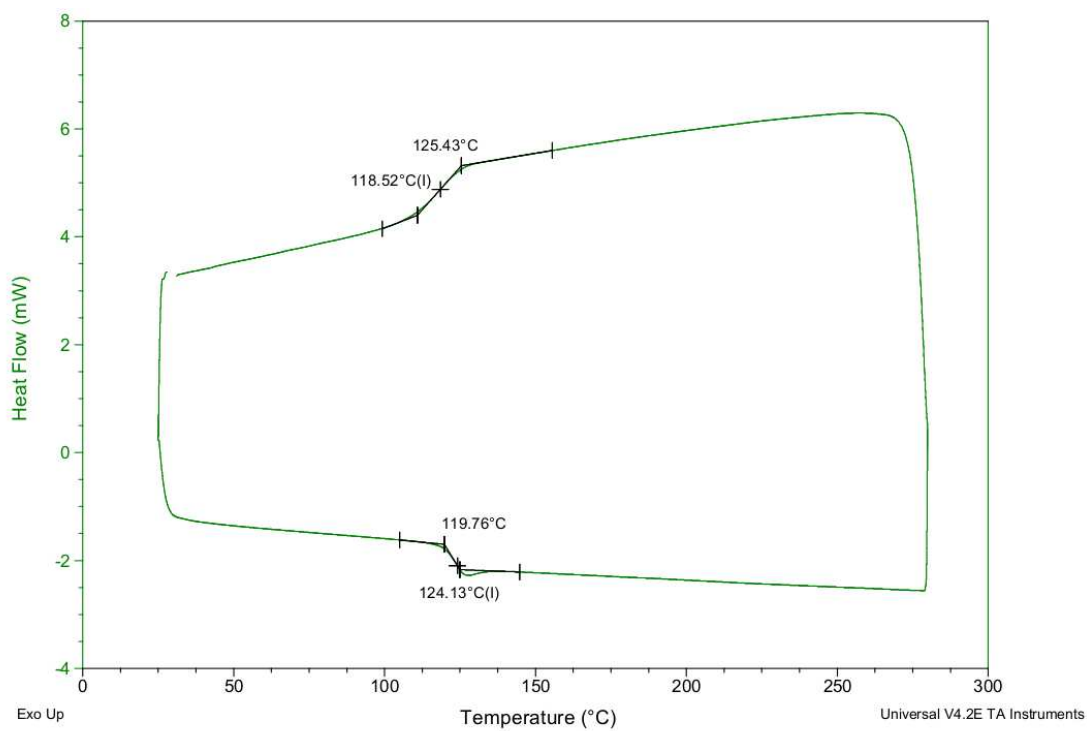
Figure D.7: DSC of a PA 6-I$_{80}$/6-F$_{20}$
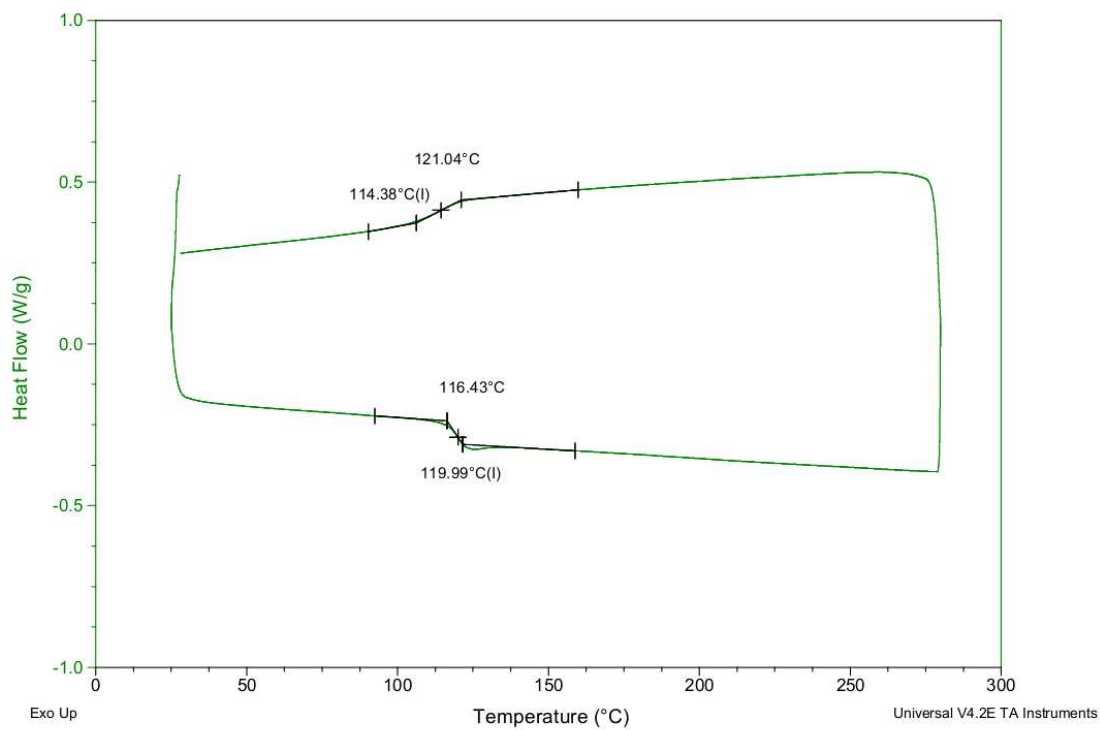
Figure D.8: DSC of a PA 6-I$_{70}$/6-F$_{30}$
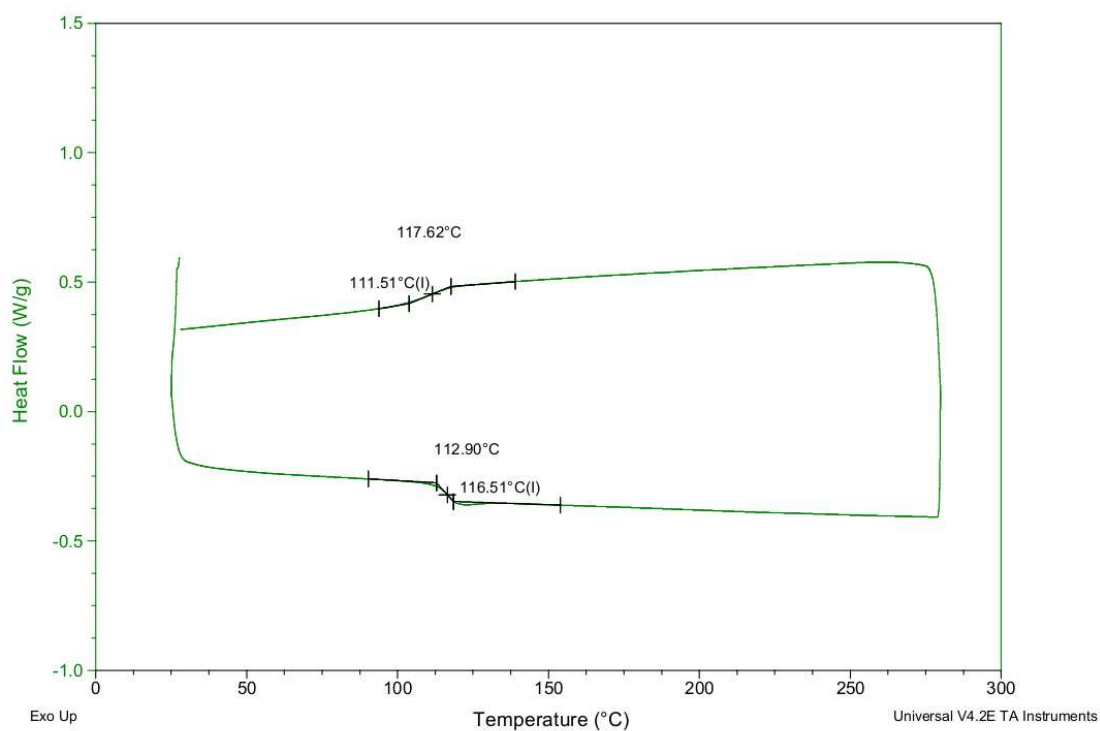
Figure D.9: DSC of a PA 6-I$_{60}$/6-F$_{40}$
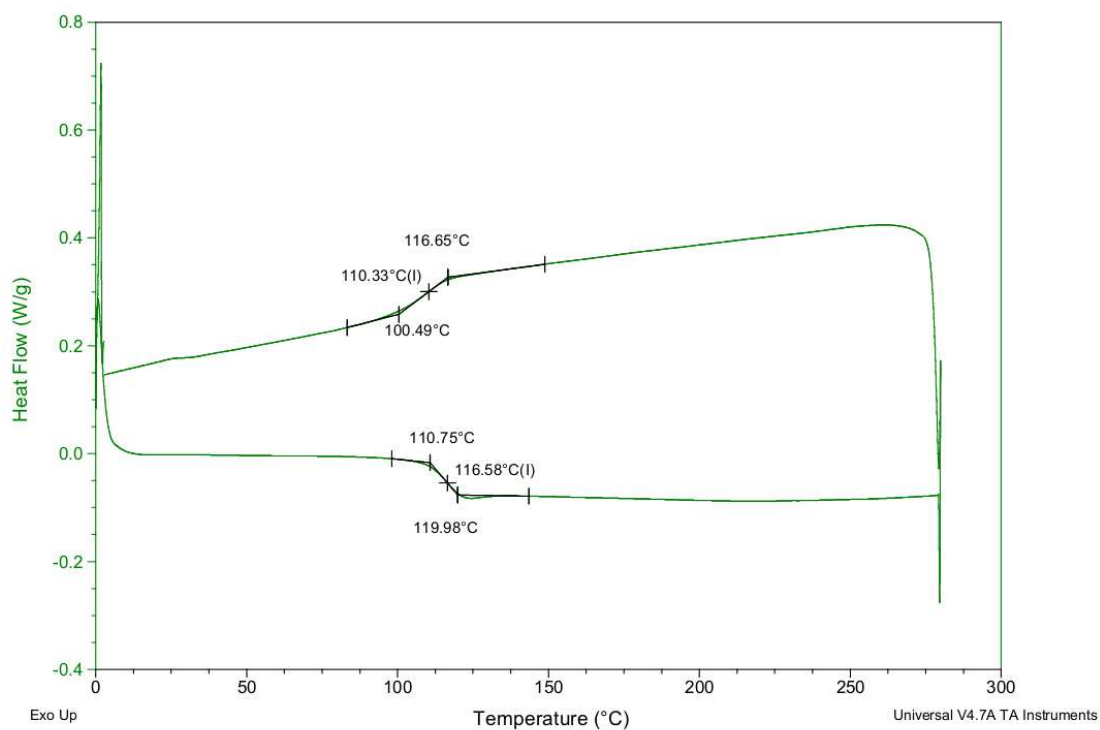
Figure D.10: DSC of a PA 6-I$_{50}$/6-F$_{50}$
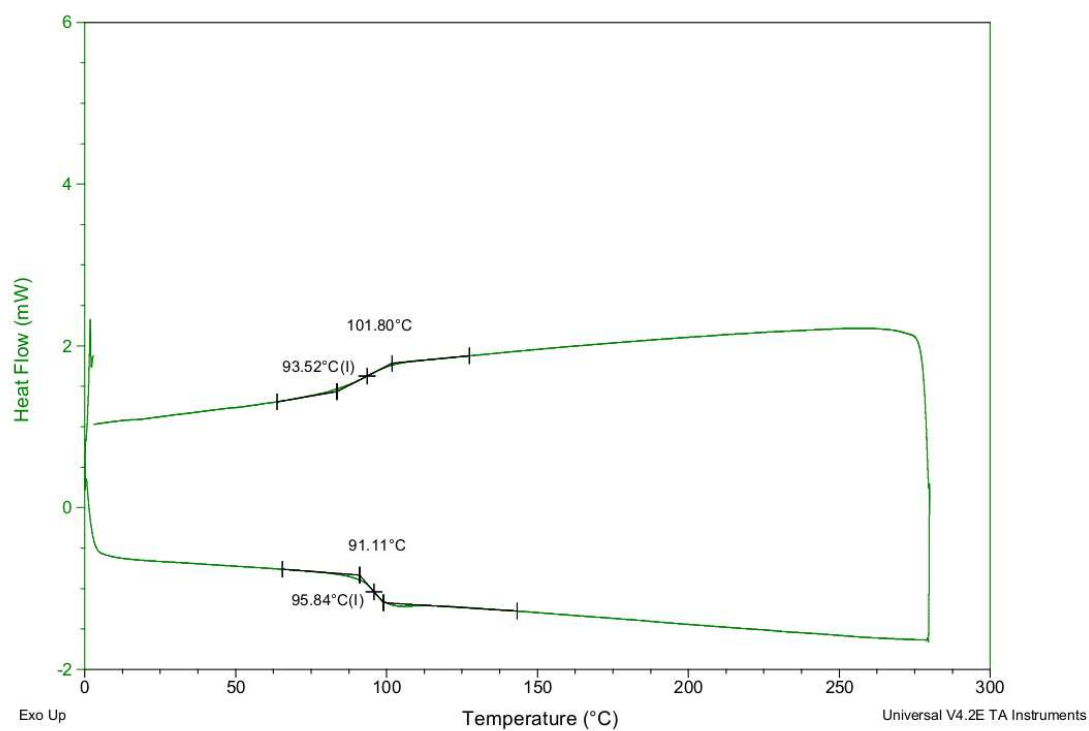
Figure D.11: DSC of a PA 6-F

FOLIO ADMINISTRATIF

THESE SOUTENUE DEVANT L'INSTITUT NATIONAL DES SCIENCES APPLIQUEES DE LYON

NOM : COUSIN   DATE de SOUTENANCE : 19 mars 2013

Prénoms : Thibault Roger

TITRE : Synthesis and molecular modelling of bio-based amorphous polyamides

NATURE : Doctorat   Numéro d'ordre : 2013 ISAL 0019

Ecole doctorale : Matériaux

Spécialité : Matériaux Polymères

RESUME :

Dans le contexte actuel de raréfaction des ressources fossiles, le développement des polymères biosourcés est d'une grande importance. Le travail de cette thèse consiste donc en la synthèse et le développement d'un polyphtalamide amorphe à base d'acide furan-2,5-oique.
Dans un premier temps, un protocole de modélisation moléculaire permettant de calculer la Tg de polyphthalamides a été développé. Pour cela, des PPA modèles (basés sur un mélange d'acides isophtaliques et téréphtaliques ainsi que l'hexaméthylène diamine) ont été synthétisés et caractérisés. En comparant les Tg obtenues par modélisation et par mesure en DSC, le protocole de modélisation a été validé.
Dans un deuxième temps, ce protocole a été appliqué à des PPA à base de FDCA. Ces polymères ont également été synthétisés et caractérisés. Il en ressort que le PA 6-F subit une importante décarboxylation durant sa synthèse, l'empêchant d'atteindre une masse molaire importante. Il a aussi été montré que l'ajout de FDCA dans des copolyphtalamides diminuait leurs propriétés thermiques et mécaniques.

MOTS-CLES : Polyamides biosourcés, polyphtalamides, modélisation moléculaire, dynamique moléculaire, acide furan-2,5-oique, FDCA

Laboratoire (s) de recherche :
Ingénierie des Matériaux Polymères IMP@INSA, CNRS UMR 5223

Directeur de thèse: Jocelyne Galy, Jérôme Dupuy

Président de jury : Dr Nadine Essayem

Composition du jury : Pr Alessandro Grandini, Pr Jean-Jacques Robin, Dr Nadine Essayem, Pr Jérôme Dupuy, Dr Jocelyne Galy, Dr Alain Rousseau